# DYNAMICAL MODELLING, CONTROL AND SIMULATION ENVIRONMENT DEVELOPMENT FOR AN EIGHT WHEEL VEHICLE

by

**TERSIA JANSE VAN RENSBURG**

**THESIS**

**submitted in the fulfilment of the requirements for the degree**

**DOCTOR INGENERIAE**

**in**

**ELECTRICAL AND ELECTRONIC ENGINEERING**

**in the**

**FACULTY OF ENGINEERING AND THE BUILT ENVIRONMENT**

**at the**

**UNIVERSITY OF JOHANNESBURG**

**PROMOTER: PROF M.A. VAN WYK**

**JANUARY 2006**

Acknowledgements

I gratefully acknowledge help from the following people and companies:

My study leader, Prof. M. A. van Wyk for his motivation and all the hours of assistance.

African Defence Systems, for sponsoring me for this study and introducing me to the world of simulators. Furthermore, for the two years of contract work on a commercial driving simulator.

Russel Lewis, for providing me with the necessary background information on simulators in general.

Thales Training And Simulation, for three months of driving simulation experience in Sydney, Australia.

My friends and family for their support.

The Applied Mathematics department of the University of Johannesburg, in particular Prof Steeb, Prof. Villet, Yorick Hardy and Dr Prentice for always being willing to assist me.

# Abstract

A driving simulator reproduces the essential features of a vehicle and provides an interface for direct human operation. It provides a safe and less expensive way of training people how to drive.

Against the backdrop of a comprehensive literature survey on driving simulators and their applications, this thesis endeavours to make five unique contributions.

Many of the military armoured vehicles have eight wheels, are able to cross trenches of approximately two meters, and can climb steps of as high as one meter. Available research, however, focuses primarily on the vehicle dynamics modelling of commercial four wheel vehicles. In this thesis, a mathematical model is given for simulating the vehicle dynamics of an eight wheel vehicle over rough terrain, taking into account the limitations of real-time driving simulation. A discussion of the model by Janse van Rensburg *et al.* is contained in a paper which is currently under review by the *International Journal of Modern Physics C (IJMPC)*.

To prove the validity of a vehicle model, it is necessary to provide a method of testing the model. Detail about the vehicle dynamics model used is not always available when developed by a third party. This thesis describes a "black box" testing method for the verification of a vehicle dynamics model. An article regarding this matter by Janse van Rensburg *et al.* has been submitted to the *IJMPC* and is currently under review.

Normally, the focus on driving simulators is on the modelling of realistic vehicle dynamics models. However, the design of a realistic

simulation environment is of equal importance. A human driver usually steers one vehicle, but the rest of the vehicles used in the simulation should be managed by a computer program. An automatic driver model is described to be used within the simulation environment. The current presentation is based on the published paper [86] by Janse van Rensburg *et al.* (*IJMPC*, 16(6):895-908, 2005).

An understanding of three-dimensional coordinate system transformations is one of the most important parts of a flight or driving simulator. Although the procedure of using Euler angles for coordinate system transformations is nothing new, almost no literature is available of how it can be applied on more complex situations. This thesis supplies more information on how a program language such as C++ could be used to apply more complex coordinate transformations in real-life situations. Results appeared in the published paper by Janse van Rensburg *et al.* (*IJMPC*, 16(6):909-920, 2005).

Finally the use of vocoders is proposed for the modelling of engine sound. For a driving simulator which should be an exact replica of a certain vehicle, an accurate sound model is of extreme importance. By using vocoders, a technique used for the manipulation of voice, a higher level of accuracy and realism can be obtained than with the methods currently discussed in literature. A paper on this matter, compiled by Janse van Rensburg *et al.* is currently under review by the *IJMPC*.

# Contents

# List of Figures

# LIST OF FIGURES

# Chapter 1

# Introduction

Simulation is a method for implementing a physical, mathematical or otherwise logical representation of a system or process over time [134]. In the same way a driving simulator can be seen as a device that reproduces the essential features of a vehicle and provides an interface for direct human operation.

A driving simulator provides a safe and less expensive way of training people how to drive. It furnishes a method for getting a person used to a specific vehicle in a specific geographic area which he possibly has never seen before. For a driver the only noticeable difference should be computer screens instead of windows and mirrors [86, 87].

Driving simulators have many fields of scientific applications, including psychology, transportation and road-safety as well as many other research areas, as discussed in section 1.1. Demonstrating the applications for driving simulators contextualizes the present study within the greater simulation environment and indicates research opportunities with regard to driving simulators.

In this thesis, several contributions are made toward the existing driving simulator technology. An eight wheel vehicle dynamics model for off-road driving is proposed, as well as a proper testing method for evaluating existing vehicle dynamics models. Within the simulation environment, realistic display and sound modelling are investigated, and an automatic driver model is presented.

To appreciate the different contributions, one needs to understand what simulation is all about and how a driving simulator works. Chapter 1, section 1.2 explains the concept of a driving simulator, the different subsystems it consist of, and how these models interact.

Section 1.3 looks at the available literature with regard to simulation. Driving simulators are not the only simulators currently in use, and technology presented for driving simulators could also be applied to other simulators. Section 1.3.1 gives a background to the history of simulation, indicating what other simulators are available for training people, such as train and motorcycle simulators. Section 1.3.2 attempts to give an overview of most of the driving simulator literature currently available. Attention is drawn to the foci of research for the different driving simulators. Although a vast amount of investigation has already been done within this area, visual display, sound, testing, eight-wheel vehicle dynamics and automated driving, as presented in this thesis, have not been addressed within literature.

The vehicle dynamics modelling forms the core of any driving simulator. Although the available literature does not contain any references to most aspects of off-road eight-wheel vehicle dynamics, many of the principles found elsewhere are also applicable for such a model. Section 1.4 discusses the available literature on vehicle dynamics modelling.

The thesis, however, has a technical focus, using a mathematical point of departure. For the modelling of realistic visual display and eight-wheel vehicle dynamics, three-dimensional coordinate system geometry is, for example, needed. Section 1.5 discusses the coordinate system convention used within this thesis.

Finally, section 1.6 gives more detail about the rest of the thesis and the contributions made within the individual chapters.

## 1.1 The Widespread use of Driving Simulators

The aim of driving simulators is not only a mathematical exercise for representing an existing vehicle's behaviour by a set of equations to be solved in real time. One should not forget the human factor that exists, that is the end-user of the driving simulators.

Several research groups use driving simulators as a tool for the verification of their research. For instance, driving simulators are used to test the *automated highway system* (AHS) technology (Section 1.1.1) where the AHS will control a vehicle on the highway, and not the driver. Simulators are also used to test the technology for unmanned vehicles (Section 1.1.2), where driving strategy needs to be determined by computer algorithms.

Driving simulators are also used in the research aimed at driving safety. In different studies, driving simulators were used to gain more insight into situations that are more likely to cause road accidents (Section 1.1.3). Research has also been done to evaluate the effect of cellphones on driving (Section 1.1.4) and to improve the design for cellphones for driving safety.

When new vehicle technology is developed, one first needs to know if it will have the desired effects on drivers, and driving simulators have been used successfully for such applications (Section 1.1.5). Within transportation research (Section 1.1.6), driving simulators are used to evaluate driver response to certain driving conditions. Ergonomics studies (Section 1.1.7), for example, use driving simulators to evaluate the effect of vehicle technologies that were developed to improve the driving conditions and to contribute towards the ease of driving.

Within the field of psychology, driving simulators have proved to be a valid method for evaluating human behaviour. For instance, driving simulators are used for analysing driving behaviour (Section 1.1.8). This includes studies of human perception, time of day variation in driving performance, and the driving behaviour within different driving conditions. Driving simulators are also used to gain more understanding of sleep patterns and the effect of fatigue on driving

(Section 1.1.9). Driving simulators are also a safe method for testing the effect of different medicine on driving behaviour (Section 1.1.10).

### 1.1.1 Automated Highway Systems

One of the technologies of the future will be *automated highway systems* (AHS). This is an attempt to increase highway capacity while improving safety. In this scenario, the human driver will not have control on the highway, but it will be done by the AHS, leaving few vehicle driving decisions to the driver.

Horowitz and Varaiya [76] describes the design of an automated highway system developed during 1990-2000 in the California PATH program. The paper focuses on the multilayer control architecture developed for the system and describes the essential components for such a system.

Miura *et al.* [124] proposed a three-level control architecture for autonomous vehicle driving in a dynamic and uncertain traffic environment. It includes the *operational level* for executing primitives for vehicle position and velocity control, the *tactical* level for selecting appropriate maneuvers and the *meta-tactical level* for timely activating an appropriate tactical-level planning procedure according to the current state. On a highway driving simulator, the architecture succeeded in adaptively changing the lane and the speed in a dynamic and uncertain traffic environment.

De Vos *et al.* [41] did research on the behavioural aspects of automatic vehicle guidance (AVG). People were asked to drive a driving simulator twice: once with AVG enabled and once without it and were asked to compare the comfort rating. Results showed that to equal the comfort level that people experience daily in dense traffic on the free way network in peek hours, the AVG headway should be no less than 0.86 seconds.

### 1.1.2 Unmanned Vehicle Control and Modelling

Driving simulators are also used to collect data to be used in advanced vehicle systems. Ohno [132] describes the collection of data for adaptive cruise control (ACC) in which a vehicle automatically maintains a constant inter-vehicle distance and speed as selected by the driver. The data were used to build a neural network in order to predict the control performance of a skilled driver using ACC.

Bernard and Gruening [26] looked at the possibility of using genetic algorithms within driving simulation. Given a terrain, the genetic algorithm is used to determine the best path for a vehicle over that terrain.

Human control strategy models which accurately emulate dynamic human behaviour, find application in a number of research areas ranging from robotics to the intelligent highway system. In a study by Xu *et al.* [180] data about human control strategy has been collected from different individuals through a real-time graphic driving simulator, and each individual's control strategy model has been identified through the flexible cascade neural network learning architecture. The driving models of different humans were then combined to produce an optimized algorithm to be used to simulate human behaviour.

Kwon *et al.* [96] investigated the model-matching control in a longitudinal autonomous driving system by vehicle dynamics simulation. This was done in order to find a solution for the stability problems in the current longitudinal and lateral controllers. To investigate this technique, it has been tested by vehicle dynamics simulation. This method enables the vehicle acceleration to follow the reference model even if the parameters of the control plant model are changed.

In a study by Kim and Kim [92] the focus for unmanned vehicle control was particularly on the hardware design and control for obstacle avoidance. The method makes use of longitudinal control for acceleration and braking and lateral control for steering. Each system recognizes obstacles surrounding it and makes a decision how fast to proceed according to circumstances. This technology can be used for military applications to send an unmanned vehicle into a mining field where it will be too dangerous for humans.

Pasquier *et al.* [137] presented an automated driver prototype using a self-organizing fuzzy rule-base system to model and subsequently emulate human driving expertise. It was, however, limited to user-specific road scenarios, and the autopilot may not be able to handle different road conditions without retraining.

### 1.1.3 Accident Analysis and Prevention

De Waard *et al.* [42] did a study to investigate which visual information is important to a driver by using an advanced driving simulator. Thirty-two drivers were tested on a $10km$ road divided into five sections of $2km$ each. At each a road element was added or removed. During the rides, performance (lateral position, speed) and heart rate were recorded continuously. It was done with the absence of markings on a road and a centre line. Elderly drivers, however, appeared to need the visual aid of the centre-line to a greater extent than younger drivers.

Since conventional driver's license tests are impractical and stressful to older drivers, studies were done to investigate the possibility of using a driving simulator to test people. Lee *et al.* [104] demonstrated an economical driving simulator approach to screen out problematic and unsafe older drivers before a more detailed but expensive road test is considered. In another article, Lee *et al* [105] discuss tests where older drivers were tested on the road and in a driving simulator and the results were compared. When the older drivers were tested with the driving simulator, the values compared well on the assessment criteria. The research support the validity of using a driving simulator to asses the driving performance of older drivers.

In a study by Charlton [32], research was done to evaluate the effectiveness of three different curve warning signs in New Zealand. People had to drive a driving simulator while talking on their cellphones. All the warnings worked reasonably well for severe curves regardless of the cellphone task. For less severe curves, the curve warnings that contain perceptual components or emphasize the physical features of the curve work best, particularly in the cognitively demanding situations such as talking on a cellphone. The drivers became less responsive to primary task demands when talking on a cellphone.

Verwey and Zaidel [176] investigated the effect of mental activity while driving. It has been found that mental activity acts as a counteract to drowsiness and improve the people's driving in general. Although people tend to be alert in more complicated driving conditions, the effect of a mental game was clearly visible when a very simple task such as driving on a long straight road was done.

Lehto *et al.* [107] investigated two collision avoidance warning systems: the *distributed signal detection theoretic* model in which the human operator and the warning mechanism are independent decision makers who work together as a team, and the *signal detection theoretic* (DST) threshold which assumes a single decision maker. The experiment focused on evaluating the quality of the decision making of the drivers. A collision avoidance system provided a warning when the probability of an inadequate overtaking gap exceeded a threshold. The findings support the conclusion that the DSDT model is a useful, quantitative tool that should be used by warning designers.



In a study by Cheng *et al.* [33], a driving simulator was used to analyse the drivers' responses to a forward collision warning. Thirty-six people were exposed randomly to three kinds of dangerous scenes while the people' attention was intentionally distracted. It has been found that the reaction time response to the warning sound, for some people, was as long as 2.4 seconds and that the timing of collision warning should take that into account. However, the braking responses to collision warnings were longer than for simple scenario tests.

Dorn and Barker [47] investigated whether professionally trained and experienced drivers exhibit safer driving behaviour in a simulated driving task compared with drivers without professional driver training. It was found that the professionally trained drivers were significantly less likely to cross the central division of the road at unsafe locations during the overtaking task and reduced their speed on approach to pedestrians at the roadside to a greater extend. They also adopted a more central lane position compared with other drivers on urban roads and at traffic lights.

Alexander *et al.* [19] used data generated from a fixed-base interactive driving simulator to built a model to predict the probability of an accident at a junction. The focus was on the scenario in which a driver turns from a major road into a minor road across an oncoming stream of traffic. It was found that the probability that a driver will have an accident or near miss when turning right across a stream of traffic is dependent on both the size of the gap that a driver will accept in an on-coming stream of traffic and the time taken to cross the intersection once the gap has been accepted. Elderly and female drivers have a lower probability to take a short gap in contrast to younger and male drivers.

Comte and Jamson [37] investigated the effectiveness of four speed-reducing methods: variable message sign, in-car advice, speed limiter and transverse bars. This was done to find ways of reducing the accidents at curves on roads with a speed limit of 100km/h. It was found that although speed limiters, which slow the vehicle down automatically, were the most effective, the provision of speed advice to drivers does result in reduced speed on the approach and negotiation of curves. It seems to matter little exactly in what mode this advice is given to the drivers.

### 1.1.4 Cellphones

Several studies on cellphones have been done with the help of driving simulators.

Rakauskas *et al.* [146] studied the effect that ordinary and demanding cellphone conversations have on driving performance by using a driving simulator. It was found that cellphone use caused participants to have higher variation in accelerator pedal position, to drive more slowly with more variation in speed, and to report a higher level of workload regardless of the demand level of the conversation.

Liu [112] used a low cost, fixed-base driving simulator to investigate the impact of a new car cellular audio phone system on driving behaviour. It was found that in low driving load environment, driving performance (mean lane position, variances in lane position, lateral acceleration and steering wheel angle) was relatively good, but in a high driving condition it decreased because the attentional resources of the people became overstretched.

Salvucci and Macuga [156] investigated the driver behaviour on different cellular dialling methods, namely manual, speed, menu and voice dialling. They found that dialling time is not an indication of driving behaviour, and that voice dialling caused the smallest deviation in driving behaviour.

Alm and Nilsson [21] studied the effect of a mobile telephone task on driver behaviour in a car-following situation. It was found that a mobile telephone task had a negative effect upon the drivers' choice reaction time, and that the effect was more pronounced for the elderly drivers. The mental workload on the people tested increased as a function of the mobile telephone task.

### 1.1.5 Testing of New Technology



Several new vehicle technologies have been validated on driving simulators.

The steer-by-wire system is a system where there is no mechanical linkage between the steering wheel and the steering gear. The steering maneuvering is detected by means of a steering angle sensor and torque sensor, and this information is transferred to a controller which uses this and other sensors' information to control front-wheel angle via a steering actuator. Segwa *et al.* [160] investigated the effectiveness of using $D^*$ control. They optimized the control parameters by using a driving simulator.

Newton *et al.* [130] used a driving simulator for the evaluation of an alternative traffic light change anticipation system. The proposed traffic light system gives the driver approaching a signalized intersection an indication when the green signal will change to amber. It was found that this will not improve intersection safety. It increased the potential for conflicting decisions between successive drivers approaching the intersection.

A vehicle stability system is an active safety system for road vehicles which stabilizes the vehicle dynamic behaviour in emergency situations such as spinning, drift out and roll over. In a study by Chung *et al.* [36] a closed loop evaluation of the vehicle stability control system is presented using a driving simulator. The real-time human-in-the-loop simulation results in realistic driving situations show that the proposed controller reduces driving effort and enhances vehicle stability.

Hoedemaeker and Brookhuis [74] describes a study that aims at assessment of driver behaviour in response to new technology, particularly Adaptive Cruise Control Systems (ACCs), as a function of driving style. They found that drivers adapt their behaviour in ways that might not be beneficial for traffic safety. Very short following distances occurred more frequently, which could be associated with increased accident likelihood.

The *Advanced Cruise-Assist Highway System* (AHS) consist of a "Support System for prevention of right turn collisions" and a "support system for prevention of collisions with crossing pedestrians" In a study done by Daimon and Kawashima [40], a motion based driving simulator was utilized in the experiment to measure how aged drivers were influenced by the content and the location of the AHS, as compared to young drivers. It was found that young drivers paid attention to the systems for helping them deciding whether it is save to turn right. However, for older drivers, the information provided by the two support systems failed to help them judge the safety of turning right.

Van Erp and Van Veen [171] used a driving simulator to test a vibrotactile display, consisting of eight vibrating elements or tactors mounted in a driver's seat. The conclusion was that this study quantitatively supports the claims that a localized vibration is an intuitive way to present directional information, and that employing the tactile channel may release other heavily loaded sensory channels, therefore potentially providing a major safety enhancement.

### 1.1.6 Transportation Research

Driving simulators have also been used for the general transportation research.

Van der Hulst *et al.* [168] investigated the performance of driving under fatigue by letting people drive 2.5 hours on a driving simulator. According to their results, performance in less central task components such as steering deteriorates in the course of time, whereas performance in high-priority sub-tasks such as hazard avoidance remains in tact.

Wrong-way entries can end tragically. Laurie *et al.* [102] investigated a 3D Do Not Enter sign painted in the same way as the conventional 2D one. The effect of this has been evaluated by testing 48 people with valid driver's licences on a driving simulator. They found that the standard 2D Do Not Enter sign combined with a "No Right Turn" was more effective than the 3D one.

McGehee *et al.* [119] assessed the time required for 80 experienced drivers to adapt to a simulator and to steer in a stable manner. Results showed that drivers' steering behaviour stabilizes within approximately 240 seconds of the start of the simulator scenario, and long extended practice periods before collecting data might be unnecessary. However, other aspects of driving simulator adaptation should still be considered.



Van Winsum *et al.* [172] used a driving simulator to gain insight in the typical maneuvers by people when they change lanes. Eight people were required to do 48 lane changes with varying vehicle speed, lane width and direction of movement. The results suggest that steering actions are controlled by the outcome of previous actions in such a way that safety margins are maintained. It also suggests that visual feedback is used by the driver during lane change manoeuvres to control steering actions, resulting in flexible and adaptive steering behaviour. Temporal information on the relation between the vehicle and lane boundaries is used by the driver in order to control the motor response.

Koutspouluos *et al.* [94] discuss the use of travel simulators to understand the traveller's response to potential *advanced traveller information systems* (ATIS). For a traveller simulator the main focus is to study the traveller's response to information acquisition and not only the human factors involved in driving. They find that all existing travel simulators fail to some degree to replicate actual behaviour. Travel simulators should be used in combination with field tests to specify the "ideal" design.

### 1.1.7 Ergonomics

With regard to driving, ergonomics pertains to the study of driving conditions, especially in the design of vehicle equipment in order to help people driving more efficiently. Driving simulators are also used to improve the ergonomics of vehicles in general.

A Kansei Engineering approach to a driver/vehicle system is a research area which involves handling a full-range of human feelings or emotions and evaluating many car product parameters. Horiguchi and Suetomi [75] discuss the high-level design of a driving simulator used by Mazda for research on how a driver perceives movement and how he controls a vehicle. They have confirmed that the reaction time is longer according to the age of the driver. Their final aim is to study high-order sensations using this simulator.

De Waard *et al.* [43] used a driving simulator to test a tutoring system in an advanced driving simulator. Drivers were provided with auditory and visual tutoring messages, with respect to a selection of offences, if deviations were detected from legally allowed behaviour. Results showed that the system was very effective in increasing law-abiding behaviour. However, the elderly drivers found it more useful than the younger drivers.

In an article by Bliss and Acton [27] results are given of the effectiveness of collision warning systems in vehicles. These are some of the inventions in new vehicles that warns a motorist of a potential collision from the rear. To test them, people were asked to drive a driving simulator with collision warning systems that were 50%, 75% and 100% effective. It was found that although the automobile swerving reactions were significantly better when alarms were more reliable, drivers still failed to avoid collisions in spite of reliable alarms.

Llaneras *et al.* [114] investigated the influence of age on driving performance. The study examined the relationships between age, functional abilities and driving performance. It was found that significant decrements in perceptual, cognitive and psychomotor abilities tend to increase with advancing age. Although age cannot be a significant predictor of driving performance, age appears to operate a moderator variable which acts to influence driving performance indirectly.

Laurie *et al.* [100] did a case study on the usability of voice activated dialling systems (VADS) while driving. They concluded that the VADS could be improved by following the principles of conversational speech such as avoiding repetition and being flexible in their handling of interruptions.

### 1.1.8 Analysing Driving Behaviour

The using of a driving simulator enables researchers to study and analyse the human behaviour while driving, which would not be possible otherwise. Salvucci and Liu [154] did research to analyse the driver's control and eye-movement behaviour as a function of time when changing lanes. This enabled the researchers to describe the sine-wave steering pattern and reduction in speed when changing lanes. It has been found that turn signals were only used half of the time and that drivers shifted their primary visual focus from the start lane to the destination lane immediately after the onset of the lane change. Such information will be used as the basis for future development of a new integrated model of driving behaviour.

In an article by Ahn *et al.* [17] possible scenarios and tests are described for evaluating the driving ability of people. Experimental results are given of the performance of different people, and the general trends are discussed. Van der Hulst *et al.* [169] studied driving behaviour in reduced visibility conditions. People had to drive a driving simulator in two different scenarios: one where a person was allowed to drive normally with no time restriction and one where a person was given a time limit. With no time restrictions and limited visibility, people compensated by reducing speed and increasing time headways. With a speed restriction, the drivers had to maintain high alertness in order to react accurately to unpredictable hazardous events.

Kemeny and Panerai [90] believes that driving simulators can be used for a more thorough understanding of human perception and control of self-motion, especially when speeds and accelerations are higher than in actual locomotion. Perception in driving simulator experiments have been evaluated. It has been found that for actual perception of vehicle speeds and distances, a large field of view is needed.

Featherstone *et al.* [50] used a driving simulator to determine under low-contrast environmental conditions whether differences exist in the driving performance of patients with bilateral array multi focal intra ocular lenses (IOLs) and those with bilateral AMO mono focal IOLs . Driving performance was evaluated under poor visibility conditions. It was found that no statistically significant differences could be measured in most of the cases, but that driver performance overall tend to be better with mono focal lenses.

Glendon *et al.* [64] investigated Risk Homeostasis Theory (RHT) in simulated environments by using the Aston Driving Simulator. RHT argues that people have a desired or target level of risk; they feel right taking a certain amount of risk and adjust their behaviour if they perceive they are exposed to more or less risk [1]. A low fidelity simulator proved to be unsuccessful and even in the more advanced simulators, although people tried to avoid accidents, they were not afraid of the consequence of an accident. Researchers found that RHT effects are limited to environments such as driving in which people have a relatively high degree of control and autonomy over their behaviour, that is in which there are few constraining parameters.



In another study on RHT using the Aston Driving Simulator [77], the role of utility and intrinsic risk as possible determinants of behavioural compensation were experimentally examined across 14 specific behaviours. They found that contrary to the traditional model of risk homoeostasis, utility is not logically necessary for behavioural compensation in response to a change in intrinsic risk.

Several studies have been done around the world to validate the reliability of using a driving simulator for analysing driving behaviour. In [167] a study was done to analyse the differences between driving through a simulated road tunnel and a real tunnel. It was found that driving speed was higher in the simulated tunnel than in the real tunnel and that the people positioned the car somewhat further away from the nearest tunnel wall in the real tunnel than in the simulated tunnel. Although absolute validity did not hold between the simulated and real scenarios, the the relative validity was good for both speed and lateral position.

Liu [113] did a study to investigate the use of a head-up display when driving a vehicle. The head-up display presents vehicle information to the driver. It was found that people paying attention to the head-up display reacted faster to variation in steering wheel angle and lateral acceleration. On simple driving conditions, it was also found that people tend to pay more attention to the road.

Iwao *et al.* [81] looked into the possibility of supplying information on a life display screen for drivers while driving a truck. With tests done on a driving simulator, it was found that a warning sound is needed with each message, otherwise the drivers will not notice half of the messages. It was also been found that the location of the messages is very important, and especially on a truck it should be placed close to the mirrors for getting information more efficiently.

Lenne *et al.* [109] investigated the time of day variations in driving performance. It was found that the performance of drivers was the worst in the early morning hours between 2:00 and 6:00 and also in the early afternoon round about 14:00.

Roge *et al.* [149] used driving simulation to investigate the driver behaviour during the performance of a monotonous task. It is known that in such a situation, certain behaviours occur that are not necessary to the performance of the task. They found that the behavioural activities generally seem to vary according to the duration of the drive in the same way as physiological signs of vigilance.

Salvucci [155] evaluated human performance of a secondary task while executing a critical primary task. Different dialling methods were tested while driving on a driving simulator. It was found that two manual-steering interfaces have significant effects on driver steering performance while two different voice-dialling interfaces have no significant effects on performance.

Kotterba *et al.* [93] tested the driving performance of people with narcolepsy, that is people with day-time sleepiness. In this experiment, they found that people who are aware of their condition, paid extra attention to the road. That means that not all people with narcolepsy should not be allowed to drive. A driving simulator was nevertheless evaluated as a valid method to test if someone should be allowed to drive on the road.

Campagne *et al.* [30] measured driving-off-the-road-incidents and large deviations to determine the number of driving errors a person made in their study. They investigated the correlation between driving errors made and vigilance level for different age groups and concluded that the correlation differs for different age groups.

Ahlgren *et al.* [16] did studies on the driving ability after a coronary artery bypass grafting. In this study it was found that cognitive functions important for safe driving may be influenced after cardiac surgery.

### 1.1.9 Fatigue and Sleep Patterns



In a study by Philip *et al.* [138] a driving simulator was used to study the effect of fatigue on driving performance. People who stopped at a rest area on a free way were asked to participate. They had to fill out a questionnaire asking information such as how many hours of driving they had done and about their sleeping patterns. People who had already spent a lot of time on the road that day found it more difficult to position the car on the road. The authors concluded that a driving simulator is a valid method for identifying fatigue.

Desmond and Matthews [44] did a study to detect the implications of fatigue effects when driving a vehicle. Several experiments were done in which fatigued drivers needed to drive under different circumstances. It was found that the fatigued drivers were still able to do more complicated driving such as driving a curved route, but when the task was easy such as driving on a straight road, performance tended to deteriorate, implying that fatigued drivers are failing to mobilise their efforts effectively.

In a survey on driving simulators used in clinical practice, George [61] looked at the use of different driving simulators for detecting patients with sleep disorders and in people made sleepy by sleep restriction. It was found that despite the varying complexity of the simulation involved, the results of the simulations were quite consistent in their outcome. Driving performance is worse in sleepy people regardless the cause for sleepiness. Moreover the magnitude of these driving performance decrements is similar to that of alcohol.

Pizza *et al.* [140] did research on the effect of sleepiness on driving. It was shown that the number of crashes and times exceeding the speed limit and lane change variability showed significant differences between simulation sessions where people had enough sleep and sessions where people had almost no sleep the night before.

Contardi *et al.* [38] used the standard deviation of lane position for evaluating sleepiness. It was shown that when awake, a person does not move from his starting position. However, after a night of sleep deprivation, he has difficulties maintaining the vehicle in the middle of the road.

Macchi *et al.* [116] investigated the effects of an afternoon nap on alertness and phsychomotor performance during a simulated night shift. They showed that a three-hour napping opportunity until 17:00 significantly improved the alertness and driving performance of drivers throughout the night.

### 1.1.10 The Effects of Medicine on Driving

Driving simulators provide a save and effective way to study the effect of a certain types of medicine on driving performance.

The studies done by Fishbain *et al.* [51], indicated that opioid (nervous system depressants) appear not to impair driving-related skills in opioid-dependent patients. Opioid is used for cases such as intense pain because of cancer. By forbidding a person to steer, dooms the person to a life of disability.

Partinen *et al.* [136] investigated the driving ability of women who took sleep medicine after midnight. It was found that certain patients were more susceptible than others to the drug effects. It underlines the necessity to strongly advocate against the late intake of sleep medicine if patients intend to drive a car early the next morning.

Verster *et al.* [175] used driving simulators in a study of the effects of sleep medication on driving ability. In this study, it has been found that the medicine such as zolpidem and zaleplon do not significantly affect driving performance in the morning, but patients treated with benzodiazepine hypnotics or zopicione should be cautioned when driving a car.

Lenne *et al.* [108] considered he effects of medicine used for heroin dependence in combination with alcohol upon simulated driving. Simulated driving skills were measured through standard deviations of lateral position, speed and steering wheel angle. Reaction time to a subsidiary task was also measured. It has been found that alcohol has the same effect on the driving of people not using other medicine than on the people using medicine for heroin dependence.



## 1.2 The Typical Driving Simulator Setup

A driving simulator consists of a vehicle dynamics model, terrain model, scenario generator, visual display, sound and a driver. Figure 1.1 shows the different subsystems of a driving simulator and how they interact. Next, each subsystem will be discussed.

### 1.2.1 Vehicle Dynamics Model

The vehicle dynamics model includes models of several subsystems of the vehicle, such as for the engine, drive train, aerodynamics, vehicle-road interaction, suspension and handling. Each component is modelled as a set of differential equations.

The vehicle dynamics calculations happen at discrete time intervals, which depend on the complexity of the model. For no suspension calculations, that is where no

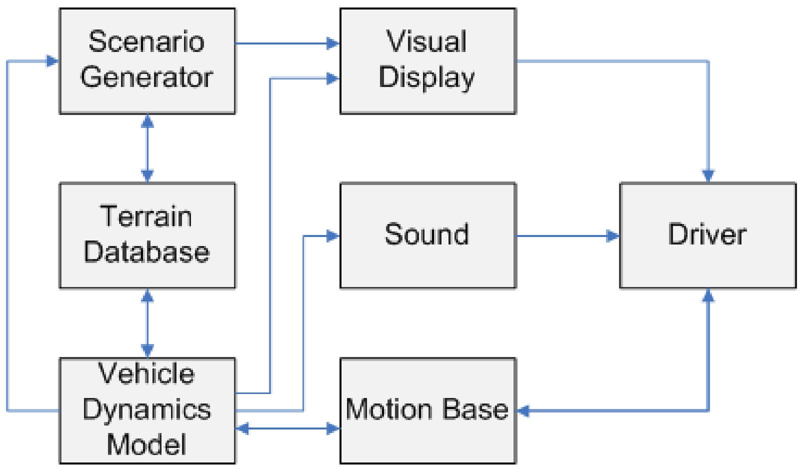


Figure 1.1: Typical driving simulator setup.

stiff differential equations are involved, a step size of $0.01s$ might be sufficient, while a complex suspension model might need a step size of $0.002s$ [70].

In each time interval, the vehicle dynamics model obtains from the motion base the driver input such as the steering wheel, throttle position, brake and the selected gear. It also queries the terrain model regarding the information such as the type and height of the terrain at the wheel positions as well as collision information. The vehicle model then solves the differential equations according to the given input, and calculates the vehicle position and orientation for the next time step. This information is then given to the scenario generator, sound and visual models and the motion base to update the vehicle and environmental information.

### 1.2.2 Terrain Model

The terrain model contains a database of all the terrain information. This information is then used to visualize the terrain by means of a graphic display. It also supplies the necessary information for the vehicle dynamics model in the required format.

The basis of the terrain database is usually the DTED (Digital Terrain Elevation Data) of a specific terrain. This is a regularly spaced grid of elevation points [6]. For most countries the elevation points are spaced $3km$ apart. This is combined with DFAD (Digital Feature Analysis Data) that contains the main landmarks of an area [5]. For a realistic terrain this information is used as a base and is further expanded to contain the small hills, the different terrains, trees and rocks, usually from aerial photographs. Specifically for defence purposes, simulators are not only made to teach a person to learn how to fly or drive, but also to get accustomed to a certain region.

The vehicle dynamics model will always be interested in the distance between the wheels and the ground in the direction of the vehicle, and information about collisions with other objects. For each time cycle, the vehicle dynamics model will supply the position and orientation of the vehicle, and the terrain model will calculate the terrain distances and possible collisions with the terrain and with other entities in the simulation.



### 1.2.3 Scenario Generator

For a realistic simulation environment, there will be other obstacles such as buildings, trees, rocks, hills and trenches, as well as distractions such as other people, vehicles, animals and changes in weather conditions. For defence purposes, a war scenario may be generated.

The time of the day will change throughout a simulation and will cause other changes as well. At night, the street lights will be switched on, and the positions of the stars will change according to the date.

The scenario generator keeps track of all the objects within the simulation, and creates background activity according to pre-defined rules. The vehicle dynamics model will supply its position and orientation to this scenario generator model, and the model will use terrain information to place its objects.

### 1.2.4 Visual Display

The visual model generates a picture of all the information given by the terrain model, the vehicle model and the scenario generator. The visual display must be able to display the scenario from different angles in order to simulate the front and side windows and the mirrors.

Several graphic engines exist. The best known open source program is Demeter [4]. The typical graphic subsystem also simulates weather conditions such as fog, snow, rain and cloud levels.

### 1.2.5 Sound

Realistic sound plays an important role in driving. The lack of an audio cue has been shown to have a detrimental effect on the driver's ability to maintain a constant velocity [121]. Audio also plays an important part in selecting the most appropriate state of the vehicle, e.g. the decision to change gears.

The vehicle sound depends on the engine and vehicle speed. The noise caused by the wind and type of terrain will also depend on the velocity and acceleration of the vehicle.

Most simulators use pre-recorded sounds from the interior of real test vehicles. These systems then manipulate sound samples using audio software in conjunction with the computer simulation to vary pitch and volume [70].

### 1.2.6 Motion Base (Haptic Subsystem)

To simulate the "look and feel" of a vehicle, the more sophisticated simulators have a motion system which might provide an exact replica of the interior of the vehicle. This includes the steering wheel, accelerator and brake pedals, gearbox and any other buttons that may be necessary for driving. The components will also supply the same force feedback than an actual vehicle.

The motion base will also simulate the suspension movements of the vehicle, as supplied by the vehicle dynamics model. It will supply the information about the status of the steering wheel, pedals, current gear and buttons to the vehicle dynamics model.

### 1.2.7 Driver

The driver is the user of the simulator. He uses his senses to combine the visual information, motion and sound feedback in order to make decisions about how to drive. The driver will usually drive a predetermined route, and will use the exercise as an opportunity to get accustomed to a specific area and a specific vehicle.

A human driver cannot steer more than one vehicle at a time. For that reason, not all the vehicles within a simulation are operated by human beings, but some might have automatic drivers [86]. The automatic driver uses the same vehicle dynamics model as the human driver would use. It also uses the vehicle characteristics in such a way to obtain the optimal performance of the vehicle.

## 1.3 Simulators found in Literature

Although the focus of this thesis is primarily on driving simulators, the kind of models presented could also be applied to other types of simulators. Section 1.3.1 discusses a few other simulators such as flight simulators, motorcycle simulators and train simulators. This is followed by an overview in section 1.3.2 of the different driving simulators that exist according to the extant literature.

### 1.3.1 Simulators in General

Aircraft simulation is found to be the earliest form of driving simulation [70]. The importance of training has been realised since the inception of manned flight. In the early days of gliding, it was customary for "pilots" to sit in the glider. The glider was exposed to a strong wind coming from the front, and the pilot could "feel" the controls by keeping the wings in a horizontal position. Thus, even before the glider flew, the pilot had some experience of the lateral controls. One of the first truly manually controlled flight training devices is shown in Fig. 1.2. The simulator consisted of two half sections of a barrel mounted and moved manually to represent the pitch and roll movements of an aeroplane. The pilot sat on top of this device and was required to line up a reference bar with the horizon.

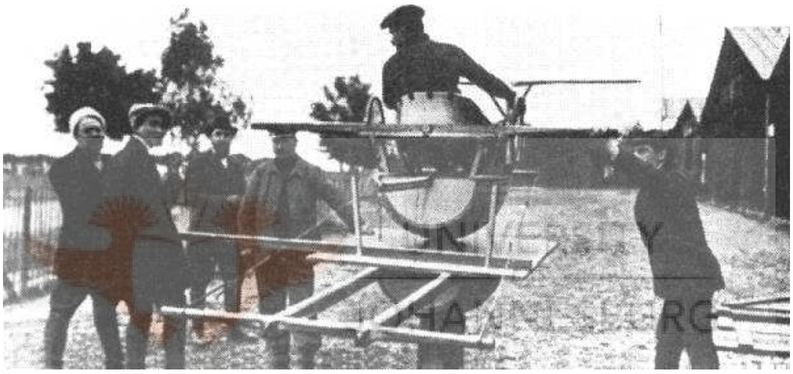

Figure 1.2: The first truly synthetic flight-training device. (Borrowed from [3].)

Modern flight simulators have come of age since the late 60's as flight simulators began relying on digital computers and more advanced visuals. They have a six degree of freedom motion system; the instrumental panel is an exact replica of the real aeroplane, and all the calculations are done very accurately. Fig. 1.3 shows a photo of an ultra modern flight simulator. We have now reached a point in commercial flying training where all conversion and recurrent training can be conducted in a simulator, so that a pilot of one type of aircraft can be cross trained to another without ever actually having flown the real target aircraft, until he or she is on board, carrying fare paying passengers [3].

The flight training simulators enable qualitative pilot training for basic training aircraft and helicopters. For a military flight simulator, training capabilities might include cockpit familiarisation, basic flying, instrument flying, navigation flying,

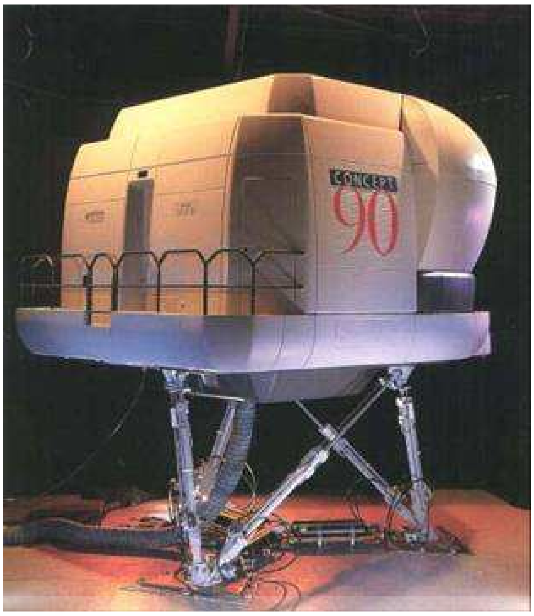

Figure 1.3: An ultra modern flight simulator. (Borrowed from [3].)



emergency and failure procedure training and training of tactical engagement and weapon systems [2]. Fig. 1.4(a) shows a photo of the Pilatus Astra Cockpit Procedural Trainer, developed by ADS.

Except for flight and driving simulators, there exist many other types of simulators as well. Marine simulators are not so well known as flight simulators, but there are several in use. The training capabilities for a military marine simulator might include navigation training, weapon system training, tactical scenario training and emergency training [2]. Fig. 1.4(b) shows the Weapon System Training system for the Minister class of the Fast Attack Craft for the South African Navy. The simulator is still in service at the South African Navy Strike Craft Training School.

Locomotive simulators are meant for training and exercising train driving skills in normal and malfunctional situations, and also to train drivers to behave correctly in emergencies and dangerous events. Locomotive simulators, such as the ICE Train Simulator (Fig. 1.4(c)) have been developed for express trains in Europe to teach drivers control of the train at 280 km/h [8].

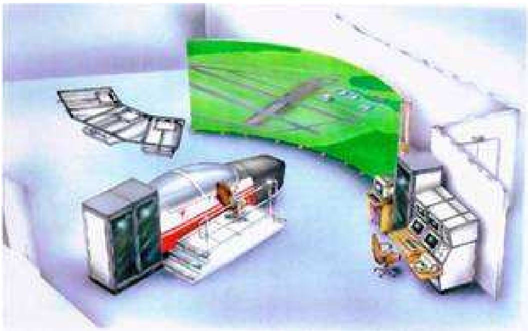

(a) The Pilatus Astra flight simulator, developed by ADS. (Borrowed from [2].)

(b) A marine simulator used by the South African Navy. (Borrowed from [2].)

(c) The ICE train simulator. (Borrowed from [8].)

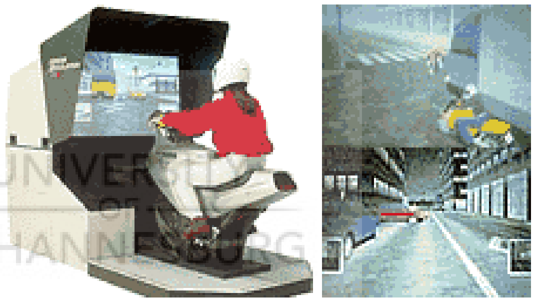

(d) The Honda riding simulator. (Borrowed from [10].)

(e) Port Crane simulator. (Borrowed from [11].)

(f) The CyberLHD simulator. (Borrowed from [12].)

Figure 1.4: Different types of simulators.

The Honda Riding Simulator (Fig. 1.4(d)) is an educational tool developed to allow motorcycle riders to safely experience potential dangers commonly encountered while riding a motorcycle, and thereby improving their ability to foresee and avoid dangerous situations. In order to make the experience as realistic as possible, the simulator closely duplicates a motorcycle's behaviour, and even mimics other conditions such as wind and surrounding noise. Riders guide their "bike" through an imaginary city where they encounter a variety of danger patterns and riding conditions that have been simulated in ways specifically designed to augment the learning process. Since its first development in 1996, the Honda Riding Simulator has been adopted by traffic education centres and driving schools throughout Japan, and has been widely used in many types of motorcycle safety training programs. In this way Honda has actively pursued both hardware and software possibilities in its quest to realize greater safety and peace of mind for those who choose to make motorcycles a part of their lives [10].

The Port Crane Simulation System (Fig. 1.4(e)) is used in an integral training program for harbour workers based on simulation. The system simulates the behaviour of five different crane models usually used in several loading and unloading tasks [11].

There are also simulators developed for the training, retraining and evaluation of drivers of load haul dumper vehicles deployed in underground mining operations. These type of simulators provide effective and efficient training in mucking, hauling and dumping skills, from basic techniques to coping with underground emergency situations [12]. Fig. 11.4(f) shows the The CyberLHD Simulator, developed for these purposes.

### 1.3.2 Driving Simulators

The development of driving simulators is becoming a popular topic within the vehicle industry. Many publications have appeared within this field. Gruening *et al.* [70] presented a general literature review of driving simulation, and discussed the important components of modern driving simulators such as graphics, haptic and audio display . They also discussed the main reasons for motion sickness within driving simulators, such as washout algorithms, display distortion, colour imbalance, geometric discontinuities and jerky motions in certain situations. Lee *et al.* [106] also described the process involved and the components needed for the development of a driving simulator. The need and use of the simulator components such as the real-time vehicle simulation system, the visual and audio system, and the motion system are described. The authors were involved in the development of a low-cost driving simulator of the Kookmin University.

Page and Smith [134] wrote an overview of military training simulation in the form of an introductory tutorial . They explained the basic terminology used within the simulation environment, and described the current trends and research foci in the military training simulation domain.

Letherwood and Gunter [110] looked at the modelling and simulation of military ground vehicles. The vehicle designs are simulated to make sure that the suggested design will have the required performance . They discussed the performance aspects of vehicles that can be simulated in order to make an intelligent decision on the reliability of a vehicle. They have also published articles on the verification of specific dynamic models such as the verification of a dynamic model of a 5-ton tractor towing an M900 series tank. [111].

Several type of algorithms have been used within in the course of the development of simulators. Mourant *et al.* [127] developed software techniques for distributed, multi-vehicle diving simulation on low cost computers. That includes standard networking techniques and cloned data acquisition. This has been implemented and tested on simple configurations with only two computers.

Park *et al.* [135] discussed the development of the PNU (Pusan International University) driving simulator. They focused specifically on the development of a motion controller for their motion platform and discussed shortly their elementary visual system and algorithms for generating the perception of motion within the driving simulator.

There are several research driving simulators developed by academic institutions.

The best known driving simulator is the Iowa Driving simulator. Freeman *et al.* [55] presented an overview of the Iowa Driving Simulator. The simulator currently supports a Ford Taurus, GM Saturn and a HMMWV. The vehicle dynamics models used are based on the real-time recursive dynamics kernel which is a general purpose multi body dynamics package making use of a minimal, joint-coordinate formulation of the equations of motion for rigid multi body systems. This simulator is mainly used for research on automated highway systems. It provides the driver with high fidelity motion, visual, auditory and force feedback cues. The Iowa Driving Simulator is shown in Fig. 1.5.

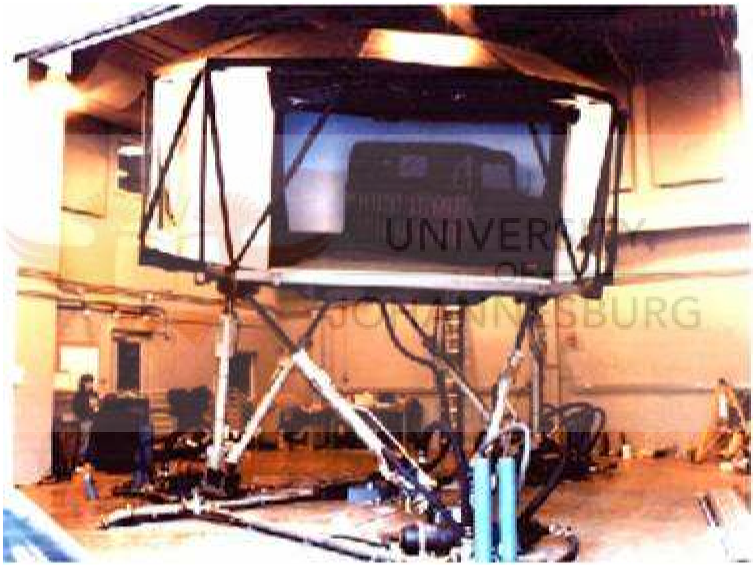

Figure 1.5: Iowa driving simulator. (Borrowed from [55].)

Low-cost simulators have been developed for several purposes. The University of Michigan developed a simple driving simulator for teaching students control systems within an embedded environment [69]. Students need to develop control modules for the simulator, such as cruise control which they then need to test by interfacing with the simulator. They used the vehicle dynamics model of Gillespie [63].

Allen *et al.* [20] described the architecture of a low cost, PC based, real-time driving simulator. Their vehicle dynamics models are based on the Ford Taurus data [35], and have a force-feedback steering unit which supplies the user with realistic visual and audio cues. The Elemental Driving Simulator (EDS) [62] is a low cost simulation of the information processing demands of driving. People with cognitive deficits, including head injury and stroke survivors will be tested to identify driving problems and prepare for intervention.

The DRI (Dynamic Research Inc.) driving simulator [163] features a computer generated graphics roadway scene, a six degree of freedom motion cueing platform, instrumented cabs, control loaders, vehicle dynamics models and data acquisition. This simulator has been used in several vehicle research and development studies, such as research on a vehicle navigation system.

Huang and Chen [78] developed a motion-based driving simulator for simulating the vehicle dynamics of a four wheel vehicle. They used Gillespie's vehicle dynamics model [63], and a motion base consisting of four cylinders to develop a four degrees of freedom vehicle dynamics model. A fairly smooth road is assumed, and not much information is given on the implementation detail of the suspension.

The JUT-ADSL driving simulator [71] is the Jilin University of Technology's driving simulator, developed in the National Key Lab of Auto-Dynamic simulation for research and development purposes. They focused on the control systems for the least delays within the simulation, a low speed tyre model, a steering model and rolling resistant modelling which take into account the computational errors that occur within a driving simulator.

Salgian and Ballard [153] developed a simulator for manual and automated driving. The virtual reality helmet for visual display can track eye movements. This simulator allows the assessment of exigencies in complex situations that can be used to guide the development of automated routines.

Driving simulators, however, have several after-effects as well, such as motion sickness. In a study by Lee *et al.* [103] eleven people were asked to perform a series of alternating left and right turns with straight sways in between. Ten of the people reported moderate sickness.

However, driving simulators have been proved to be a valid method for research on driving methodology. Godley *et al.* [65] validated the possibility for using driving simulators for speed research. It has been found that the participants used for the experiments generally drove faster in the instrumented car than the simulator. However, the speed profiles were much the same and the conclusion is made that speed is a defensible variable for research using the simulator.

## 1.4 Vehicle Dynamics Modelling

Vehicle dynamics modelling forms the core of any driving simulator. Although the available literature does not contain any references to most aspects of off-road eight-wheel vehicle dynamics, many of the principles used elsewhere are also applicable for such a model. Most of the vehicle dynamics models are based on the fundamental prototypes given in the following books:

Gillespie [63] presented a basic vehicle model and discussed all the fundamental concepts of vehicle dynamics. This is one of the most popular books on vehicle dynamics, and it discusses the acceleration and braking performance, aerodynamics, vehicle-road interaction, suspension, handling roll-over and the mechanics of the steering system of road vehicles.

Wong [179] wrote the classic reference manual on the dynamics of road and off-road vehicles. This book covers the mechanics of pneumatic tyres, the vehicle-terrain interaction of off-road vehicles, the acceleration, braking, handling and steering characteristics of road and tracked vehicles, vehicle ride characteristics and the principles of air cushion vehicles.

Genta [60] focused on the modelling and simulation of vehicles dynamics. He derived mathematical models for the forces between the road and wheel, aerodynamic, longitudinal dynamics, handling, suspension and road accident reconstruction of road vehicles. However, several parameters have been defined for each model, but no information is given on how these parameters could be estimated.

Kiencke and Nielsen [91] looked at engine and vehicle models necessary for controller design. That includes the thermodynamic engine cycles, engine management systems, engine control systems, driveline control, vehicle modelling, vehicle parameters and states, vehicle control systems and road and driver models.

Pacejka [133] focused specifically on the modelling of tyres. That includes a basic tyre model and all forces acting on different types of tyres.

Dixon [45] discussed all the variables of the modelling of tyres, as well as the aerodynamics and suspension of vehicles, focusing on the vehicle dynamics of racing cars.

Garret [59] gave more detail on the principles of the motor vehicle in general. The principles of the engine is discussed, as well as the transmission such as clutches, gearboxes and torque converters, and detail is given about the mechanics of brakes, steering mechanisms and suspension systems.

The vehicle dynamics literature that appeared in journals within the last few years, were predominantly based on the vehicle dynamics models of two specific vehicles for the National Advanced Driving Simulator (NADS).

Salani and Heydinger [151] presented an evaluation of a complete vehicle dynamics model for a 1997 Jeep Cherokee to be used for the NADS. Vehicle handling and power train dynamics results are compared with experimental field testing. It is shown that the NADS simulation predicts the fundamental mechanics of the vehicle handling responses. The vehicle dynamics aspects focused on is slowly increasing steer, step steer, lane changing and straight line acceleration and braking maneuvers.

Chrstos and Grygier [35] discussed the experimental and field testing of the vehicle dynamics of the 1994 Ford Taurus GL passenger car by the Vehicle Research and Test Center (VRTC) in East Liberty, California. Each of the test maneuvers is described, along with instrumentation setup, control actuation, test location and driver procedures. The testing performed is to provide the data needed to evaluate the NADS software and to make more vehicle dynamics information available to other researchers.

Shiiba and Suda [161] used a multibody analysis technique for a driving simulator of a four wheel vehicle to a six degrees of freedom motion system. A real-time analysis method for vehicle dynamics is proposed to reduce the calculation complexity, and it proved to give realistic results for driving the Ford Taurus [35] on a road.

Romano [150] proposed a modular modelling methodology for the simulation of real-time multi-body vehicle dynamics. Based on recursive techniques a set of reusable components were developed for use in a graphical simulation and modelling environment. The components were then connected to form a real-time multi-model version of a Ford Taurus [35]. It was found that the model is accurate and could perform the calculations much faster than needed for real-time simulations.



## 1.5 Coordinate System Transformations

For the vehicle dynamics modelling, the visual display and the automated driver, one needs to work according to a certain coordinate system convention. In total there are twelve possible conventions. Within the thesis, the coordinate system convention utilized will be the following:

(i) Earth axis or world coordinate system $(X, Y, Z)$:
The origin of this axis system is a fixed, point, usually at sea level, with the positive $X$-axis pointing north, positive $Y$-axis pointing east, and the positive $Z$-axis pointing down.

(ii) Body (chassis) axis system $(x, y, z)$:
The origin of the body axis system (Fig. 1.6) is the centre of gravity of the vehicle, measured when the vehicle is stationary, with the positive $x$-axis pointing forward, the positive $y$-axis pointing to the right of the vehicle, and the positive $z$-axis pointing down relative to the vehicle. The three rotational movements are rotation about the body $x$-axis (roll, $\phi$), rotation

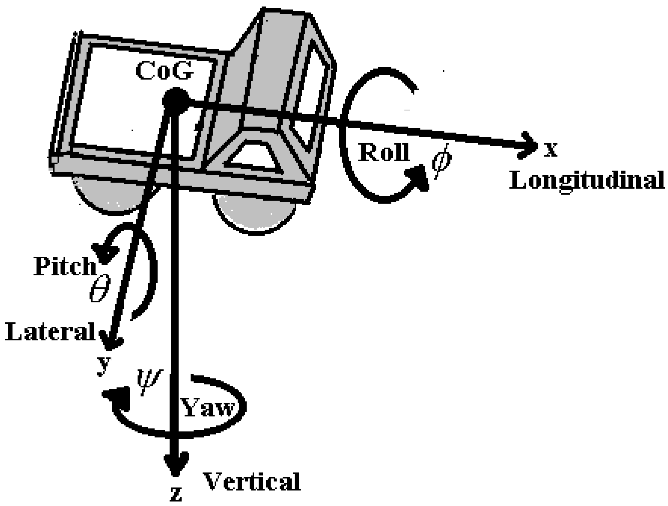


Figure 1.6: Body axis coordinate system.

about the body $y$-axis (pitch, $\theta$) and rotation about the body $z$-axis (yaw, $\psi$). The direction of angular velocities are derived by applying the right hand rule: By using the right hand, if the thumb is pointing at the positive axis, the other four fingers point to the direction of positive rotation about that axis.

To keep track of the position of the vehicle in terms of the earth axis, Euler has defined three angles $\theta$, $\phi$ and $\psi$ to describe the rotation of one axis system in terms of the other. The sequence of rotations is not commutative. Therefore, the Euler angles can be used in 12 different ways [67]. For the purpose of vehicle simulation, we will use the Euler angles sequence which is the standard in flight simulation as accepted by the Society of Automotive Engineers (SAE) [60, 63, 179]:

Assume the vehicle's centre of gravity is at the origin of the world axis. Then the earth axis position $(X, Y, Z)$ can be given as a body axis position by three rotations in this sequence:

(i) Rotate $(X, Y, Z)$ about the $Z$-axis by an angle $\psi$

$$\begin{pmatrix} X_\psi \\ Y_\psi \\ Z_\psi \end{pmatrix} = \begin{pmatrix} \cos\psi & \sin\psi & 0 \\ -\sin\psi & \cos\psi & 0 \\ 0 & 0 & 1 \end{pmatrix} \begin{pmatrix} X \\ Y \\ Z \end{pmatrix} \tag{1.1}$$

(ii) Rotate $(X_\psi, Y_\psi, Z_\psi)$ about the new $Y_\psi$-axis by an angle $\theta$

$$\begin{pmatrix} X_{\theta\psi} \\ Y_{\theta\psi} \\ Z_{\theta\psi} \end{pmatrix} = \begin{pmatrix} \cos\theta & 0 & -\sin\theta \\ 0 & 1 & 0 \\ \sin\theta & 0 & \cos\theta \end{pmatrix} \begin{pmatrix} X_\psi \\ Y_\psi \\ Z_\psi \end{pmatrix} \tag{1.2}$$

(iii) Rotate $(X_{\theta\psi}, Y_{\theta\psi}, Z_{\theta\psi})$ about the new $X_{\theta\psi}$ -axis by an angle $\phi$

$$\begin{pmatrix} x \\ y \\ z \end{pmatrix} = \begin{pmatrix} X_{\phi\theta\psi} \\ Y_{\phi\theta\psi} \\ Z_{\phi\theta\psi} \end{pmatrix} = \begin{pmatrix} 1 & 0 & 0 \\ 0 & \cos\phi & \sin\phi \\ 0 & -\sin\phi & \cos\phi \end{pmatrix} \begin{pmatrix} X_{\theta\psi} \\ Y_{\theta\psi} \\ Z_{\theta\psi} \end{pmatrix} \tag{1.3}$$

By multiplying out, we get:

$$\begin{pmatrix} x \\ y \\ z \end{pmatrix} = \boldsymbol{B} \begin{pmatrix} X \\ Y \\ Z \end{pmatrix} \tag{1.4}$$

where

$$\boldsymbol{B} = \begin{pmatrix} \cos\theta\cos\psi & \cos\theta\sin\psi & -\sin\theta \\ \sin\phi\sin\theta\cos\psi - \cos\phi\sin\psi & \sin\phi\sin\theta\sin\psi + \cos\phi\cos\psi & \sin\phi\cos\theta \\ \cos\phi\sin\theta\cos\psi + \sin\phi\sin\psi & \cos\phi\sin\theta\sin\psi - \sin\phi\cos\psi & \cos\phi\cos\theta \end{pmatrix} \tag{1.5}$$

This matrix is orthogonal and therefore its transpose is equal to its inverse, i.e. $\boldsymbol{B}^{-1} = \boldsymbol{B}^T$ [67]. Since rotation about an axis does not change the direction of that specific axis, we know that $\hat{\boldsymbol{X}}_{\theta\psi} = \hat{\boldsymbol{X}}_{\phi\theta\psi} = \hat{\boldsymbol{x}}$, $\hat{\boldsymbol{Y}}_\psi = \hat{\boldsymbol{Y}}_{\theta\psi}$ and $\hat{\boldsymbol{Z}} = \hat{\boldsymbol{Z}}_\psi$.

## 1.6 Thesis Outline and Major Contributions

Against the backdrop of the comprehensive literature survey on driving simulators and their applications, this thesis endeavours to make five new contributions, as described below:

Firstly, although the design of driving simulators is common practice within the simulation industry, the focus is primarily on the vehicle dynamics modelling of commercial four wheel vehicles. Even with truck driver simulators, the assumption is made that the road surface is fairly smooth. Many of the military armoured vehicles have six or eight wheels, are able to cross trenches of approximately two meters, and can climb steps of as high as one meter. In Chapter 2, a mathematical model is given for simulating the vehicle dynamics of an eight wheel vehicle over rough terrain, taking into account the limitations of real-time driving simulation. A discussion of the model by Janse van Rensburg *et al.* is contained in a paper [88] which is currently under review by the *International Journal of Modern Physics C*.

To prove the validity of a vehicle model, it is necessary to provide a method of testing the model. Proper testing of a driving simulator is not only the verification of standard vehicle dynamics equations. Integration methods and other numerical methods used may also influence the final result. Detail about the vehicle dynamics model used is not always available when developed by a third party. This testing scenario has not yet been discussed within the literature. Chapter 3 describes a "black box" testing method for the verification of a vehicle dynamics model. An article regarding this matter [89] by Janse van Rensburg *et al.* has been submitted to the *International Journal of Modern Physics C* and is currently under review.

Normally, the focus on driving simulators is on the modelling of realistic vehicle dynamics models. However, the design of a realistic simulation environment is of equal importance. A human driver usually steers one vehicle, but the rest of the vehicles used in the simulation should be managed by a computer program. In Chapter 4 an automatic driver model to be used within the simulation environment, is described. The current presentation is based on the published paper [86] by Janse van Rensburg *et al.*. The automatic driver uses the same vehicle dynamics model as the human driver would use. It also uses the vehicle characteristics in such a way to obtain the optimal performance of the vehicle.

An understanding of three-dimensional coordinate system transformations is one of the most important parts of a flight or driving simulator. Although the concept of using Euler angles for coordinate system transformations is nothing new, almost no literature is available of how it can be applied for more complex situations. In Chapter 5, more information is given on how a program language such as C++ could be used to apply more complex coordinate transformations in real-life situations. Results appeared in the published paper by Janse van Rensburg *et al.* [87].

Chapter 6 proposes the use of vocoders for the modelling of engine sound. For a driving simulator which should be an exact replica of a certain vehicle, an accurate sound model is of extreme importance. The most games select between three or more pre-recorded engine sounds, depending on the engine speed. Other methods use linear interpolation between engine sounds for a more accurate model, but are still not ideal. By using vocoders, a technique used for the manipulation of voice, a much higher level of accuracy and realism can be obtained. This essence of this chapter, compiled by Janse van Rensburg *et al.* [85] is currently under review by the *International Journal of Modern Physics C*.

Concluding remarks and recommendations for further research follow in Chapter 7.

# Chapter 2

# Modelling and Simulation of Eight Wheel Vehicle Dynamics

## 2.1 Introduction



Vehicle dynamics modelling is an essential component for the development of a driving simulator. If it is supplied with information on the steering wheel, accelerator, brake and gear position, the current status of the vehicle as well as data of the terrain on which the vehicle is driving, a vehicle dynamics model should be able to predict the position and velocity of the vehicle mathematically.

Most of the existing vehicle dynamics models presented in literature, such as the model developed for the *National Advanced Driving Simulator* [55], focus primarily on the vehicle dynamics modelling necessary for the simulation of automated highway systems. That includes the exact modelling of slowly increasing steer, step steer, lane changing and straight line acceleration and braking maneuvers [35, 151].

These models, however, are not suitable for a driving simulator of an eight wheel military vehicle. An eight wheel vehicle can easily climb a step of $0.5m$ and cross a trench of at least $1.8m$. It can even ascent stairs, and drive with only half of its wheels touching ground [13].

In this chapter, a practical model is given for simulating the vehicle dynamics of an eight wheel vehicle. Although an exact suspension model of an eight wheel vehicle will not be possible [60], a realistic model is presented for predicting the suspension behaviour of the vehicle for off-road driving.

Section 2.2 describes the necessary background information on coordinate system transformations for simulating vehicle dynamics in three dimensions. In section 2.3, a basic eight wheel vehicle model is given for modelling the acceleration, braking and steering properties of a vehicle. Section 2.4 presents a model for simulating the suspension behaviour of an eight wheel vehicle. Section 2.5 describes how the interaction of the vehicle dynamics model with a terrain could be simulated. In section 2.6, a complete model is given for simulating the vehicle dynamics over time. In section 2.7, some experimental results are given and concluding remarks follow in section 2.8.



## 2.2 Coordinate System Transformations

In this thesis, the following coordinate system convention is assumed as discussed in section 1.5.

### 2.2.1 Derivatives of Euler Angles

According to the choice of Euler angles, $\dot{\boldsymbol{\phi}}$ will be in the $\hat{\boldsymbol{x}}$-direction, $\dot{\boldsymbol{\theta}}$ in the $\hat{\boldsymbol{Y}}_{\theta\psi}$-direction and $\dot{\boldsymbol{\psi}}$ in the $\hat{\boldsymbol{Z}}_{\psi}$-direction. Therefore

$$\begin{aligned}
\dot{\boldsymbol{\phi}} &= \dot{\phi}\hat{\boldsymbol{x}} \\
\dot{\boldsymbol{\theta}} &= \begin{pmatrix} 1 & 0 & 0 \\ 0 & \cos\phi & \sin\phi \\ 0 & -\sin\phi & \cos\phi \end{pmatrix} \begin{pmatrix} 0 \\ \dot{\theta} \\ 0 \end{pmatrix} \cdot \begin{pmatrix} \hat{\boldsymbol{x}} \\ \hat{\boldsymbol{y}} \\ \hat{\boldsymbol{z}} \end{pmatrix} \\
&= \dot{\theta}\cos\phi\hat{\boldsymbol{y}} - \dot{\theta}\sin\phi\hat{\boldsymbol{z}} \\
\dot{\boldsymbol{\psi}} &= \begin{pmatrix} 1 & 0 & 0 \\ 0 & \cos\phi & \sin\phi \\ 0 & -\sin\phi & \cos\phi \end{pmatrix} \begin{pmatrix} \cos\theta & 0 & -\sin\theta \\ 0 & 1 & 0 \\ \sin\theta & 0 & \cos\theta \end{pmatrix} \begin{pmatrix} 0 \\ 0 \\ \dot{\psi} \end{pmatrix} \cdot \begin{pmatrix} \hat{\boldsymbol{x}} \\ \hat{\boldsymbol{y}} \\ \hat{\boldsymbol{z}} \end{pmatrix}
\end{aligned}$$

$$= \quad -\dot{\psi}\sin\theta\hat{\boldsymbol{x}} + \dot{\psi}\cos\theta\sin\phi\hat{\boldsymbol{y}} + \dot{\psi}\cos\theta\cos\phi\hat{\boldsymbol{z}}.$$

Let $\boldsymbol{\omega}$ be the total rotational rate vector. Then

$$\begin{aligned}\boldsymbol{\omega} &= \dot{\boldsymbol{\psi}} + \dot{\boldsymbol{\theta}} + \dot{\boldsymbol{\phi}} \\ &= \omega_x\hat{\boldsymbol{x}} + \omega_y\hat{\boldsymbol{y}} + \omega_z\hat{\boldsymbol{z}}\end{aligned}$$

where

$$\begin{aligned}\omega_x &= \dot{\phi} - \dot{\psi}\sin\theta \\ \omega_y &= \dot{\theta}\cos\phi + \dot{\psi}\cos\theta\sin\phi \\ \omega_z &= \dot{\psi}\cos\theta\cos\phi - \dot{\theta}\sin\phi.\end{aligned}$$

This can be rewritten as

$$\begin{aligned}\dot{\phi} &= \omega_x + (\omega_y\sin\phi + \omega_z\cos\phi)\tan\theta \\ \dot{\theta} &= \omega_y\cos\phi - \omega_z\sin\phi \\ \dot{\psi} &= (\omega_y\sin\phi + \omega_z\cos\phi)\sec\theta. \qquad (2.1)\end{aligned}$$

### 2.2.2 Transformation of Position Vectors

#### Transformation from Body Axis to Earth Axis

Suppose the centre of gravity of the vehicle is at the position $(X_{CoG}, Y_{CoG}, Z_{CoG})$. Then, any body axis coordinate $(x, y, z)$ is given in terms of world coordinates $(X, Y, Z)$ by:

$$\begin{pmatrix} X \\ Y \\ Z \end{pmatrix} = \begin{pmatrix} X_{CoG} \\ Y_{CoG} \\ Z_{CoG} \end{pmatrix} + \begin{pmatrix} B_{11} & B_{21} & B_{31} \\ B_{12} & B_{22} & B_{32} \\ B_{13} & B_{23} & B_{33} \end{pmatrix} \begin{pmatrix} x \\ y \\ z \end{pmatrix}.$$

### Transformation from Earth Axis to Body Axis

Recall that $\boldsymbol{B}^{-1} = \boldsymbol{B}^T$. Therefore, by taking the inverse of Eq. (1.5), it can be shown that

$$\begin{pmatrix} x \\ y \\ z \end{pmatrix} = \begin{pmatrix} B_{11} & B_{12} & B_{13} \\ B_{21} & B_{22} & B_{23} \\ B_{31} & B_{32} & B_{33} \end{pmatrix} \begin{pmatrix} X - X_{CoG} \\ Y - Y_{CoG} \\ Z - Z_{CoG} \end{pmatrix}.$$

## 2.2.3 Transformation of Velocity and Acceleration

### Transformation of Velocity

Let $\boldsymbol{V}$ be the absolute velocity of a point $\boldsymbol{r}$ on the vehicle relative to the earth and $\boldsymbol{v}$ the velocity relative of that point to the vehicle. If the vehicle has an angular velocity $\boldsymbol{\omega}$, the following equation holds [54]:

$$\boldsymbol{V} = \boldsymbol{v} + \boldsymbol{\omega} \times \boldsymbol{r}.$$

The velocity of the vehicle is given as the velocity of its centre of gravity, that is where $\boldsymbol{r} = 0$ and therefore $\boldsymbol{V} = \boldsymbol{v}$. In vector format, using the transformation vector $\boldsymbol{B}$, this can written as

$$\begin{pmatrix} V_X \\ V_Y \\ V_Z \end{pmatrix} = \boldsymbol{B}^T \begin{pmatrix} v_x \\ v_y \\ v_z \end{pmatrix} \tag{2.2}$$

### Transformation of Acceleration

The absolute acceleration $\dot{\boldsymbol{V}}$ of a point on the vehicle relative to earth is given by [54, 67]

$$\underbrace{\dot{\boldsymbol{V}}}_{Relative\ to\ Earth} = \underbrace{\dot{\boldsymbol{V}}}_{Relative\ to\ Vehicle} + \boldsymbol{\omega} \times \boldsymbol{V}. \tag{2.3}$$

For the vehicle's centre of gravity, $\boldsymbol{r} = 0$ and therefore $\boldsymbol{V} = \boldsymbol{v}$ and Eq. (2.3) can be written as

$$\dot{\boldsymbol{V}} = \dot{\boldsymbol{v}} + \boldsymbol{\omega} \times \boldsymbol{v} \tag{2.4}$$

where $\dot{\boldsymbol{v}}$ and $\boldsymbol{v}$ are the acceleration and velocity of the point relative to the vehicle and $\boldsymbol{\omega}$ is the angular velocity of the vehicle.

Let $\boldsymbol{\omega} = \omega_x \hat{\boldsymbol{x}} + \omega_y \hat{\boldsymbol{y}} + \omega_z \hat{\boldsymbol{z}}$, $\dot{\boldsymbol{v}} = \dot{v}_x \hat{\boldsymbol{x}} + \dot{v}_y \hat{\boldsymbol{y}} + \dot{v}_z \hat{\boldsymbol{z}}$ and $\boldsymbol{v} = v_x \hat{\boldsymbol{x}} + v_y \hat{\boldsymbol{y}} + v_z \hat{\boldsymbol{z}}$. By multiplying out the cross product, Newton's second law, $\boldsymbol{F} = m\dot{\boldsymbol{V}}$, can be written as [18]

$$\begin{pmatrix} F_x \\ F_y \\ F_z \end{pmatrix} = m \begin{pmatrix} \dot{v}_x + v_z\omega_y - v_y\omega_z \\ \dot{v}_y + v_x\omega_z - v_z\omega_x \\ \dot{v}_z + v_y\omega_x - v_x\omega_y \end{pmatrix}$$

or

$$\begin{pmatrix} \dot{v}_x \\ \dot{v}_y \\ \dot{v}_z \end{pmatrix} = \begin{pmatrix} F_x/m - v_z\omega_y + v_y\omega_z \\ F_y/m - v_x\omega_z + v_z\omega_x \\ F_z/m - v_y\omega_x + v_x\omega_y \end{pmatrix}.$$

To calculate the acceleration of the vehicle relative to the earth, one could transform the forces to the earth axis system and apply Newton's second law relative to the earth

$$\begin{pmatrix} F_X \\ F_Y \\ F_Z \end{pmatrix} = \boldsymbol{B}^T \begin{pmatrix} F_x \\ F_y \\ F_z \end{pmatrix} = m \begin{pmatrix} \dot{V}_X \\ \dot{V}_Y \\ \dot{V}_Z \end{pmatrix},$$

then

$$\begin{pmatrix} \dot{V}_X \\ \dot{V}_Y \\ \dot{V}_Z \end{pmatrix} = \frac{1}{m} \begin{pmatrix} F_X \\ F_Y \\ F_Z \end{pmatrix}.$$

### 2.2.4 Calculation of Angular Acceleration

Let $\boldsymbol{H}$ be the angular momentum of the vehicle. Euler's second law in terms of angular momentum is given by [120]

$$\boldsymbol{H} = \sum_i \left(\boldsymbol{R}_i \times m_i \dot{\boldsymbol{R}}_i\right)$$

where $\boldsymbol{R}_i$ and $m_i$ are the position vector and mass of the $i^{th}$ particle making up the vehicle. If the particle's position is fixed relative to the vehicle, then [18]

$$\dot{\boldsymbol{R}}_i = \boldsymbol{\omega} \times \boldsymbol{R_i}.$$

Taking the integral of $\boldsymbol{H}$ yields

$$\boldsymbol{H} = \int_V \left(\boldsymbol{R} \times \dot{\boldsymbol{R}}\right) dm.$$

If $\boldsymbol{\omega} = \omega_x \hat{\boldsymbol{x}} + \omega_y \hat{\boldsymbol{y}} + \omega_z \hat{\boldsymbol{z}}$ and $\boldsymbol{R} = x\hat{\boldsymbol{x}} + y\hat{\boldsymbol{y}} + z\hat{\boldsymbol{z}}$, then, by calculating the cross product, $\dot{\boldsymbol{R}}$ can be represented by

$$\dot{\boldsymbol{R}} = (\omega_y z - \omega_z y)\,\hat{\boldsymbol{x}} + (\omega_z x - \omega_x z)\,\hat{\boldsymbol{y}} + (\omega_x y - \omega_y x)\,\hat{\boldsymbol{z}}$$

and

$$\begin{aligned} \boldsymbol{R} \times \dot{\boldsymbol{R}} \quad = \quad & \left(\omega_x(y^2+z^2) - \omega_y xy - \omega_z zx\right)\hat{\boldsymbol{x}} \\ & + \left(\omega_y(z^2+x^2) - \omega_z yz - \omega_x xy\right)\hat{\boldsymbol{y}} \\ & + \left(\omega_z(x^2+y^2) - \omega_x zx - \omega_y yz\right)\hat{\boldsymbol{z}}. \end{aligned}$$

Substituting the moments of inertia

$$I_{xx} = \textstyle\int_V (y^2+z^2)\,dm, \quad I_{yy} = \int_V (x^2+z^2)\,dm, \quad I_{zz} = \int_V (x^2+y^2)\,dm$$

and products of inertia [159]

$$I_{xy} = \textstyle\int_V (xy)\,dm, \quad I_{yz} = \int_V (yz)\,dm, \quad I_{zx} = \int_V (zx)\,dm$$

the angular momentum can be written as

$$\begin{aligned}\boldsymbol{H} &= (\omega_x I_{xx} - \omega_y I_{xy} - \omega_z I_{zx})\,\hat{\boldsymbol{x}} \\ &\quad + (\omega_y I_{yy} - \omega_z I_{yz} - \omega_x I_{xy})\,\hat{\boldsymbol{y}} \\ &\quad + (\omega_z I_{zz} - \omega_x I_{zx} - \omega_y I_{yz})\,\hat{\boldsymbol{z}}.\end{aligned}$$

If $\boldsymbol{M}$ is the total external moment acting on the vehicle then

$$\begin{aligned}\boldsymbol{M} &= \dot{\boldsymbol{H}} \\ &= (\dot{\boldsymbol{H}})_r + \boldsymbol{\omega} \times \boldsymbol{H}\end{aligned}$$

where $(\dot{\boldsymbol{H}})_r$ is the rate of change of angular momentum observed from vehicle axis system [18], that is

$$\begin{aligned}(\dot{\boldsymbol{H}})_r &= (\dot{\omega}_x I_{xx} - \dot{\omega}_y I_{xy} - \dot{\omega}_z I_{zx})\,\hat{\boldsymbol{x}} \\ &\quad + (\dot{\omega}_y I_{yy} - \dot{\omega}_z I_{yz} - \dot{\omega}_x I_{xy})\,\hat{\boldsymbol{y}} \\ &\quad + (\dot{\omega}_z I_{zz} - \dot{\omega}_x I_{zx} - \dot{\omega}_y I_{yz})\,\hat{\boldsymbol{z}}\end{aligned}$$

and

$$\begin{aligned}\boldsymbol{H_w} &= \boldsymbol{\omega} \times \boldsymbol{H} \\ &= (\omega_y H_z - \omega_z H_y)\dot{\boldsymbol{x}} + (\omega_z H_x - \omega_x H_z)\dot{\boldsymbol{y}} + (\omega_x H_y - \omega_y H_x)\dot{\boldsymbol{z}} \\ &= H_{\omega x}\hat{\boldsymbol{x}} + H_{\omega y}\hat{\boldsymbol{y}} + H_{\omega z}\hat{\boldsymbol{z}}.\end{aligned}$$

Let $\boldsymbol{M} = M_x\hat{\boldsymbol{x}} + M_y\hat{\boldsymbol{y}} + M_z\hat{\boldsymbol{z}}$. Then

$$\begin{aligned}M_x &= \dot{\omega}_x I_{xx} - \dot{\omega}_y I_{xy} - \dot{\omega}_z I_{zx} + H_{\omega x} \\ M_y &= \dot{\omega}_y I_{yy} - \dot{\omega}_z I_{yz} - \dot{\omega}_x I_{xy} + H_{\omega y} \\ M_z &= \dot{\omega}_z I_{zz} - \dot{\omega}_x I_{zx} - \dot{\omega}_y I_{yz} + H_{\omega z}\end{aligned} \tag{2.5}$$

where the components of $\boldsymbol{H_\omega}$ can be calculated as

$$\begin{aligned}H_{\omega x} &= I_{yz}\left(\omega_z^2 - \omega_y^2\right) + \omega_y\omega_z\left(I_{zz} - I_{yy}\right) + \omega_z\omega_x I_{xy} - \omega_x\omega_y I_{zx} \\ H_{\omega y} &= I_{zx}\left(\omega_x^2 - \omega_z^2\right) + \omega_z\omega_x\left(I_{xx} - I_{zz}\right) + \omega_x\omega_y I_{yz} - \omega_y\omega_z I_{xy} \\ H_{\omega z} &= I_{xy}\left(\omega_y^2 - \omega_x^2\right) + \omega_x\omega_y\left(I_{yy} - I_{xx}\right) + \omega_y\omega_z I_{zx} - \omega_z\omega_x I_{yz}\end{aligned}$$

For simulation purposes, one needs to find the value of $\dot{\boldsymbol{\omega}}$. This can be done using the algebraic mathematical program such as MuPad:

$$\dot{\boldsymbol{\omega}} = \frac{1}{D}\begin{pmatrix} -I_{yy}I_{zz} + I_{yz}^2 & I_zI_{xy} - I_{zx}I_{yz} & I_yI_{zx} - I_{xy}I_{yz} \\ I_zI_{xy} - I_{zx}I_{yz} & -I_{xx}I_{zz} + I_{zx}^2 & I_{xx}I_{yz} - I_{xy}I_{zx} \\ I_{yy}I_{zx} - I_{xy}I_{yz} & I_{xx}I_{yz} - I_{xy}I_{zx} & -I_{xx}I_{yy} + I_{xy}^2 \end{pmatrix}\begin{pmatrix} M_x - H_{\omega x} \\ M_y - H_{\omega y} \\ M_z - H_{\omega z} \end{pmatrix}$$

where

$$D = -I_{xx}I_{yy}I_{zz} - 2I_{xy}I_{yz}I_{zx} + I_{xx}I_{yz}^2 + I_{yy}I_{zx}^2 + I_{zz}I_{xy}^2.$$

For aircraft simulation purposes, these equations are much simpler, since an aircraft is symmetric about the $xz$-plane and therefore $I_{xy} = I_{yz} = 0$ [159, 165]. For a normal vehicle, that will also be the case. However, for an armed vehicle equipped with a turret and a gun, this will only be the case if the turret is stationary in the body $x$-direction.



If a body is symmetrical about two axis planes, the value of $\dot{\boldsymbol{\omega}}$ is given by

$$\begin{pmatrix} \dot{\omega}_x \\ \dot{\omega}_y \\ \dot{\omega}_z \end{pmatrix} = \begin{pmatrix} \frac{1}{I_{xx}} & 0 & 0 \\ 0 & \frac{1}{I_{yy}} & 0 \\ 0 & 0 & \frac{1}{I_{zz}} \end{pmatrix}\begin{pmatrix} M_x - (I_{zz} - I_{yy})\,\omega_y\omega_z \\ M_y - (I_{xx} - I_{zz})\,\omega_z\omega_x \\ M_z - (I_{yy} - I_{xx})\,\omega_x\omega_y. \end{pmatrix}$$

## 2.3 Acceleration, Braking and Turning Properties of a Vehicle

### 2.3.1 Wheel Radius

Three types of tire radii are generally recognized. These are the *unloaded* radius $R_u$, the *loaded* radius $R_L$ and the *effective* radius $R_e$.

(i) The *unloaded* radius is the unloaded tire circumference divided by $2\pi$.

(ii) The *loaded* tire radius depends on the particular load. It is approximately the height of the centre of the tyre above the ground when the vehicle is stationary.

(iii) The *effective* radius is also called the rolling radius and can be measured as the vehicle speed divided by the wheel angular speed. The effective radius can be approximated by [45]

$$R_e = R_u - \frac{1}{3}\left(R_u - R_L\right).$$

### 2.3.2 Forces Acting on a Vehicle

Several forces have an influence on the vehicle speed. This includes the weight of the vehicle, the tractive force of the engine, the applied braking force, the rolling resistance forces and aerodynamic drag forces.

**Weight of the Vehicle ($\boldsymbol{W}$)**

The weight of the vehicle acts in the $Z$-direction. Therefore, if the vehicle has a mass $M$, the weight of the vehicle in terms of body coordinates is given by

$$\begin{pmatrix} W_x \\ W_y \\ W_z \end{pmatrix} = \boldsymbol{B} \begin{pmatrix} 0 \\ 0 \\ Mg \end{pmatrix} = \begin{pmatrix} -Mg\sin\theta \\ Mg\sin\phi\cos\theta \\ Mg\cos\phi\cos\theta \end{pmatrix}.$$

**Tractive Force of the Engine ($F_e$)**

The output torque of the engine is a function of the engine speed and the throttle position.

The torque curve of an engine as a function of the engine speed is a standard specification of any engine. This torque curve is measured at full throttle, that is when the accelerator is pressed at a maximum. It is also measured at standard atmospheric conditions as specified by the SAE, and should be recalculated for different barometric pressures and ambient temperatures.

The engine torque used by various vehicle accessories such as the water pump, air conditioning and power-assisted steering and braking, should also be subtracted to calculate the engine torque $T_e$ available for vehicle dynamics [179].

When the clutch is fully engaged, the engine speed $\eta_e$ can be determined by [179]

$$\eta_e = \frac{v_x \epsilon_0}{R_e\left(1 - i\right)}$$

where $i$ is the slip of the running gear, normally between 2% and 5%, $\epsilon_0$ the overall gear reduction ratio between the output of the clutch or torque converter and wheel axle, and $R_e$ the effective rolling radius of the tyre.

The tractive force of the engine can be determined as [63, 179]

$$F_e = \frac{T_e C_{tr} \epsilon_0 \eta_0}{R_L}$$

where $T_e$ is the engine torque available for vehicle dynamics, $\eta_0$ the overall efficiency of the gearbox and drive axle, normally about 90% and $C_{tr}$ the torque ratio of the torque converter or clutch.

**Braking Force** ($F_b$)

For each surface, a maximum braking force can be determined before the wheels will lock and the vehicle will start sliding. If the braking force is below the limit of tyre-road adhesion, the braking force $F_b$ is [91]

$$F_b = \frac{T_b - \sum I \alpha_{an}}{R_e}$$

where $T_b$ is the applied braking torque, $I$ the rotational inertia connected with the wheel being decelerated and $\alpha_{an}$ the corresponding angular deceleration.

**Rolling Resistance** ($F_r$)

Rolling resistance of tyres is one of the major vehicle resistance forces on level ground [179]. The rolling resistance occurs because of several mechanisms such as energy loss due to the deflection of the tyre, scrubbing in the contact patch, deflection of the road surface and air drag on the inside and outside of the tyre [63].

The rolling resistance force of a vehicle is equal to

$$F_r = f_r W_z$$

where $f_r$ is the rolling resistance coefficient which is a function of the vehicle speed and the type of road surface. Several empirical formulas exist for calculating the rolling resistance coefficient [63, 179].

**Aerodynamic Drag** ($F_a$)

The aerodynamic resistance is mainly generated by the airflow over the exterior of the vehicle body. The aerodynamic drag is characterized by the equation

$$F_a = \frac{1}{2}\rho V^2 C_D A,$$

where $C_D$ is the aerodynamic drag coefficient of the vehicle determined experimentally by a vehicle manufacturer, $A$ the frontal area of the vehicle, $\rho$ the air density and $V$ the vehicle speed relative to the wind speed.

### 2.3.3 A Basic Handling Model

The handling performance of a vehicle refers to the directional behaviour of a vehicle during a turn [179]. The most general method to model a turning vehicle, is the so called bicycle model [60, 63, 179], as shown in Fig. 2.1. The front wheel represents the turning axes, and the rear wheel the non-turning wheels of the vehicle. The position of each wheel is the average position of the axes it represents.

For an eight wheel vehicle, it might be the case that not all the wheels are touching ground. This will not affect the model. All off road-vehicles are equipped with differentials which manage the power flow to each wheel. It will lock up a wheel which turns too fast, and will direct the torque to the other wheels. Several types

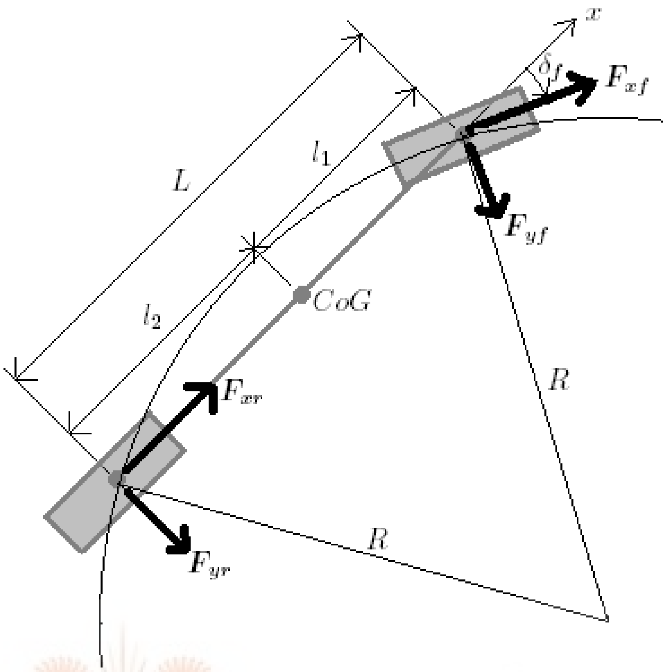


Figure 2.1: Bicycle handling model.

of differentials exist such as solid differentials, locking differentials and limited-slip differentials.

When a vehicle is turning at a moderate or high speed, a centrifugal force develops toward the outside of the circle. This centrifugal force, $F_{cf}$ equals

$$F_{cf} = \frac{W_z}{g}\frac{v_x^2}{R}.$$

To balance that force, the wheels develop a cornering force toward the centre of the turning circle. The forces on the wheels will be proportional to the weight on that wheel. This can be approximated by [179]

$$\begin{aligned} F_{yf} &= \frac{l_2}{l} F_{cf} \\ F_{yr} &= \frac{l_1}{l} F_{cf}. \end{aligned} \tag{2.6}$$

If the vehicle is turning on a slope, the wheels will also develop a force to balance the effect of gravity in the vehicle's $y$-direction. Let the force be given by $F_{fy}$.

In general, this force will be a frictional force in the vehicle $y$-direction equal to $-W_y$, but on a very steep slope, or on snow or loose sand, it will be a frictional force smaller than the weight of the vehicle in the $y$-direction. Therefore, on a slope, Eq (2.6) will be equal to

$$\begin{aligned} F_{yf} &= \frac{l_2}{l}\left(F_{cf} - F_{fy}\right) \\ F_{yr} &= \frac{l_1}{l}\left(F_{cf} - F_{fy}\right). \end{aligned}$$

Because of the tyre forces, there is an angle between the direction in which the wheel is heading and the direction in which the wheel is actually travelling. This is called the side-slip angle [63]. The turning radius will therefore depend not only on the steering geometry, but also on the properties of the tyres. The turning radius can be approximated by [179]

$$R = \frac{L + K_{us}\frac{v_x^2}{g}}{\delta_f}.$$



$K_{us}$ is usually referred to as the understeer coefficient and is expressed in radians. It can be determined experimentally in several ways such as the constant steering angle test, where the vehicle is driven with a fixed steering wheel angle at various forward speeds [179].

If the vehicle is all-wheel drive, and the torque is evenly distributed between the front and rear wheels, the longitudinal wheel forces can be approximated by

$$\begin{aligned} F_{xf} &= \frac{F_e}{2} - \frac{F_b}{2} - f_r\frac{l_2}{l}W_z \\ F_{xr} &= \frac{F_e}{2} - \frac{F_b}{2} - f_r\frac{l_1}{l}W_z. \end{aligned}$$

The equations of motion for the vehicle in the $x$- and $y$-direction and its yaw moment can therefore be described by

$$\begin{aligned} F_x &= F_{xr} + F_{xf}\cos\delta_f - F_{yf}\sin\delta_f - F_a + W_x \\ F_y &= F_{yr} + F_{xf}\sin\delta_f + F_{yf}\cos\delta_f + W_y \\ M_z &= l_1F_{yf}\cos\delta_f - l_2Fyr + l_1F_{xf}\sin\delta_f. \end{aligned} \tag{2.7}$$

## 2.4 Suspension modelling

To model the suspension properties of a vehicle, the best known model is the *Quarter Car Model* [31, 45, 60, 63, 91, 133]. The suspension movement of the vehicle is approximated by considering the suspension on one wheel only. This model has two degrees of freedom.

Another model used is the *walking beam tandem suspension* model [31]. This is a three degree of freedom model which estimates the pitch movement of the vehicle as well.

Several more advanced suspension models exist for modelling the suspension vibrations of road vehicles. These models make the assumption that the tyre deflections are very small, and make use of linearisation techniques according to this assumption.

For an off-road driving simulator, no assumption can be made about small deflections in the tyre and suspension. The aim of the suspension model is not to simulate small vibrations which will in any case be filtered out by the visual system to prevent motion sickness. According to the website that gives detail on all the current defence projects [13] the eight wheel military vehicles have trench crossing abilities of about $1.8m$, and most of them could easily manage to climb a step of $0.5m$ or more. The task is therefore to give an indication of how a vehicle will manage such obstacles and a rough terrain, where not all the wheels are necessary touching the ground at the same time. Although an exact model of a car with more than three wheels is not possible [60], an approximation could still be made of the behaviour of the vehicle.

### 2.4.1 The Quarter Car Model

For the quarter car model, the suspension of a car is modelled by considering the suspension on one wheel only, as shown in Fig. 2.2. The weight of the wheel, axis and suspension components are given by $m_w$, also called the *unsprung mass* of

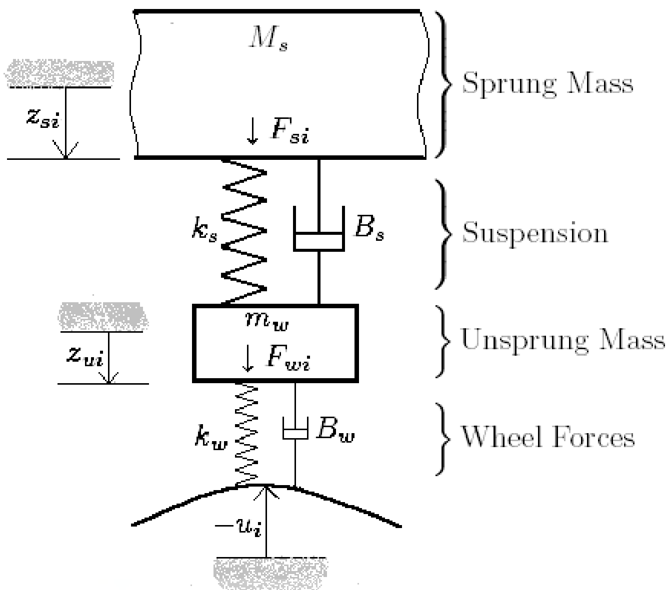


Figure 2.2: Quarter car model.



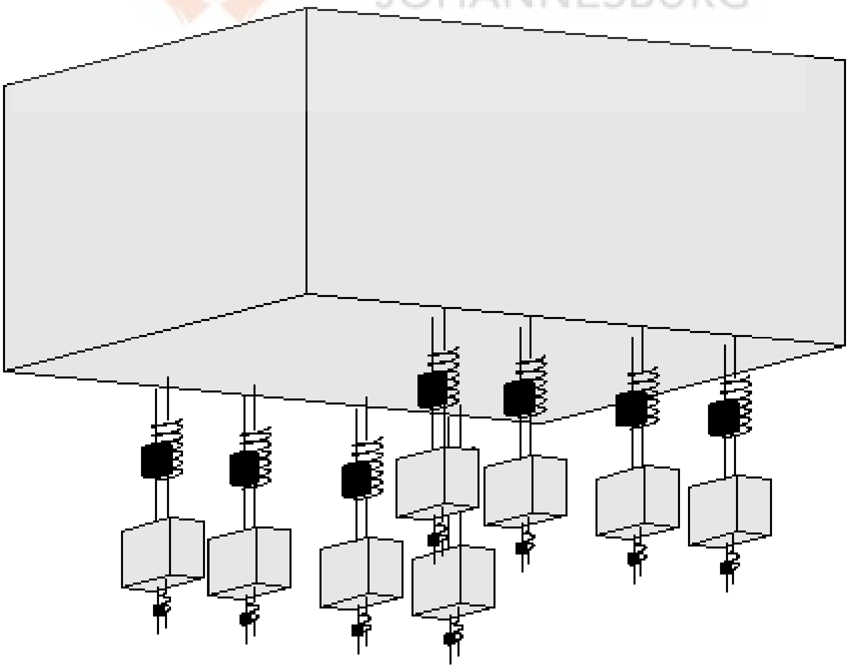

Figure 2.3: Suspension model representation for an eight wheel vehicle.

the system. The rest of the vehicle mass is called the *sprung mass* and is given by $M_s$.

It is approximated that a quarter of the weight of a four-wheel car acts on the suspension, and the weight of the sprung mass is approximated by $W_u$. The wheel is represented by a spring and damper with constants $k_w$ and $B_w$, and the actual suspension with $k_s$ and $B_s$. Both springs are constrained to move vertically [31]. The terrain deflections $u_i$ is modelled as a Gaussian random variable of which parameters are chosen according to the type of terrain.

The force on the $i_{th}$ suspension excluding the weight of the sprung mass on that suspension, $F_{si}$, is given by

$$F_{si} = -k_s(z_{si} - z_{ui}) - B_s(\dot{z}_{si} - \dot{z}_{ui}). \tag{2.8}$$

The force acting on the $i_{th}$ wheel will be

$$\begin{aligned} F_{wi} &= W_{wi} - F_{si} - k_t(z_{ui} - u_i) - B_t(\dot{z}_{ui} - \dot{u}_i) \\ &= W_{wi} + k_s(z_{si} - z_{ui}) + B_s(\dot{z}_{si} - \dot{z}_{ui}) \\ &\quad -k_t(z_{ui} - u_i) - B_t(\dot{z}_{ui} - \dot{u}_i) \end{aligned} \tag{2.9}$$

where $W_{wi}$ is the weight of the $i_{th}$ wheel in the direction of the suspension.

### 2.4.2 Applying the Quarter Car Model to Off-Road Driving

With off-road driving, a wheel does not always touch the ground. Therefore, it should be remembered that there is no extension force possible on a wheel or suspension force in this configuration.

Introduce the step function $u(z)$

$$u(z) = \begin{cases} 1 & \text{if z} \geq 0 \\ 0 & \text{otherwise.} \end{cases}$$

For the case where it can't be guaranteed that all wheels will be touching ground, Eq. (2.8) and (2.9) should be written as

$$\begin{aligned} F_{si} &= -k_s(z_{si} - z_{ui}) - B_s(\dot{z}_{si} - \dot{z}_{ui}) \\ F_{wi} &= m_{wi}g + [k_s(z_{si} - z_{ui}) + B_s(\dot{z}_{si} - \dot{z}_{ui})] \\ & \quad -u(z_{ui} - u_i)\left[k_t(z_{ui} - u_i) + B_t(\dot{z}_{ui} - \dot{u}_i)\right]. \end{aligned} \tag{2.10}$$

The off-road vehicles, that include $4 \times 4$-vehicles and six and eight wheel military vehicles, usually have independent suspensions. This suspension allows each wheel to move vertically without affecting the opposite wheel [63]. Therefore, it should be possible to approximate the suspension properties of an eight wheel vehicle by a quarter car model for each wheel, but with a combined unsprung mass, as shown in Fig. 2.3.

To model each suspension independently, it will be necessary to see each wheel as an independent coordinate system. Therefore, it will be necessary to keep track of each wheel position independently. To calculate the actual movement of the vehicle as a result of the vehicle, the forces and moments generated by each suspension component will be taken into account.

### Determining the Wheel Positions

To determine the wheel positions at every time interval, the vertical speed of each wheel as well as the speed of the wheel caused by its suspension should be taken into account.

If the starting point of the $i^{th}$ wheel's suspension is at $\boldsymbol{r}_{si} = (x_{si}, y_{si}, z_{si})$ relative to the vehicle, its position in earth axis coordinates is given by $\boldsymbol{R}_{si} = B^T\boldsymbol{r}_{si}$. If the earth axis position of the $i^{th}$ wheel is $\boldsymbol{R}_{wi}$, the direction of the wheel speed as a result of suspension movements, in earth axis coordinates, will therefore be $\hat{\boldsymbol{R}}_{si} = \frac{\boldsymbol{R}_{si} - \boldsymbol{R}_{wi}}{|\boldsymbol{R}_{si} - \boldsymbol{R}_{wi}|}$.

Let $\boldsymbol{V}_{CoG}$ denote the vehicle speed in world coordinates and $V_i$ the speed of the $i^{th}$ wheel. The component of the vehicle speed which is perpendicular to the suspension direction vector will affect the wheel speed, that is $\left[\boldsymbol{V}_{CoG} - \left(\boldsymbol{V}_v \cdot \hat{\boldsymbol{R}}_s\right)\hat{\boldsymbol{R}}_s\right]$. The speed of the wheel in the direction of the suspension will be determined by the suspension forces only.

The yaw rotation ($\dot{\psi}$) which is a result of turning the vehicle, will also contribute to the speed of the wheel, but not the pitch and roll rotation ($\dot{\theta}$ and $\dot{\phi}$) caused by the suspension.

The wheel also has a velocity in the same direction as the suspension, that is in the direction $\boldsymbol{R}_{si}$. Using the formula $\boldsymbol{V}_E = \boldsymbol{V}_R + \boldsymbol{\omega} \times \boldsymbol{R}$ and Eq. (1.4) for transforming body axis velocity into earth axis velocity, the velocity of the $i^{th}$ wheel in earth axis coordinates is given by

$$
\begin{aligned}
\begin{pmatrix} V_{wiX} \\ V_{wiY} \\ V_{wiZ} \end{pmatrix} &= \int_t^{t+\Delta t} \frac{\boldsymbol{F}_{wi}}{m_w} dt + \left[\boldsymbol{V}_{CoG} - \left(\boldsymbol{V}_{CoG} \cdot \hat{\boldsymbol{R}}_s\right)\hat{\boldsymbol{R}}_s\right] \\
&\quad + \boldsymbol{B}^T \left[\left.\left( \begin{array}{c} \dot{\phi} - \dot{\psi}\sin\theta \\ \dot{\theta}\cos\phi + \dot{\psi}\cos\theta\sin\phi \\ \dot{\psi}\cos\theta\cos\phi - \dot{\theta}\sin\phi. \end{array} \right) \times \begin{pmatrix} x_i \\ y_i \\ z_i \end{pmatrix} \right]\right|_{\dot{\theta},\dot{\phi}=0} \\
&= \int_t^{t+\Delta t} \frac{\boldsymbol{F}_{wi}}{m_w} dt + \left[\boldsymbol{V}_{CoG} - \left(\boldsymbol{V}_{CoG} \cdot \hat{\boldsymbol{R}}_s\right)\hat{\boldsymbol{R}}_s\right] \\
&\quad + \boldsymbol{B}^T \left[ \dot{\psi} \begin{pmatrix} -\sin\theta \\ \cos\theta\sin\phi \\ \cos\theta\cos\phi \end{pmatrix} \times \begin{pmatrix} x_i \\ y_i \\ z_i \end{pmatrix} \right] \\
&= \int_t^{t+\Delta t} \frac{\boldsymbol{F}_{wi}}{m_w} dt + \left[\boldsymbol{V}_{CoG} - \left(\boldsymbol{V}_{CoG} \cdot \hat{\boldsymbol{R}}_s\right)\hat{\boldsymbol{R}}_s\right] \\
&\quad + \dot{\psi}\boldsymbol{B}^T \begin{pmatrix} z_i\cos\theta\sin\phi - y_i\cos\theta\cos\phi \\ x_i\cos\theta\cos\phi + z_i\sin\theta \\ -y_i\sin\theta - x_i\cos\theta\sin\phi \end{pmatrix}. \qquad (2.11)
\end{aligned}
$$

### The Forces and Moments taking Suspension into Account

Let $\boldsymbol{r}_{si}$ be the position of the $i^{th}$ suspension relative to the vehicle's centre of gravity and $z_{CoG}$ the distance of the centre of gravity to the ground in the vehicle $z$-direction. Make the assumption that all the suspensions are approximately in the same direction, $\hat{\boldsymbol{r}}_s = r_{sx}\hat{\boldsymbol{x}} + r_{sy}\hat{\boldsymbol{y}} + r_{sz}\hat{\boldsymbol{z}}$, which is not necessary perpendicular to the vehicle.

Taking into account the forces generated by the handling model as given by Eq. (2.7), the total moment of the vehicle is given by

$$\begin{aligned} \boldsymbol{M} \;=\; & \underbrace{\sum_{i=1}^{8} (\boldsymbol{r}_{si} \times F_{si})}_{Terrain\ moment} \\ & - \underbrace{(F_{yr} + F_{xf}\sin\delta_f + F_{yf}\cos\delta_f)\, z_{CoG}}_{Acceleration\ pitch\ moment}\hat{\boldsymbol{x}} \\ & + \underbrace{(F_{xr} + F_{xf}\cos\delta_f - F_{yf}\sin\delta_f)\, z_{CoG}}_{Turning\ roll\ moment}\hat{\boldsymbol{y}} \\ & + \underbrace{(l_1 F_{yf}\cos\delta_f - l_2 Fyr + l_1 F_{xf}\sin\delta_f)}_{Turning\ yaw\ moment}\hat{\boldsymbol{z}}. \end{aligned} \tag{2.12}$$



Let

$$F_{sTotal} = \sum_{i=1}^{8} F_{si} \tag{2.13}$$

then the total force acting on the vehicle is given by

$$\begin{aligned} \boldsymbol{F} \;=\; & (F_{xr} + F_{xf}\cos\delta_f - F_{yf}\sin\delta_f - F_a + W_x + r_{sx}F_{sTotal})\,\hat{\boldsymbol{x}} \\ & + (F_{yr} + F_{xf}\sin\delta_f + F_{yf}\cos\delta_f + W_y + r_{sy}F_{sTotal})\,\hat{\boldsymbol{y}} \\ & + (W_{uz} + r_{sz}F_{sTotal})\,\hat{\boldsymbol{z}}. \end{aligned} \tag{2.14}$$

The actual roll centre of the suspension is also somewhat lower than the centre of gravity. However, for a military vehicle, the centre of gravity is very low, so its position could be approximated to be close enough to the centre of gravity of the vehicle.

## 2.5 Vehicle-Terrain Interaction

### 2.5.1 Limitation of Terrain Database Engines

For a driving simulator, the terrain and vehicle dynamic models are separate models. In this way, the vehicle dynamics model can be used on any modelled terrain. The vehicle dynamics model could request information about the terrain, but it has no complete picture of the terrain. Most of the terrain databases support the following requests:

- Terrain feedback queries, where the terrain model supplies the height of the terrain and the normal of the terrain at the requested list of $(x, y)$ positions.
- Ray tracing queries, where, for a given vector with a starting position of $(x_s, y_s, z_s)$, direction $(x_d, y_d, z_d)$ and length $l_v$ the terrain model returns the distance to, and normal of the surface closest to $(x_s, y_s, z_s)$ which crosses that vector. If there is no surface within the distance $l_v$ from the starting point of the vector, no results will be returned.
- Collision information, where a normal vector and collision depth will be given of any object colliding with the collidable volume of the vehicle. The collision volume of the vehicle will be smaller than the actual vehicle, because the vehicle will be able to drive over objects smaller than its maximum step climbing ability

Although the ray tracing facility looks like the ideal solution to the terrain modelling problem, it uses a lot of computational time to execute, as one could expect. The modelled terrain might be several kilometres long and wide. Within a military driving simulator, the ray tracing facility might rather be used for ballistic modelling, where the model needs to know when a bullet had hit another object within the visual database, so that an explosion could be shown by the visual display. Enough computation time must also be given to the database to return collision information. Therefore, the less memory-intensive option needs to be used for the vehicle to enable the driving simulator to perform at real-time.

### 2.5.2 Selection of Terrain Feedback Positions

Since it is too complex to model a complete wheel, the suspension model considers the wheel to be a point mass. The obvious choice of positions to select terrain feedback will be at the centre of each wheel. However, this might not be the ideal position for a military vehicle.

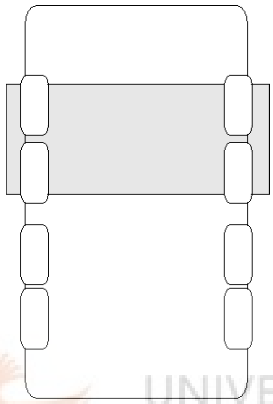



Figure 2.4: An eight wheel vehicle crossing a 1.8m trench.

Several eight-wheel military vehicles can cross a trench of at least 1.8 meters [13]. Fig. 2.4 shows a standard size eight wheel vehicle crossing a 1.8$m$ trench. Looking at the figure, it is clear that at least two of the four front wheels will be touching the ground most of the time. However, at a low speed, the centre of the front wheels will not be touching ground for quite a while. If the centre of each wheel is used, the vehicle will get stuck in the trench according to the suspension model, because the model will not have received the information on time that the front wheels have already reached the end of the trench.

If the vehicle is required to ascend a step, and the terrain model uses only the centre of the wheel positions, a similar problem will occur. The step will only be observed at the moment that the vehicle should already have reached the top of it. This will result in an inaccurate representation of the terrain. Therefore, one needs to know the terrain height at the beginning of the front wheels. This should be taken into account when the terrain height is supplied to the suspension model.

Since the vehicle is not supposed to reverse very often on rough terrain, the ten vertices $\{\boldsymbol{p}_i\}$, as chosen in Fig. 2.5, will give enough information about the terrain.

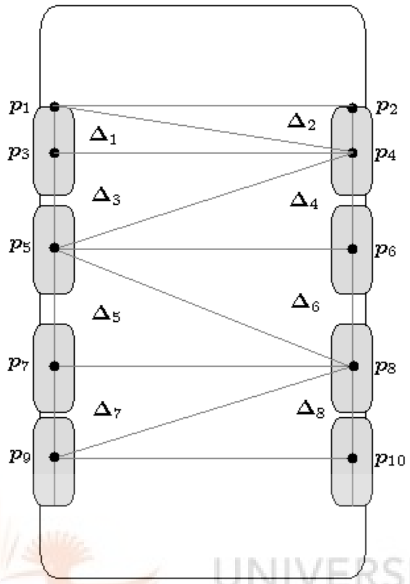


Figure 2.5: Selection of vertices for terrain feedback.

### 2.5.3 Supplying the Terrain Information to the Suspension Model

For the accurate simulation of suspension, an integration frequency of at least 500Hz is recommended [70]. This means terrain information every $2ms$, while the standard terrain database engines cannot always supply terrain information faster than every $30ms$. The suspension model also needs the terrain information in the direction of the wheels, and not vertical downwards. These limitations mean that the vehicle dynamics model should adjust the terrain database information so that it could be used for the simulation of the suspension.

One probability would be to use the normal vector supplied at each $(x, y)$-position where terrain information was requested, and to use that as an estimate of the surface around that position. This solution, however, proved not to be a success. If terrain information is requested on a kerb stone or on the edge of a trench, the terrain will have a very small $z$-component. That means that a calculated terrain height a few centimetres from that point could be infinitely large.

Another option would be to use the cubic spline techniques as used by graphics programs to build a terrain of small surfaces. Using these methods, adjacent surfaces will have the same terrain heights and normals at the $(x_i, y_i)$-positions where the terrain database has supplied the terrain information. However, nothing could be said about the terrain heights and normals on the rest of the line where the two surfaces meet. These methods are ideal for the rendering of a figure where the distance between two given $(x_i, y_i)$-positions are very small. Therefore, using these methods could result in an inaccurate representation of the terrain, especially where the type of normals occur as mentioned above. It will also be memory-intensive and use a lot of computational time.

Therefore, extreme normal vectors could always cause problems, and should be filtered. This could be done by representing the terrain by triangles, using the heights of adjacent $(x, y)$ positions and ignoring the supplied terrain normals. This method has a low computational complexity, and has successfully been implemented in a commercial driving simulator.

A possible method for dividing the terrain into triangles is given in Fig. 2.5. In order to supply the terrain information to the vehicle dynamics model of the driving simulator, several mathematical formulas are needed which are discussed below.

### Equation of a Plane defined by three Vertices

Let the three vertices be $\boldsymbol{r}_i = (x_i, y_i, z_i)|_{i=1}^{3}$. The cross product between $(\boldsymbol{r}_3 - \boldsymbol{r}_1)$ and $(\boldsymbol{r}_2 - \boldsymbol{r}_1)$ is given by

$$\begin{aligned}
(\boldsymbol{r}_3 - \boldsymbol{r}_1) \times (\boldsymbol{r}_2 - \boldsymbol{r}_1) &= a_n\hat{\boldsymbol{x}} + b_n\hat{\boldsymbol{y}} + c_n\hat{\boldsymbol{z}} \\
&= \begin{vmatrix} \hat{\boldsymbol{x}} & \hat{\boldsymbol{y}} & \hat{\boldsymbol{z}} \\ (x_3 - x_1) & (y_3 - y_1) & (z_3 - z_1) \\ (x_2 - x_1) & (y_2 - y_1) & (z_2 - z_1) \end{vmatrix} \\
&= \left[(y_3 - y_1)(z_2 - z_1) - (y_2 - y_1)(z_3 - z_1)\right]\hat{\boldsymbol{x}}
\end{aligned}$$

$$
\begin{aligned}
&+\left[\left(z_3-z_1\right)\left(x_2-x_1\right)-\left(z_2-z_1\right)\left(x_3-x_1\right)\right]\hat{\boldsymbol{y}} \\
&+\left[\left(x_3-x_1\right)\left(y_2-y_1\right)-\left(x_2-x_1\right)\left(y_2-y_1\right)\right]\hat{\boldsymbol{z}}.
\end{aligned}
\tag{2.15}
$$

The normal on the surface will be the normalized cross product, in an upwards direction, that is

$$
\begin{aligned}
\hat{\boldsymbol{r}} &= a\hat{\boldsymbol{x}} + b\hat{\boldsymbol{y}} + c\hat{\boldsymbol{z}} \\
&= -\frac{c_n}{|c_n|}\frac{1}{\sqrt{a_n^2+b_n^2+c_n^2}}\left(a_n\hat{\boldsymbol{x}} + b_n\hat{\boldsymbol{y}} + c_n\hat{\boldsymbol{z}}\right).
\end{aligned}
$$

The equation of the plane defined by these vertices will therefore be

$$ax + by + cz + d = 0$$

where $d$ can be calculated by substituting one of the vertices in the equation of the plane, that is

$$d = -\left(ax_1 + by_1 + cz_1\right). \tag{2.16}$$

### Distance between a Point and a Plane in a given Direction

Let the equation of the plane be given by $ax + by + cz + d = 0$, and let the situation be that the suspension model requests the distance between the point $(x_p, y_p, z_p)$ and the plane in the direction $(x_r, y_r, z_r)$.

Assume the distance is equal to $k$. Then, the point $(x_p + kx_r, y_p + ky_r, z_p + kz_r)$ must lie on the plane, that is

$$a\left(x_p + kx_r\right) + b\left(y_p + ky_r\right) + c\left(z_p + kz_r\right) + d = 0.$$

Rearranging the terms, $k$ can be calculated as

$$k = -\frac{ax_p + by_p + cz_p + d}{ax_r + by_r + cz_r}. \tag{2.17}$$

### Calculating the Wheel Forces on Rough Terrain

As mentioned before, if the centre of a wheel does not touch the ground, it does not mean that the wheel is not touching ground. This scenario is illustrated in Fig. 2.6.

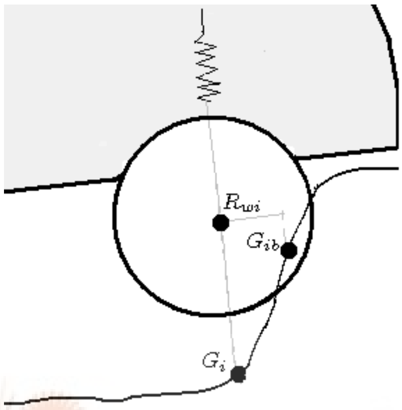


Figure 2.6: Vehicle crossing a trench.

In such a case, one still needs to estimate the wheel force acting in the direction of the suspension, to prevent the vehicle from falling into a trench while its wheels are already touching ground on the other side of the trench.

Let the starting position of the $i^{th}$ suspension be at $\boldsymbol{r}_{si} = (x_{si}, y_{si}, z_{si})$ relative to the vehicle, then its position in world coordinates will be given by $\boldsymbol{R}_{si} = \boldsymbol{B}^T \boldsymbol{r}_{si}$. If the position of the $i^{th}$ wheel is at $\boldsymbol{R}_{wi}$, the suspension is in the direction

$$\hat{\boldsymbol{R}}_i = \frac{\boldsymbol{R}_{wi} - \boldsymbol{R}_{si}}{|\boldsymbol{R}_{wi} - \boldsymbol{R}_{si}|}$$

and the length of the $i^{th}$ suspension can be calculated as

$$z_{si} - z_{ui} = |\boldsymbol{R}_{wi} - \boldsymbol{R}_{si}| - s_{length} \tag{2.18}$$

where $s_{length}$ is the normal length of the suspension. Let $k_i$ denote the distance from $\boldsymbol{R}_{wi}$ to the ground in the direction $\hat{\boldsymbol{R}}_i$, as calculated using Eq. (2.17). Then the world coordinate of that point is given by $\boldsymbol{G}_i = \boldsymbol{R}_{wi} + k_i \hat{\boldsymbol{R}}_i$.

To change the problem to a two-dimensional problem, one needs to find the world coordinate of another vertex on the ground in the wheel plane. For instance, take the point $\boldsymbol{R}_{wib} = \boldsymbol{R}_{wi} + \boldsymbol{B}^T(0,0,0.1)^T$, calculate the distance to the ground in the direction $\hat{\boldsymbol{R}}_i$, and determine the world coordinates $G_{ib}$ of that point as for $\boldsymbol{G}_i$. This problem can then be simplified as shown in Fig. 2.7.

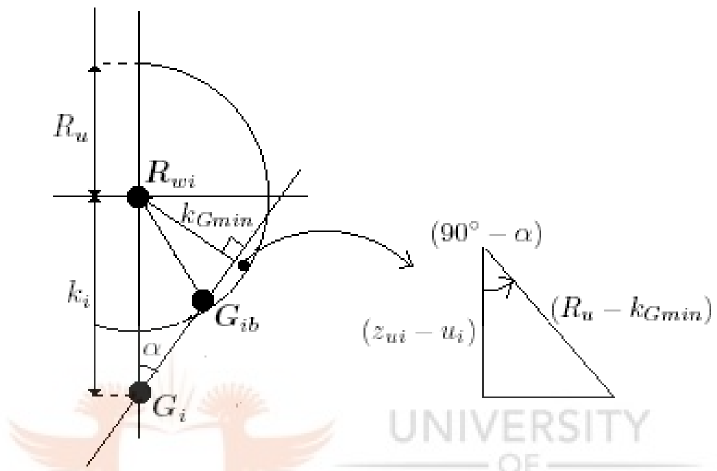




Figure 2.7: The 2D representation of Fig. 2.6 rotated so that $G_i$ lies on the $y$-axis.

The angle $\alpha$ can be determined using the cosine rule:

$$\alpha = \arccos\left(\frac{|\boldsymbol{R}_{wi} - G_i|^2 + |\boldsymbol{G}_{ib} - G_i|^2 - |\boldsymbol{R}_{wi} - G_{ib}|^2}{2\,|\boldsymbol{R}_{wi} - G_i|\,|\boldsymbol{G}_{ib} - G_i|}\right). \tag{2.19}$$

The closest point of contact will be the perpendicular distance between $\boldsymbol{R}_{wi}$ and the line $l_{Gi}$, that is

$$k_{Gmin} = k_i \sin\alpha,$$

which will result in a compression of the wheel of $(R_u - k_{Gmin})$. Since it is assumed that the wheel force will act in the same direction as the suspension, this compression will give the same force as if one estimates $z_{ui} - u_i$ by

$$z_{ui} - u_i = (R_u - k_{Gmin})\sin\alpha. \tag{2.20}$$

### 2.5.4 Adjusting the Terrain Model for Step Climbing

Most military vehicles can climb a step of at least $0.5m$. A wheel climbing a step, will almost "drive" up the step while pressing against it. The given suspension model will, however not be able to simulate the exact movement of the wheel. By filtering the terrain effectively, this problem could be overcome.

A step can be defined as a change in height of a vertex $\boldsymbol{p}_i$ of more than $l_{stepMin}$ and less than $l_{stepMax}$, the maximum step climbing ability of the vehicle.

For a left wheel, the vertices are defined by $\boldsymbol{p}_{2k-1}$, $\boldsymbol{p}_{2k+1}$ and $\boldsymbol{p}_{2n}$. The direction of the terrain points is

$$\hat{\boldsymbol{p}}_{left} = \frac{\boldsymbol{p}_2 - \boldsymbol{p}_1}{|\boldsymbol{p}_2 - \boldsymbol{p}_1|}.$$

If the vehicle is driving forward, and $\boldsymbol{p}_1$ detects a step (see Fig. 2.5), that position should be kept in a list $\boldsymbol{p}^i_{stepLeft}\big|_i$ until the last left vertex, $\boldsymbol{p}_9$, is past that point, that is until

$$\left(\boldsymbol{p}^i_{stepLeft} - \boldsymbol{p}_1\right) \cdot \hat{\boldsymbol{p}}_{left} > (\boldsymbol{p}_9 - \boldsymbol{p}_1) \cdot \hat{\boldsymbol{p}}_{left} \tag{2.21}$$

For the calculation of a terrain distance within $\Delta_{2k+1}$, $\boldsymbol{p}_{2k+1}$ should be replaced by $\boldsymbol{p}_{stepLeft}$ if

$$(\boldsymbol{p}_{2k+1} - \boldsymbol{p}_{\mathbf{1}}) \cdot \hat{\boldsymbol{p}}_{left} \leq (\boldsymbol{p}_{stepLeft} - \boldsymbol{p}_{\mathbf{1}}) \cdot \hat{\boldsymbol{p}}_{left} \leq (\boldsymbol{p}_{2k+3} - \boldsymbol{p}_{\mathbf{1}}) \cdot \hat{\boldsymbol{p}}_{left} \tag{2.22}$$

In that way, the vehicle would be able to "ride" up the step realistically, although the exact vehicle dynamics of the step climbing has not been modelled.

Similar conditions hold for detecting a step on the right hand side and if the vehicle is moving backwards.

## 2.6 Implementation of the Suspension Model

To implement the suspension model, one needs to simulate the vehicle dynamics model over time. A sequence of calculations is necessary every time interval to keep track of the position and rotation of the vehicle and all the wheels. The variables needed is given in Table 2.1 and Table 2.2 and the control sequence for the implementation is given below.

### 2.6.1 Starting Conditions

To start the vehicle simulation the starting $(x, y)$-position and the direction of the vehicle $\psi$ should be known.

To determine the exact orientation of the vehicle, estimate its orientation by a minimization method such as the least squares method, and then put it a meter higher so that it can "drop" down and follow the control sequence. Once the difference of pitch and roll orientation between two time cycles become infinitely small, one can assume that the vehicle has stabilized. Assume the vehicle is stationary, that is there are no forces in the $x$ and $y$-directions, no yaw moment, no extension or compression of the suspension and zero velocity and acceleration.



### 2.6.2 Control Sequence

In the previous sections, all the necessary building blocks were given for the modelling of an eight wheel vehicle. However, to simulate the vehicle dynamics, every variable must be updated continuously after each time interval. This needs to be done in a logical sequence, and this sequence is described below.

(i) Determine the following world coordinates:

  (a) The new rotation matrix $\boldsymbol{B}$.
  (b) Positions where terrain heights will be requested: $\boldsymbol{R}_{gj} = \boldsymbol{R}_{CoG} + \boldsymbol{B}^T \boldsymbol{r}_{gj}$.
  (c) Suspension starting positions: $\boldsymbol{R}_{si} = \boldsymbol{R}_{CoG} + \boldsymbol{B}^T \boldsymbol{r}_{si}$.
  (d) The direction vector of the suspension: $\hat{\boldsymbol{R}}_s = \frac{\boldsymbol{R}_{w1} - \boldsymbol{R}_{s1}}{|\boldsymbol{R}_{w1} - \boldsymbol{R}_{s1}|}$.

(ii) Suspension forces:

  (a) Use Eq. (2.18) to determine the distance $z_{si} - z_{ui}$.

(b) Use the current and previous values of $z_{si} - z_{ui}$ to estimate $\dot{z}_{si} - \dot{z}_{ui}$.
(c) Determine the suspension force $F_{si}$ in the direction $\hat{\boldsymbol{R}}_s$ using Eq. (2.8).

(iii) Wheel suspension forces:

(a) Request the terrain height at each $\boldsymbol{R}_{gi}$ to obtain $\boldsymbol{p}_i$ .
(b) Check if a step occurs.
(c) Use Eq. (2.21) and Eq. (2.22) to analyse the existing steps and to replace certain vertices $\boldsymbol{p}_k$ by step values if necessary.
(d) For each wheel, determine the equation of the plane $a_i x + b_i y + c_i z + d = 0$ defined by the vertices of $\Delta_i$, as described in Eq. (2.15) to (2.16).
(e) Use Eq. (2.19) to (2.20) to determine the distance $z_{ui} - u_i$.
(f) Use the current and previous values of $z_{ui} - u_i$ to estimate $\dot{z}_{ui} - \dot{u}_i$.
(g) Determine the wheel force $F_{wi}$ in the direction $\hat{\boldsymbol{R}}_s$ using Eq. (2.10).

(iv) Total force and moment:

(a) Determine the total force acting on the vehicle using Eq. (2.14).
(b) Calculate the total momentum acting on the vehicle using Eq. (2.12).

(v) Orientation of the vehicle

(a) Determine the angular acceleration $\dot{\boldsymbol{\omega}}$ of the vehicle as given by Eq. (2.5).
(b) Integrate the angular acceleration $\dot{\boldsymbol{\omega}}$ to obtain the angular velocity $\boldsymbol{\omega}$.
(c) Determine the derivatives of the Euler angles $\dot{\boldsymbol{\Omega}}$ using Eq. (2.1).
(d) Integrate the derivatives of the Euler angles to obtain the new orientation of the vehicle $\boldsymbol{\Omega} = (\psi, \theta, \phi)$.

(vi) Position and velocity of the vehicle

(a) Convert the total force acting on the vehicle to earth axis coordinates to obtain $F_X$, $F_Y$ and $F_Z$, and divide by $m$ to obtain the acceleration of the vehicle $\dot{\boldsymbol{V}} = (\dot{V}_X, \dot{V}_Y, \dot{V}_Z)$.
(b) Integrate the acceleration of the vehicle $\dot{\boldsymbol{V}} = (\dot{V}_X, \dot{V}_Y, \dot{V}_Z)$ to determine the new vehicle speed $\boldsymbol{V} = (V_X, V_Y, V_Z)$. Transform the vehicle speed to body axis coordinates to determine the vehicle speed relative to the vehicle $\boldsymbol{v}_{CoG} = (v_x, v_y, v_z)$ (see Eq. (2.2)).
(c) Integrate the velocity of the vehicle $(V_X, V_Y, V_Z)$ to obtain the new vehicle position $\boldsymbol{R}_{CoG} = (X, Y, Z)$.

(vii) Position and velocity of each wheel.

(a) Determine the velocity of each wheel (see Eq. (2.11)).

(b) Integrate the wheel velocities to determine the new wheel positions.

(viii) Set $t = t + \Delta t$ and start again at (i).

Table 2.1: Static vehicle information for a complete vehicle dynamics and suspension simulation. In general, $i = 1, \ldots, 8$ and $j, k, l = 1, \ldots, 10$.

| **Category** | **Variable** | **Description** |
|---|---|---|
| Suspension Constants | $k_w$ | Wheel spring constant |
| | $B_w$ | Wheel damping coefficient |
| | $k_s$ | Suspension spring constant |
| | $B_s$ | Suspension damping coefficient |
| Suspension Dimensions | $s_{length}$ | Normal length of the suspension |
| | $w_{length}$ | Length of wheel tube |
| | $R_u$ | The unloaded radius of the wheel |
| Vehicle Dimensions | $\boldsymbol{r}_{si} = (x_{si}, y_{si}, 0)$ | Suspension starting positions relative to the vehicle's centre of gravity |
| | $l_1 = \frac{1}{2}(x_{s1} + x_{s3})$ | Average position of the front axes |
| | $l_2 = \frac{1}{2}(x_{s5} + x_{s7})$ | Average position of the rear axes |
| Mass | $M_{vehicle}$ | Mass of the vehicle |
| | $m_w$ | Mass of a wheel and its suspension components |
| | $M_s = M_{vehicle} - 8m_w$ | Sprung mass of the vehicle |
| Inertia components | $I_{xx}, I_{yy}, I_{zz}$ | The moments of inertia of the vehicle |
| | $I_{xy}, I_{xz}, I_{yz}$ | The products of inertia of the vehicle |

Table 2.1 – continued from previous page.

| Category | Variable | Description |
|---|---|---|
| Terrain constants | $\boldsymbol{r}_{gi} = (x_{gi}, y_{gi}, z_{gi})$ | The positions relative to the vehicle's CoG to ask for terrain feedback. These positions form the vertices of the terrain feedback triangles. |
| | $\boldsymbol{\Delta}_i = (\boldsymbol{p}_j, \boldsymbol{p}_k, \boldsymbol{p}_l)$ | The vertices that will be used to determine the equation of the plane at each wheel |
| Direction vectors | $\hat{\boldsymbol{r}}_s$ | The direction vector of the suspension in vehicle coordinates |
| Simulation constants | $\Delta t$ | Simulation time interval |
| Step constants | $l_{stepMin}$ | The minimum change in terrain height that will be considered as a step |
| | $l_{stepMax}$ | The maximum step climbing ability of the vehicle |

Table 2.2: The variables needed for a complete vehicle dynamics and suspension simulation. In general, $i = 1, \ldots, 8$ and $j = 1, \ldots, 10$.

| Category | Variable | Description |
|---|---|---|
| Forces | $\boldsymbol{F}_{si}$ | Resultant force of each suspension |
| | $\boldsymbol{F}_{wi}$ | Resultant force acting on each wheel |
| Suspension | $z_{si} - z_{ui}$ | The compression or extention of each suspension |
| | $z_{ui} - u_i$ | The compression of each wheel |
| | $\dot{z}_{si} - \dot{z}_{ui}$ | The rate of compression of each suspension |

Table 2.2 – continued from previous page.

| Category | Variable | Description |
|---|---|---|
| | $\dot{z}_{ui} - \dot{u}_i$ | The rate of compression of each wheel |
| Simulation constants | $\Delta t$ | Simulation time interval |
| | $\hat{\boldsymbol{R}}_{si} = (R_{siX}, R_{siY}, R_{siZ})$ | The direction vector of the $i^{th}$ suspension in world coordinates |
| Direction vectors | $\hat{\boldsymbol{r}}_{si} = (r_{six}, r_{siy}, r_{siz})$ | The direction vector of the $i^{th}$ suspension in vehicle coordinates |
| Position vectors | $\boldsymbol{R}_v = (X, Y, Z)$ | The position of the vehicle's centre of gravity in world coordinates |
| | $\boldsymbol{R}_{wi} = (X_{wi}, Y_{wi}, Z_{wi})$ | The world coordinates of each wheel |
| | $\boldsymbol{R}_{si} = (X_{si}, Y_{si}, Z_{si})$ | Suspension starting positions in world coordinates |
| | $\boldsymbol{R}_{gi} = (X_{gi}, Y_{gi}, Z_{gi})$ | The terrain positions in world coordinates where terrain heights will be needed. |
| Velocity | $\boldsymbol{V}_{CoG} = (V_X, V_Y, V_Z)$ | The velocity of the vehicle in world coordinates. |
| | $\boldsymbol{v}_{CoG} = (v_x, v_y, v_z)$ | The velocity of the vehicle in vehicle coordinates. |
| | $\boldsymbol{V}_{wi} = (V_{wix}, V_{wiy}, V_{wiz})$ | The velocity of the $i^{th}$ wheel in world coordinates. |
| Rotation | $\boldsymbol{\omega} = \{\omega_x, \omega_y, \omega_z\}$ | Angular velocity |
| | $\dot{\boldsymbol{\omega}} = \{\dot{\omega}_x, \dot{\omega}_y, \dot{\omega}_z\}$ | Angular acceleration |
| | $\boldsymbol{\Omega} = (\psi, \theta, \phi)$ | Euler Angles |
| | $\dot{\boldsymbol{\Omega}} = \left(\dot{\psi}, \dot{\theta}, \dot{\phi}\right)$ | Derivatives of Euler Angles |
| | $\boldsymbol{B}$ | The World-to-Body-Coordinates rotation matrix |

## 2.7 Experimental Results

To illustrate the vehicle dynamics model, the algorithm for this model has been implemented in Matlab. Since eight wheel vehicles are mostly military vehicles, no exact vehicle data could be obtained. The estimated values are given in Table 2.3. Fig. 2.8 gives a verification of the result. The vehicle and wheel positions are shown when the vehicle was dropped from a height of $4.3m$.

To illustrate the suspension model, a terrain was modelled where the vehicle was required to climb a $0.5m$ step. Due to the complexity of the simulation, a graphical representation of the simulation parameters was not deemed to be suitable. For that reason, a separate MATLAB program was written to draw a simple picture of a terrain and an eight wheel vehicle, where the hull and wheels can be positioned separately.

Fig. 2.9 illustrates by means of 28 pictures (to be viewed from left to right and top to bottom) the phases of an eight wheel vehicle climbing the step. The time difference between two consecutive frames is $0.1s$. In this figure it can be seen that the wheels can flatten themselves up to the rim, as is the case with real eight wheel vehicles. The wheels and suspension are extremely flexible. However, while driving at a low speed, a person in the vehicle itself might not even realise that he is climbing such a high step.

This model therefore succeeds in simulating the vehicle dynamics modelling of an eight wheel vehicle in extreme off-road conditions. However, more can still be done about several numerical analysis aspects of the problem. As regards the given results, a first order Euler method was used for the integration, but the model tends to become unstable after the simulation is run for some time. For that reason, the proper implementation of numerical ODE solvers such as the Runge Kutta methods for stiff differential equations need to be considered in future applications. The possibility of using predictor-corrector methods for running two methods in parallel could also be considered.

Table 2.3: The values used for the results shown in Fig. 2.8 and Fig. 2.9.

| Variable | Value |
|---|---|
| $k_w$ | 100 000 $N/m$ |
| $B_w$ | 15 000 $Ns/m$ |
| $k_s$ | 150 000 $N/m$ |
| $B_s$ | 40 000 $Ns/m$ |
| $s_{length}$ | 1.3 $m$ |
| $R_u$ | 0.5 $m$ |
| $M_{vehicle}$ | 12000 $kg$ |
| $m_w$ | 200 $kg$ |
| $\Delta t$ | 0.001 |



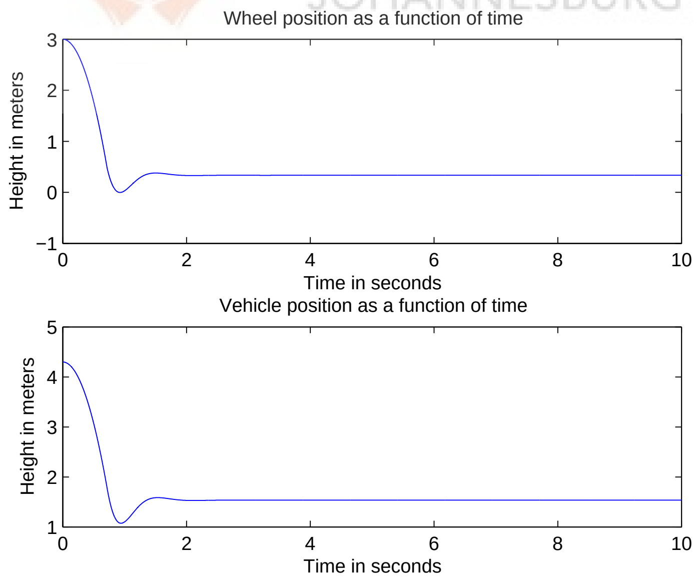


Figure 2.8: Wheel and suspension dynamics when vehicle is dropped.

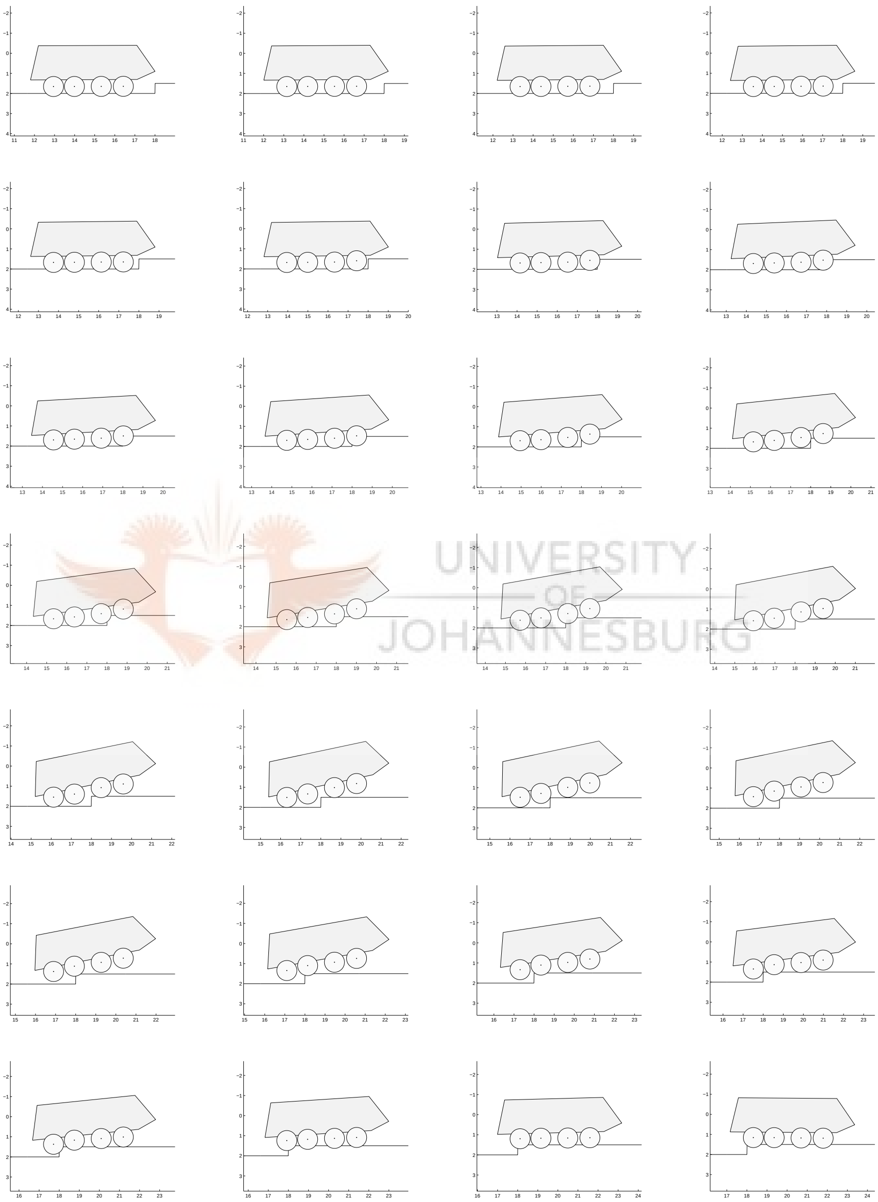



Figure 2.9: An eight wheel vehicle climbing a 0.5$m$ step. (Displacement of the floor and step is merely an artefact of the very basic interface.)

## 2.8 Conclusion

In this chapter, an eight wheel vehicle dynamics model was described for use in an off road driving simulator. An overview was given of the coordinate transformations and transformation of speed, linear and angular velocity and acceleration between two coordinate systems in three dimensions. The basic vehicle dynamics modelling components such as acceleration, braking and turning properties of the vehicle are explained. A suspension model for eight wheel vehicles is suggested together with a terrain model for addressing extreme terrain conditions such as trenches and steps. A control sequence is given to show how all the models could be integrated for a real-time simulation, where all parameters change after each time interval. The experimental results illustrated the model's ability to realistically simulate the climbing of a 0.5m step. Further results need to focus on the incorporation of proper numerical analysis techniques for ensuring stability and a higher level of accuracy within the model.

# Chapter 3

# Simulating a Test Environment for Vehicle Dynamics Models

## 3.1 Introduction



Most of the driving simulators are developed for the training of people. Within the military environment in particular, a driving simulator should correctly imitate the surroundings. It is of no use to drill into someone a specific procedure for a certain route if the latter does not correspond with reality. The consequence may be fatal.

To prove the validity of a vehicle model, it is necessary to provide a method of testing the model. Proper testing of a driving simulator is not only the verification of standard vehicle dynamics equations. Integration methods and other numerical methods used may also influence the final result. Detail about the vehicle dynamics model used is not always available when developed by a third party. This testing scenario has not yet been discussed within the literature.

This chapter describes a “black box” testing method for verification of the vehicle dynamics model. The general driving simulator setup is described in section 1.2. Section 3.2 discusses the necessary tests to be done on a vehicle model. Section 3.3 shows how the simulator setup needs to be changed to do the tests on the vehicle dynamics model. In section 3.4, some experimental results are discussed. Concluding remarks follows in section 3.5.

## 3.2 Typical Vehicle Dynamics Tests

The basic tests for testing a vehicle dynamics model are acceleration, braking and turning or handling tests. For an off road model, obstacle tests could also be done. All tests should be done according to the environmental conditions as defined by the SAE (Society of Automotive Engineers). The conditions are hard road, a temperature of $25^oC$ and an engine air inlet pressure of about $100kPa$ [179].



### 3.2.1 Acceleration

The graphs of speed and acceleration as a function of time is obtained by accelerating from standstill to maximum acceleration in the shortest time possible. Thus it is required that gear changing must occur at optimal time instants and as swiftly as possible.

The tractive force of the engine available at the wheels can be determined as [63, 179]

$$F_e = \frac{T_e C_{tr} \epsilon_0 \eta_0}{R_L}$$

where $T_e$ is the engine torque available for vehicle dynamics, $\eta_0$ the overall efficiency of the gearbox and drive axle, and $C_{tr}$ the torque ratio of the torque converter or clutch. The acceleration of the vehicle is calculated by taking into account the tractive force of the engine, aerodynamic drag, gravity and rolling resistance.

### 3.2.2 Braking

For a braking test, the vehicle will first accelerate to maximum speed and thereafter maximum braking power will be applied. The distance and the speed of the vehicle will then be recorded as a function of time.

The braking force available at the wheels is equal to

$$F_b = \frac{T_b - T_i}{R}$$

where $T_b$ is the applied braking torque, $T_i$ the torque absorbed by the wheel being decelerated and $R$ is the radius of the tyre.

For braking of heavy vehicles, two types of braking are involved, namely normal braking and so called engine braking. Engine braking applied to a diesel engine causes the engine to absorb energy rather than to supply energy to the wheels. The engine brakes can be activated by a switch on the dash. The brake will then be activated once the clutch is engaged and the throttle is closed [9].



For normal braking, a braking force is applied to the wheels to slow down the vehicle. If the force applied is more than the value of the static friction on a road surface, the tyres will lock and the vehicle will start sliding. ABS braking (Antilock Braking System) prevents the tyres from locking. A sensor monitors the angular speed of the tyres and the ABS controls the braking force applied to the tyres. For this chapter ABS is not considered.

### 3.2.3 Turning

When a vehicle is turning at a moderate or high speed, a centrifugal force develops toward the outside of the circle. This centrifugal force, $F_{cf}$ equals

$$F_{cf} = \frac{W}{g}\frac{v^2}{R}$$

where $W$ is the weight of the vehicle, $g$ the gravitational constant, $v$ the velocity of the vehicle and $R$ the radius of the curve.

To balance the centrifugal force, the wheels develop a cornering force toward the centre of the turning circle. The forces on the wheels will be proportional to the weight on that wheel. Because of the tyre forces, there is an angle between the direction in which the wheel is heading and the direction in which the wheel is actually travelling. This is called the side-slip angle [63]. These two forces generate a yaw moment about the centre of the wheel. The turning radius will therefore depend not only on the steering geometry, but also on the properties of the tyres and the vehicle speed. Several tests can be done to determine the properties of the tyres.

### 3.2.4 Obstacle Crossing

Military vehicles and commercial 4WD vehicles are designed for off-road driving. Most military vehicles can cross trenches of at least 0.8m, climb steps of $0.5m$ or more, drive up a hill of as much as 60% slope, and can handle a side slope of 35% [13]. It is a tall order for a driving simulator to handle such characteristics, and most of the driving simulators use short-cuts for simulating the off-road behavior. It is therefore necessary to test if the specifications are simulated correctly under all conditions. For example, a vehicle shouldn't be able to cross a longer trench at a higher velocity.

### 3.2.5 Swimming Tests for Amphibious Vehicles

Many of the armoured vehicles also have amphibious abilities. The LAV III, developed in Switzerland has a maximum speed of $10km/h$ in water [13]. In the water, the vehicle should have the correct vehicle dynamics response to turning, acceleration, braking and collisions. All these properties should also be checked against specifications thereof.

## 3.3 Modification of Subsystems for Testing Purposes

To test a vehicle dynamics model with a "black box" testing method, one needs to utilize the same interfaces that exists for interfacing with all the subsystems. However, in order to develop a standalone test program, one needs to use different subsystems to simulate all the necessary inputs.

Fig. 3.1 shows how the simulator setup (see section 1.2) needs to be modified for the design of a test program. The vehicle dynamics model remains the core of the simulator. The driver is replaced by an automatic driver, and the main test program gives the instructions to the automatic driver regarding what test to perform. The automatic driver uses the vehicle dynamics model's output directly and the models for the visual display, sound and motion are omitted. The output supplied to these models is now written to an output file. The scenario generator and terrain database are replaced by the terrain simulation model that performs both these functions.

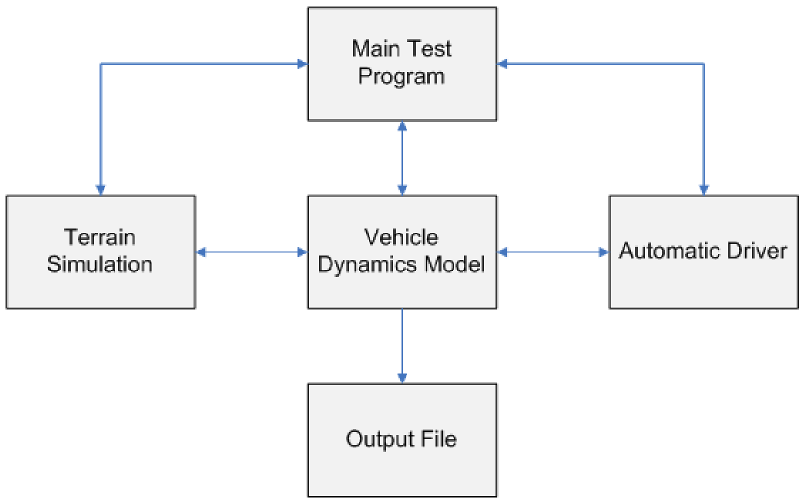


Figure 3.1: Modifications of the driving simulator setup for testing.

### 3.3.1 Main Test Program

In a normal driving simulator, the driver will drive according to instructions of an instructor or he will follow a route that he has planned beforehand. For a testing simulator, the driver needs to perform several tests on the vehicle. For each test, the driver needs to drive on a certain route or terrain, and the necessary data for that test must be recorded. The main test program interacts with the other subsystems, schedules them and issues the instructions to them for each test scenario. The automatic driver notifies the main program if a certain test is completed after which the main program will then request another test to be executed.

### 3.3.2 Terrain Interface

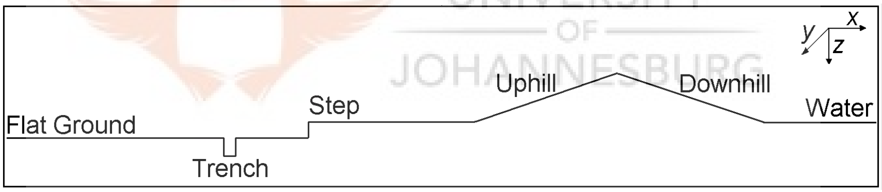


Figure 3.2: Terrain model developed for testing.

For proper testing of a vehicle dynamics model, one needs an appropriate terrain that includes all the surface profiles needed for proper testing such as flat road, slopes, obstacles and water. Although it might be possible to render a testing terrain, it is unnecessary. Since the collision detecting capability is not needed in general, an independent program could rather be written to simulate the terrain model. That will give one the possibility to change the slope of a road or the road surface at runtime. The terrain model we used for testing is given in Fig. 3.2. The terrain height is only dependent on $x$, and the length of each terrain type, the trench and step sizes and the slope angle are configurable. This terrain model uses a right hand coordinate system with the $X$-axis pointing north, the $Y$-axis east and the Z-axis downwards.

For a road with a slope of $\alpha$ radians starting at $(x_0, y, z_0)$, the equation of the plane is given by

$$x \tan\alpha - z + (z_0 + x_0 \tan\alpha) = 0.$$

The normal on a surface will therefore be

$$\hat{\boldsymbol{r}} = (\tan\alpha, 0, -1).$$

The vehicle dynamics model will usually request the distance from the centre of a wheel $(x_p, y_p, z_p)$ to the ground in the direction of the vehicle $(x_r, y_r, z_r)$. Assume this distance is equal to $k$. Then, the point $(x_p + kx_r, y_p + ky_r, z_p + kz_r)$ must lie on the above mentioned plane, that is,

$$(x_p + kx_r)\tan\alpha - (z_p + kz_r) + (z_0 + x_0 \tan\alpha) = 0.$$

Rearranging the terms, $k$ can be calculated to be

$$k = -\frac{x_r \tan\alpha - z_r}{x_p \tan\alpha - z_p + (z_0 + x_0 \tan\alpha)}.$$

For each test scenario, the main test program will prompt the terrain model a starting position for the vehicle given a certain type of terrain. The vehicle dynamics model will then be set accordingly.

### 3.3.3 Automatic Driver

For the evaluation of a driving simulator, a driver could operate the simulator, but then the human factors should also be dealt with. Many simulations will be needed of the same action to analyse the results statistically. For more realistic simulations, more drivers will be needed. For a person who is not an expert at driving, it will be very difficult to accelerate in the most efficient way, and also to maintain a constant speed and to turn at a certain radius. For these reasons, it is more effective to incorporate an automatic driver for the tests [86]. The tests will then be accurate and repeatable.

For an acceleration test, the vehicle will start at a hard road, and the automatic driver will try to achieve optimal acceleration. To do so, acceleration will be at full throttle, and the gear will be changed as swiftly as possible and at the optimal vehicle speed. A gear selection will happen as soon as it is calculated that the vehicle has reached a speed at which the engine will supply the same torque for a higher gear as for the current gear [60].

The braking, obstacle crossing and amphibious properties can be verified as described in the definition of the tests.

For the turning tests, the vehicle should be able to turn at a prescribed speed. To calculate a turning radius, the vehicle speed should be kept constant during the duration of one turning radius test. To do this, the automatic driver needs to adjust the vehicle inputs continuously. For determining the turning radius of a certain steering input, the vehicle will be placed such that it points in the x-direction. The vehicle will then accelerate on level ground until the vehicle is stabilized at the required speed, and thereafter the steering input will be increased incrementally to the requested steering input. When this is done, the vehicle position $(x_{\text{start}}, y_{\text{start}})$ will be recorded. The automatic driver will monitor the speed so that the vehicle will be always within $1km/h$ of the required speed [86]. If the $y$-position of the vehicle is smaller than the previous $y$-position, a quarter of a circle has been completed and the turning radius can be calculated. Let the previous position then be $(x_{\text{start}}, y_{\text{start}})$. The turning radius can then be estimated as the average of $|x_{\text{end}} - x_{\text{start}}|$ and $|y_{\text{start}} - y_{\text{end}}|$.

### 3.3.4 Output file

In a driving simulator, output is mainly used by other systems to provide the cues for the driver about how to drive. For a test program, the evaluation of driving behaviour happens with the analysis of the output during the simulation. For each time instant, the information such as the vehicle position and orientation, speed, gear and engine speed must be logged.

## 3.4 Experimental Results

To illustrate the application and usefulness of an independent test program, tests were done on a preliminary version of an automatic, off-road truck driver simulator.

A C++ program was written to simulate the testing environment, as described above. When the program is executed, it performs all the tests in sequence and generates output files for each test. A MATLAB program is then used to interpret the output data for each test and to draw a graph of it. An analysis of a few of the test results is given below.

### 3.4.1 Acceleration Test

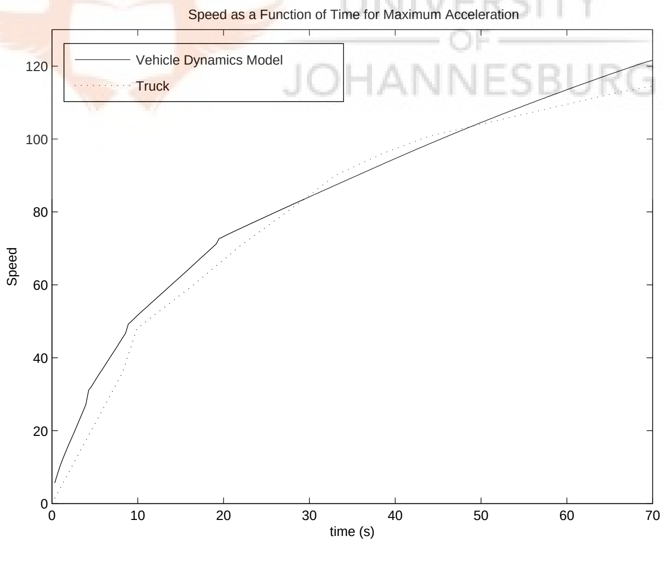


Figure 3.3: Evaluating the maximum acceleration of the vehicle dynamics model.

Fig. 3.3 shows the result of the evaluation of the acceleration properties of the vehicle. In general, if a gear change takes place, there is a time of $0.5s - 1s$ that the engine and driveshaft are not coupled. The torque of the engine will therefore not reach the wheels and the vehicle will not be able to accelerate. On a graph evaluating the acceleration of a vehicle, the slope breakpoints will therefore denote the gear changes. In this case, it can be seen that the gear-selecting model for the automatic gearbox is not correct. The simulated model changes gears much earlier than the actual vehicle.

By comparing the slopes of the two graphs, it can be seen that for any given gear, the simulated model accelerates much faster and has a higher maximum speed than the actual vehicle. This can be the result of gear ratios not chosen properly, or that the aerodynamics and road resistance were not simulated properly.

Although the errors do not look that significant on a graph, it should be remembered that a driving simulation might last for half an hour or longer. With a difference of as little as $1km$ on the maximum vehicle speed, it will mean that a driver reaches a landmark much quicker than it should be able to.



### 3.4.2 Braking Test

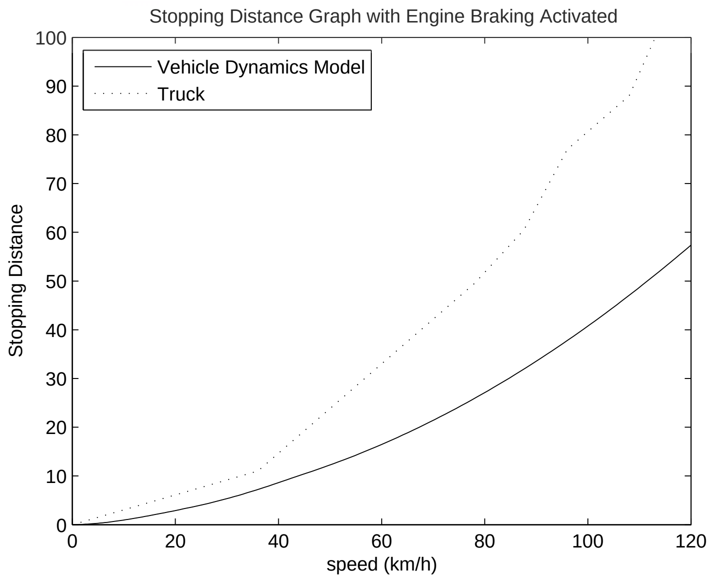


Figure 3.4: Evaluating the braking ability of the vehicle dynamics model when engine braking is involved.

The braking abilities of the vehicle dynamics model is shown in Fig. 3.4. Although the braking properties compared favourable with the normal braking of the actual vehicle, it is clear that the vehicle dynamics model brakes much faster than it should be able to. There is a maximum braking force that can be applied to a vehicle for a specific road surface [179]. Thereafter, the tyres will lock and the vehicle will start slipping and it will take a longer distance to stop. In this case, it seems as if this has not been taken into account, which then gives the vehicle dynamics model unrealistic braking abilities.

### 3.4.3 Turning Test

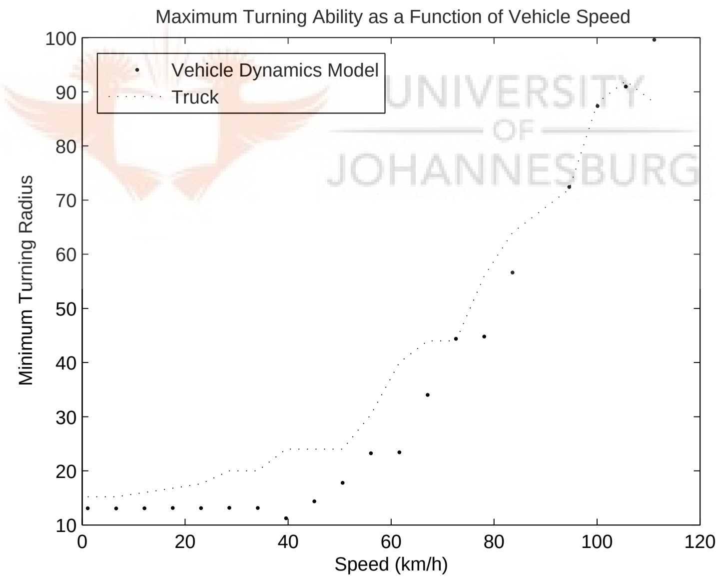


Figure 3.5: Evaluating the maximum turning ability of the vehicle dynamics model.

To test the handling of the vehicle, one test was to determine the minimum turning radius of the vehicle for a given vehicle speed. For a given vehicle speed the steering angle of the vehicle was slowly increased until the vehicle became unstable and all the wheels did not touch the ground any longer.

When the tests are done on the actual vehicle, it can be expected that the test driver would record the vehicle to be unstable much quicker that the automated driver. The automated driver has no fear of an accident resulting. For that reason, the results given in Fig. 3.5 can be regarded as quite accurate. However a much smoother curve for the vehicle dynamics model should be expected. The minimum turning radius graph should be strictly increasing. For a given turning radius, it cannot be expected that a vehicle is more unstable at a high speed than a lower speed.

### 3.4.4 Step Climbing Test

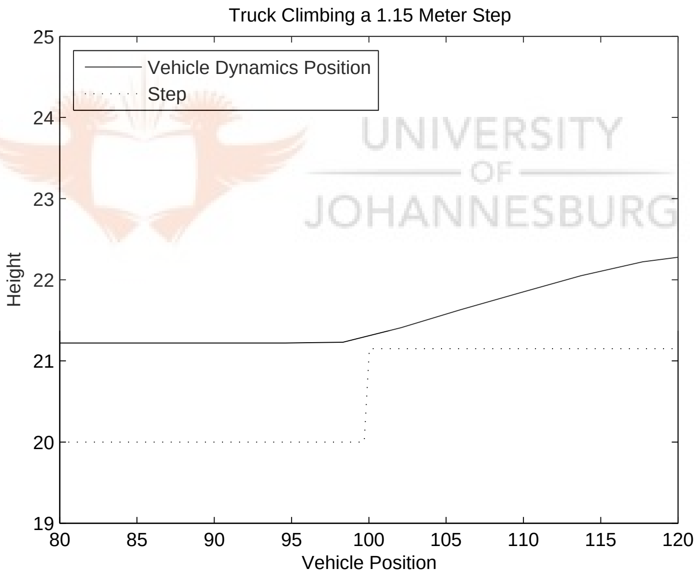



Figure 3.6: Evaluating the step climbing ability of the vehicle dynamics model.

The results of the step climbing test are shown in Fig. 3.6. This test should have failed completely, since the vehicle's wheels were smaller than that height. For such results one could query the existence of a suspension model. However, the terrain model did not include a collision model. The vehicle dynamics model could maybe react to certain collisions to indicate oversized steps, rather than to try to detect a step with the terrain information obtained. Since off-road vehicles have independent suspensions for each wheel, the suspension of the wheel and the coils could have been modelled as one system. Then, the identification of a step cannot be done without collision information.

## 3.5 Conclusion

In this chapter, the simulation of a “black box” testing environment for a vehicle dynamics model was elucidated. Such a simulation is necessary for the validation of a commercial off-the-shelf vehicle model where the implementation detail is unknown. The subsystems of a standard driving simulator, that is the vehicle dynamics model, terrain model, scenario generator, visual display, sound, motion base and driver were discussed. It has been shown how these interfaces can be adjusted to use a main test program, terrain model and automatic driver to simulate various test scenarios and log the vehicle dynamics output. In the discussion of experimental results on an off-road truck, the value of a proper test simulator has been shown.

# Chapter 4

# Mathematical Modelling of an Automatic Driver

## 4.1 Introduction



Within the simulation environment, other vehicles will also be on the road. It should not be possible for these vehicles to have different acceleration, braking or turning characteristics than the actual vehicle. Therefore, they should use the same vehicle dynamics model as the actual vehicle, simulated by the driving simulator. The automatic drivers of these vehicles should also be aware of the vehicle characteristics. For example, an automatic driver should also be aware of the time to start braking and be careful not to turn too fast.

In this chapter, an automatic driver model is described which can be used within the simulation environment. Section 4.2 below describes the setup used for the driving simulator. Section 4.3 discusses the automatic driver model. Section 4.4 gives some experimental results obtained, and concluding remarks follow in section 4.5.

## 4.2 Setup for the Automatic Driver

The task of the automatic driver is to use the vehicle dynamics model in order to drive on a predefined route. The route is indicated by way points. It will be assumed that the way points were chosen in such a way that no collisions with other objects will occur. There could be speed limitations on the route and places where the driver should stop for a predetermined period of time. The set of way points used to describe the route, should contain the following information:

- The $(x, y)$ coordinates of the way point,
- The desired speed or maximum speed allowed when driving toward the way point $V_{wayPoint}$
- The time (in seconds) the automatic driver should pause when it reaches the way point before driving toward the next way point.



For example, the task could be to drive the route as indicated in Fig. 4.1. The set of way points that could describe the route is given in Table 4.1.

Table 4.1: Set of way points to describe the route in Fig. 4.1.

| no | $x$ | $y$ | speed | pause time |
|---:|---:|---:|---:|---:|
| 1 | 298 | 0 | 45 | 30 |
| 2 | 300 | 300 | 60 | 0 |
| 3 | 600 | 600 | 65 | 0 |
| 4 | 5 | 598 | 55 | 60 |
| 5 | 0 | 0 | 60 | 0 |

An authorized user of the program will be able to change, add or delete way points at any time during an exercise. For instance, the second way point might be a traffic light, and when the driver arrives, he should wait until the traffic light is green again. Therefore, the automatic driver will only be able to use the current way point's information when determining the vehicle inputs.

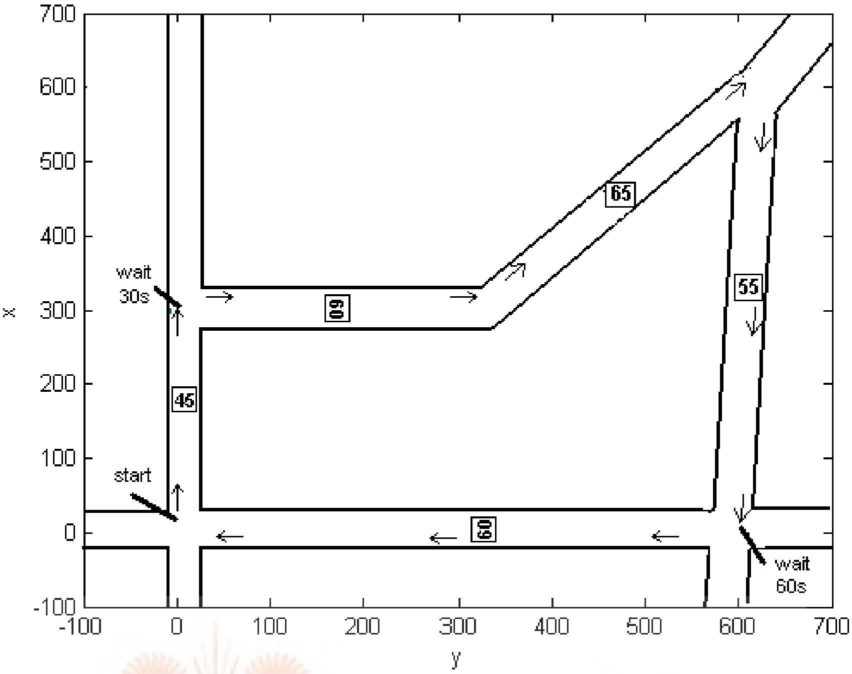


Figure 4.1: A possible route to be followed by an automatic driver.

It is practically impossible to always reach each way point perfectly, that is, to position the vehicle's centre of gravity exactly at the $(x, y)$ coordinate of the way point. If the automatic driver is allowed to reverse at any time, he could do so, but such actions are not allowed on a highway, for example. The minimum turning radius of the vehicle limits the smallest distance to a way point that can be reached. For example, in the case depicted in Fig. 4.2, an automatic driver will end up driving forever in a circle in the hope to reach the way point. For a computer program, that will cause an infinite loop. To prevent this, define a constant $R_{wayPoint}$ as the radius of a circle around a way point within which it will be considered that the way point has been reached. Denote the vehicle's minimum turning radius by $R_{vehicleMin}$. If there is no control over the placement of the way points, the constant value $R_{wayPoint}$ could not be smaller than $R_{vehicleMin}$, since the worst case is that the next way point is exactly at the centre of the vehicle's minimum turning circle. The vehicle will be displaced by a distance $2R_{vehicleMin}$ if it needs to turn 180°. It is easy to verify that any way point which is a distance

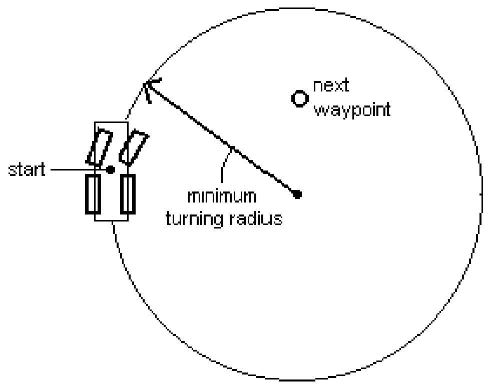


Figure 4.2: A vehicle trying to reach a way point inside its smallest turning circle.

further than $2R_{vehicleMin}$ away from the vehicle's centre of gravity will always be in reach of the autodriver. Therefore, if it could be guaranteed that two consecutive way points will always be further apart than $2R_{vehicleMin}$, $R_{wayPoint}$ could be chosen to be a small positive value.

## 4.3 The Automatic Driver Model

For a smooth graphical display of the driving simulator, the vehicle position should be updated at a frequency of at least 30 times per second. Define $\Delta t$ to be the extent of a time cycle, that is, the time that has elapsed since the previous time that the vehicle position has been updated.

Every time cycle, the automatic driver determines the vehicle inputs for the next $\Delta t$ seconds. Thereafter, the vehicle dynamics model will determine the vehicle outputs. The audio and visual display routines will then give the correct cues to the driver according to the outputs of the vehicle dynamics model. Every cycle, the automatic driver is called to execute the steps listed in Fig. 4.3.

First, the current way point and vehicle parameters are obtained. The automatic driver then determines the way point status, taking into account the vehicle's position, speed and engine speed, distance to the way point and direction of the way point. According to the state of the vehicle and the vehicle's current input parameters, it determines the vehicle inputs for the next cycle and passes the values to the vehicle dynamics model.

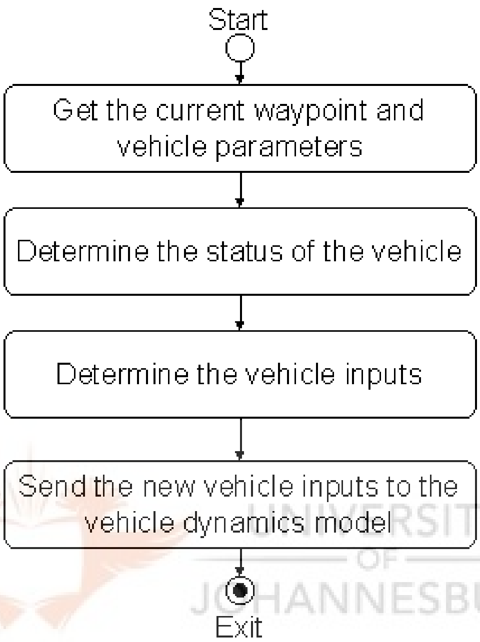


Figure 4.3: The main flow diagram of the automatic driver model.

### 4.3.1 Current Way Point and Vehicle Parameters

Since the way points may change at any time during the exercise, the automatic driver needs to read the current way point again each cycle. It also needs the current vehicle coordinates ($m$), the vehicle speed ($m/s$) and engine speed ($rpm$) every cycle to determine the vehicle inputs for the next cycle.

The way points may be deleted at any time as well, and therefore the number of way points need not be the same each cycle. It could also happen that the current way point has been deleted and that there is suddenly no more way points left. Therefore, if the current way point is read again, several possibilities should be considered.

- If the current way point still exists, that is, if the number of way points is not less than the current way point number, the same way point is read again.
- If the current way point no longer exist, revert to the last existing way point.
- If there are no way points defined, drive to a default position.

### 4.3.2 Status of the Vehicle

The automatic driver can be in one of six possible states which will affect the determination of the vehicle inputs:

- startVehicle
- searchDirection
- driveNormal
- almostThere
- inPauseTime
- finished



The driver follows the procedure given in Fig. 4.4 to determine the status of the automatic driver.

Unless the vehicle has reached the last way point, or is currently pausing at a way point, the highest priority is to make sure that the engine is running and if not, to start the vehicle again. The automatic driver will then turn slowly until it aims at the next way point. Once its direction is correct, it will start driving toward the current way point at the indicated way point speed. If it is in reach of the next way point, it will start braking in time to reach the way point at a low, predefined speed, or to stop if the way point has a defined pause time. As soon as the pause time elapsed, it will then start turning toward the next way point. Once the last way point has been reached, the automatic driver will switch off the engine, but if another way point has been added, it will immediately start the vehicle again and repeat the same cycle once more.

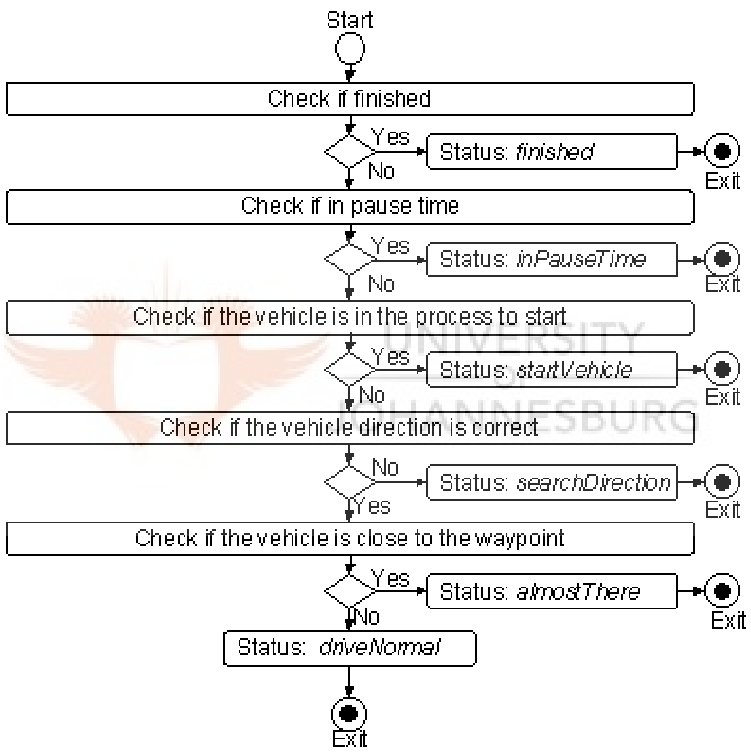


Figure 4.4: The flow diagram for determining the status of the automatic driver.

#### Checking if Finished

For the automatic driver to be temporarily finished with the exercise, the current way point should be the last way point of the way point list and the vehicle should be closer than $R_{wayPoint}$ to the last way point.

#### Checking if in Pause Time

Once a way point has been reached, the current way point will be set to point towards the next way point in the way point list. However, it will not start moving towards it before the pause time defined at the previous way point has been executed. If $t_{current}$ denotes the current time, $t_{waypointReached}$ the time when the previous way point has been reached, and $T_{pause}$ the pause time of the previous way point, the vehicle will be in pause time if

$$t_{current} - t_{waypointReached} < T_{pause} \tag{4.1}$$

#### Checking if Vehicle is in the Process to Start

When an actual vehicle dynamics model is used, a vehicle does not start instantaneously. Let $rpm_{min}$ be the idle speed of the engine and $rpm_{current}$ the current engine speed. Then the vehicle is in start mode if

$$rpm_{current} < rpm_{min} \tag{4.2}$$

#### Checking if the Vehicle Direction is Correct

Define $\psi$ as the yaw angle of the vehicle, that is, the direction angle of the vehicle measured clockwise with respect to north. Assume a right-hand coordinate

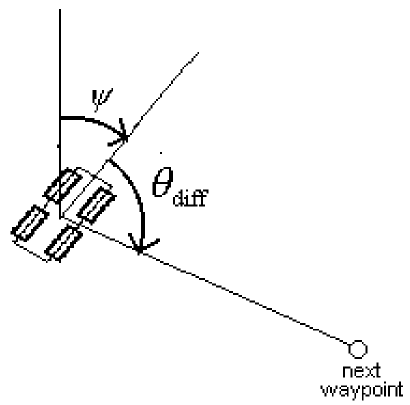


Figure 4.5: Determining the error in the direction of the vehicle.

system with the positive $x$-axis pointing north, the positive $y$-axis pointing east and the positive $z$-axis pointing down. Let $\theta_{diff}$ be the difference between the yaw angle of the vehicle and the direction of the way point with respect to the vehicle. See Fig. 4.5 for a graphical representation of $\psi$ and $\theta_{diff}$. $\theta_{diff}$ is calculated in Eq. (4.3).

$$\begin{aligned}
\Delta x &= x_{waypoint} - x_{vehicle} \\
\Delta y &= y_{waypoint} - y_{vehicle} \\
\text{if } \Delta x := 0 \text{ then } \theta_{waypoint} &:= \frac{\pi}{2} \\
\text{else } \theta_{waypoint} &:= \arctan\left(\frac{\Delta y}{\Delta x}\right) \\
\text{if } \Delta x < 0 \text{ then } \theta_{waypoint} &:= \pi - \theta_{waypoint} \\
\text{if } \Delta y < 0 \text{ then } \theta_{waypoint} &:= -\theta_{waypoint} \\
\theta_{diff} &:= \theta_{waypoint} - \psi \qquad (4.3)
\end{aligned}$$

First, convert $\theta_{diff}$ to an angle between $\pi$ and $-\pi$. Since the vehicle movement is discrete, it can be updated once per time cycle. In a time period $\Delta t$, the vehicle could turn more than the necessary correction needed to be in the exact direction of the way point such that $\theta_{diff} = 0$. If the vehicle turned too much left, next time cycle it might turn too much to the right again. At the end it could be permanently correcting distance without ever being able to get the correct direction to aim perfectly at the way point. Therefore, define $\theta_{diffMax}$ to be the biggest value of $\theta_{diff}$ so that the vehicle is still considered to be moving in the correct direction. Then the vehicle is driving in the correct direction if

$$|\theta_{diff}| < \theta_{diffMax} \tag{4.4}$$

### Checking if the Vehicle is close to the Way Point

For any vehicle, one of the standard specifications is the stopping distance curve, which indicates the stopping distance and vehicle speed as a function of time. This test, according to the Society of Automotive Engineers' standard, is done on a flat road. Maximum braking power is applied to the vehicle when travelling at maximum speed. The distance from the position that maximum braking power is applied as well as the vehicle speed is then recorded [179].

Unless there is a very strong wind, the vehicle aerodynamics in different circumstances will not make a noticeable difference to the braking properties of the vehicle [60, 63]. The rolling resistance on other surfaces such as grass is higher than on a tar road, and therefore the vehicle will brake faster than expected [28], which will not affect the automatic driver. The slope of the road, however, cannot be ignored. For a vehicle driving up a hill with slope $\alpha$ (see Fig. 4.6), the braking force of the vehicle, taking into account the vehicle aerodynamics and vehicle-road interaction, is estimated to be

$$\begin{aligned} F_{brakingForce} &= m_{vehicle} \times a \\ &= -\frac{m_{vehicle} u^2}{2 s_{graph}(u)} \end{aligned} \tag{4.5}$$

where $m_{vehicle}$ is the vehicle mass and $s_{graph}(u)$ is the stopping distance of the vehicle at a speed $u$.

The gravity force in the direction in which the vehicle travels is

$$F_{gravity} = -m_{vehicle} g \sin(\alpha). \tag{4.6}$$

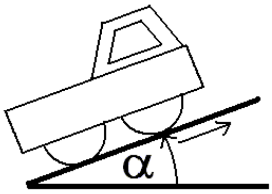


Figure 4.6: Braking of a vehicle against a hill with slope $\alpha$.

Therefore, the total braking force when gravity has been taken into account is given by

$$F_{totalBraking} = -m_{vehicle}\frac{u^2}{2s_{graph}(u)} - m_{vehicle}g\sin(\alpha). \tag{4.7}$$

The deceleration of the vehicle is therefore

$$\begin{aligned} a_{totalBraking} &= \frac{F_{totalBraking}}{m_{vehicle}} \\ &= -\frac{u^2}{2s_{graph}(u)} - g\sin(\alpha), \end{aligned} \tag{4.8}$$



and the stopping distance when the slope has been taken into account is

$$\begin{aligned} s_{totalBraking} &= -\frac{u^2}{2a_{totalBraking}} \\ &= \frac{u^2}{2\left(\frac{u^2}{2s_{graph}(u)} + g\sin(\alpha)\right)}. \end{aligned} \tag{4.9}$$

Unless there is a pause time specified for a way point, the vehicle only needs to slow down at a way point in order to be able to turn toward the next way point. Define the constants $v_{min}$ and $v_{max}$ to be the minimum and maximum speed at a way point respectively. Then

$$s_{totalBraking} = \frac{u^2}{2\left(\frac{u^2}{2s_{graph}(u)} + g\sin(\alpha)\right)} - \frac{v_{min}^2}{2\left(\frac{v_{min}^2}{2s_{graph}(v_{min})} + g\sin(\alpha)\right)}. \tag{4.10}$$

If the current distance to the way point is denoted by $s_{wayPoint}$ the vehicle is *close to a way point* if

$$s_{totalBraking} \geq s_{wayPoint} \tag{4.11}$$

### 4.3.3 Determining the vehicle inputs

**Actions**

(i) *Accelerating*
In a time $\Delta t$, a human driver will not be able to press the accelerator or brake pedal more than a few millimetres. Therefore, it will be unrealistic to define an ideal brake or accelerator position for a certain action. Define $P_{max}$ as the percentage that an accelerator or brake pedal could be pressed or depressed in the given time $\Delta t$. If the brake pedal is currently pressed, the accelerating action it will release the brake pedal with amount $P_{max}$, but not to less than 0%. Otherwise, the accelerator pedal will be pressed with an amount $P_{max}$, but not to more than 100%.

(ii) *Braking*
The braking action works on the same principle as the acceleration. If the accelerator pedal is currently pressed, it will released with an amount $P_{max}$, but not to less than 0%. Otherwise, the brake pedal will be pressed with an amount $P_{max}$, but not to more than 100%.

(iii) *Maintaining Speed*
While the vehicle is searching for a certain direction, it needs to stay within the predefined speed limits $V_{min}$ and $V_{max}$. Also when driving normally, the automatic driver must try to stay at the speed $V_{wayPoint}$ defined at the way point with a variation of less than $\Delta V_{allowed}$. To maintain a certain speed, the automatic driver needs to accelerate if the vehicle speed is less than the allowed speed and brake if the vehicle speed is more than the allowed vehicle speed.

(iv) *Evaluating Gear*
The best gear selection at a certain stage is dependent on the vehicle and engine speed. Define $Gear_{minSpeed}(k)$ and $Gear_{maxSpeed}(k)$ as the minimum and maximum speed for which gear $k$ will be appropriate. The speed intervals for the gears will coincide, that is $Gear_{maxSpeed}(k) > Gear_{minSpeed}(k + 1)$. For example, for 0 - 30km/h, first gear is recommended, while for 20-50km/h $2^{nd}$ gear is acceptable. Let $rpm_{toHigherGear}$ be the minimum engine

speed at which a higher gear selection is recommended, and $rpm_{toLowerGear}$ the maximum engine speed at which a lower gear selection is recommended. Then, if the current engine speed is larger than $rpm_{toHigherGear}$ and the current speed is larger than $Gear_{maxSpeed}(k)$, change to a higher gear. If the current engine speed is less than $rpm_{toLowerGear}$, and the current speed is less than $Gear_{minSpeed}(k)$, and the vehicle is not currently in first gear, change to a lower gear.

(v) *Turning*

To model the turning action of the automatic driver, one should take into account that the steering wheel could not be turned more than $\Delta Turn$ in a time $\Delta t$. For a given vehicle speed $v$ and slope $\phi$, the steering wheel may not be turned more than $MaxTurn(\phi, v)$ so that it is guaranteed that no roll-over takes place. Therefore, if the vehicle is requested to turn left, the steering percentage should be decreased by a percentage $\Delta Turn$, but not less than $-100\%$ or $-MaxTurn(\phi, v)$. If the vehicle is requested to turn right, the steering percentage should be increased by a percentage $\Delta Turn$, but not more than $100\%$ or $MaxTurn(\phi, v)$.

### Determining inputs

In order to determine the vehicle input, the automatic driver should decide which actions is necessary to take according to its current status. This is represented by Table 4.2. The actions *Accelerating* and *Braking* will be used by the *maintaining speed* action.

## 4.4 Experimental Results

The vehicle dynamics model of a truck driver simulator has been used to test the automatic driver model. Table 4.3 shows the constant values chosen for the model.

Table 4.2: Determining the vehicle inputs.

| Vehicle Status | Turn Left | Turn Right | Maintain Speed | Gear |
|---|---|---|---|---|
| *StartVehicle* | 0 | 0 | 0 | Neutral |
| *InPauseTime* | 0 | 0 | 0 | Neutral |
| *Finished* | 0 | 0 | 0 | Neutral |
| *SearchDirection* | if $\theta_{diff} > \theta_{diffMax}$ | if $\theta_{diff} < -\theta_{diffMax}$ | $> V_{min}$ and $< V_{max}$ | Select Gear |
| *DriveNormal* | 0 | 0 | $V_{wayPoint}$ | Select Gear |
| *AlmostThere* | 0 | 0 | $V_{min}$ | Select Gear |



Table 4.3: Constant values chosen for the automatic driver.

| Constant | Value |
|---|---|
| $R_{wayPoint}$ | $0.2m$ |
| $\Delta t$ | $30ms$ |
| $Rpm_{min}$ | $800rpm$ |
| $\theta_{diffMax}$ | $0.01rad$ |
| $V_{max}$ | $8km/h$ |
| $V_{min}$ | $5km/h$ |
| $P_{max}$ | $1\%$ |
| $Rpm_{higherGear}$ | $1400rpm$ |
| $Rpm_{lowerGear}$ | $1800rpm$ |
| $\Delta V_{allowed}$ | $0.3km/h$ |
| $\Delta Turn$ | $0.01rad$ |

### 4.4.1 Verification of the Route followed by the Automatic Driver

To verify that the automatic driver has the ability to stay on a road, the way points described in Table 4.1 has been used. The $(x, y)$ positions of the truck have been recorded and are shown in Fig. 4.7. In the figure, it can be seen that the automatic driver passed all the way points and stayed on the road at all times.

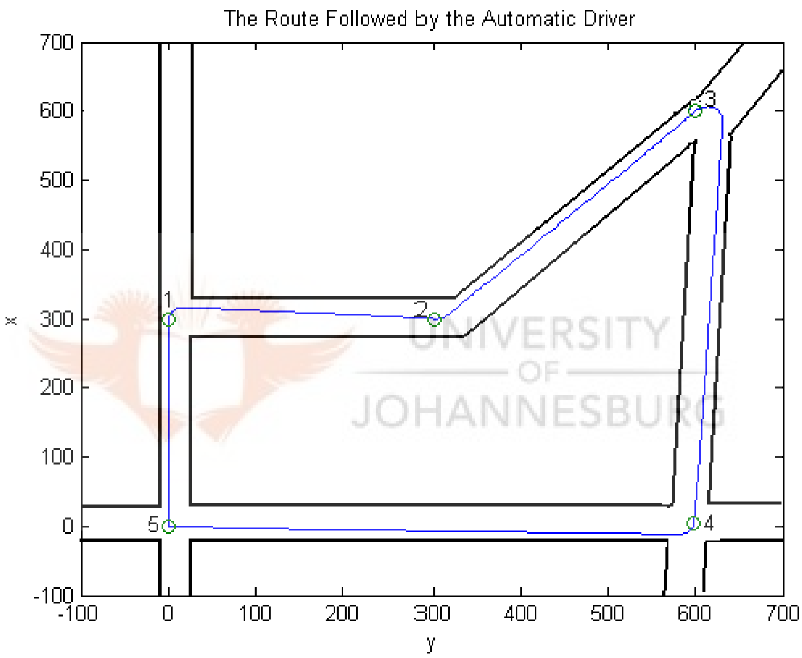


Figure 4.7: The route followed by the automatic driver for the way points of Table 4.1.

### 4.4.2 Verification of the requested Vehicle Speed and Pause Times

To verify the speed and pause times of the way points, the same route was used as in Fig. 4.1, but on a much larger scale. Table 4.4 shows the way points used for this experiment. The speed of the vehicle as a function of time has been recorded and the results are shown in Fig. 4.8. These results show that the speed and pause time requirements of the way points were followed very accurately by the automatic driver. Although it looks as if the acceleration and braking happened instantaneously, one should notice that the time scale used is in minutes. It took the truck driver simulator almost 20s to accelerate to 60km/h.

Table 4.4: Set of way points to verify the requested vehicle speed and pause times.

| no | $x$ | $y$ | speed | pause time |
|---|---|---|---|---|
| 1 | 2995 | 0 | 45 | 300 |
| 2 | 3000 | 3000 | 60 | 0 |
| 3 | 6000 | 6000 | 65 | 0 |
| 4 | 5 | 5995 | 55 | 600 |
| 5 | 0 | 0 | 60 | 0 |

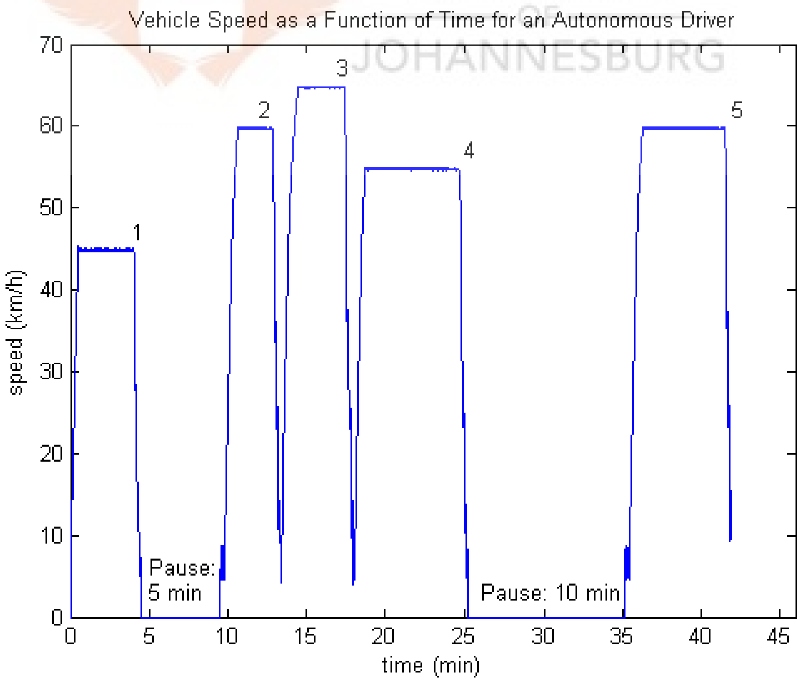


Figure 4.8: The speed of the vehicle as a function of time when the input to the automatic driver was the set of way points described in Table 4.4.

## 4.5 Conclusion

In this chapter, an automatic driver model was described which can be used within the simulation environment. By using the vehicle output and the way points defined, the automatic driver determines the inputs to the vehicle dynamics model. It uses the vehicle specifications to achieve the optimal performance of the vehicle. By using this automatic driver model, the movement of vehicles controlled by the computer could be simulated much more realistically.

# Chapter 5

# Three Dimensional Geometry within a Driving Simulator

## 5.1 Introduction



An understanding of three-dimensional coordinate system transformations is one of the most important parts of a flight or driving simulator. All velocities and forces relative to the aeroplane or vehicle should be transformed into the world coordinates [18, 39, 63, 165]. These coordinate transformations are used for robotics to keep track of the position of a robot arm [34]. Game programming or any other three-dimensional graphics programming cannot be done without a proper understanding of how it works. It is also an essential part of camera or observer positioning within a driving simulator.

Although the procedure of using Euler angles for coordinate system transformations is nothing new [67], almost no literature is available on how it can be applied for more complex situations. In this chapter, more information is given on how a program language such as C++ could be used to apply more complex coordinate transformations in real-life situations.

For commercial purposes, in order to have a driving simulator approved, proof must be given that all mathematical models developed are true representations of the real vehicle. However, years of work for a simulator worth a few million dollars can only really be appreciated by a realistic display for the driver accompanied by impressive sounds and movements.

The ideal driving simulator should give the driver the impression that he/she is driving a real vehicle. The only noticeable difference should be computer screens instead of windows and mirrors. The typical set-up for a commercial driving simulator within the military environment is given in Fig. 5.1

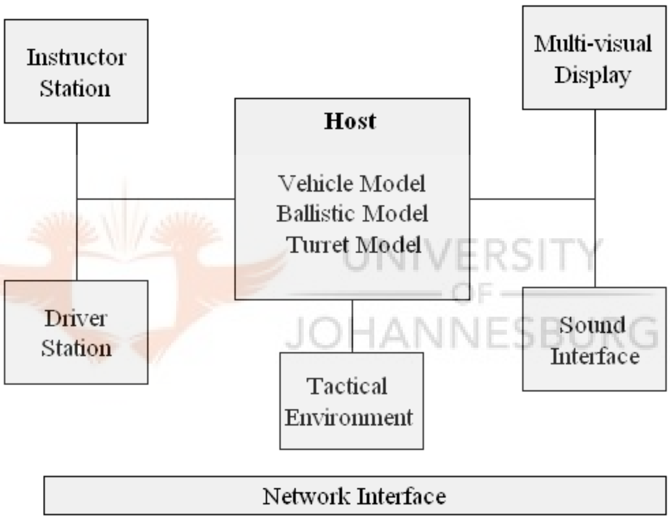


Figure 5.1: The typical set-up for a driving simulator.

For the multi-visual display, simulator companies often make use of existing graphics packages such as SpaceMagic or VTree. The network interface to the graphics program is usually very primitive, allowing only the most basic single translation and rotation functions. Therefore all the three-dimensional transformation calculations need to be performed before the transformations could be send as single instructions to the graphics program module.

For the display on a computer screen an observer or camera viewpoint on the visual object needs to be created. The observers's position and orientation are then defined relative to the visual object's position and orientation.

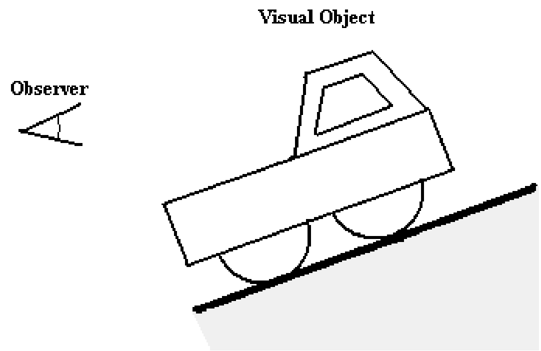


Figure 5.2: Positioning of a camera on a visual object.

However, it is sometimes deemed necessary for an observer or object to follow a particular vehicle. In this case, the observer will not have a fixed position relative to the vehicle. In the same way as for the human eye, there will be a reaction time involved. For instance, the vehicle will turn, and about half a second later the observer will turn as well. If the vehicle vibrates when driving on an uneven road, the observer will not experience it to the same extent. Therefore, a thorough understanding of coordinate system transformations is of vital importance to implement it within a driving simulator.



## 5.2 Coordinate System Convention

In this thesis, the following coordinate system convention is assumed as discussed in section 1.5.

### 5.2.1 Transformation from Body Axis to Earth Axis

Suppose the centre of gravity of the vehicle is at the position $(X_{CoG}, Y_{CoG}, Z_{CoG})$. Then, any body axis coordinate $(x, y, z)$ is given in terms of world coordinates $(X, Y, Z)$ by

$$\begin{pmatrix} X \\ Y \\ Z \end{pmatrix} = \begin{pmatrix} X_{CoG} \\ Y_{CoG} \\ Z_{CoG} \end{pmatrix} + \begin{pmatrix} B_{11} & B_{21} & B_{31} \\ B_{12} & B_{22} & B_{32} \\ B_{13} & B_{23} & B_{33} \end{pmatrix} \begin{pmatrix} x \\ y \\ z \end{pmatrix}. \tag{5.1}$$

### 5.2.2 Transformation from Earth Axis to Body Axis

Recall that $\boldsymbol{B}^{-1} = \boldsymbol{B}^T$. Therefore, by taking the inverse of Eq. (5.1), we get

$$\begin{pmatrix} x \\ y \\ z \end{pmatrix} = \begin{pmatrix} B_{11} & B_{12} & B_{13} \\ B_{21} & B_{22} & B_{23} \\ B_{31} & B_{32} & B_{33} \end{pmatrix} \begin{pmatrix} X - X_{CoG} \\ Y - Y_{CoG} \\ Z - Z_{CoG} \end{pmatrix}. \tag{5.2}$$

## 5.3 Adding Transformations

Let the vehicle's centre of gravity be at $\boldsymbol{R}_{CoG} = (X_{CoG}\ Y_{CoG}\ Z_{CoG})^T$. Denote its body coordinates by $\boldsymbol{r} = (x\ y\ z)^T$, and its world coordinates by $\boldsymbol{R} = (X\ Y\ Z)^T$.

If the vehicle is first rotated by $(\psi_1, \theta_1, \psi_1)$, defined by matrix $\boldsymbol{B}_1$, and thereafter by $(\psi_2, \theta_2, \psi_2)$, defined by matrix $\boldsymbol{B}_2$, the total rotation is given by

$$\boldsymbol{r} = (\boldsymbol{B}_2 \boldsymbol{B}_1)\,(\boldsymbol{R} - \boldsymbol{R}_{CoG}). \tag{5.3}$$

Therefore, the matrix $\boldsymbol{B} = \boldsymbol{B}_2 \boldsymbol{B}_1$ will do the same transformations with a single matrix.

## 5.4 Transformations between Left-Hand and Right-Hand Coordinate Systems

All the above transformation formulas are for right hand coordinate systems. For left hand coordinate systems, the $z$-axis is in a different direction, and therefore the pitch and roll angles will also be in a different direction. Thus, one needs to work in the coordinate system in which the Euler angles were defined. For instance, if the Earth axis is a left hand coordinate system, one will first need to make it right-handed by the equation $Z_{earth} = -Z_{earth}$, then to do all the calculations, and subsequently change $Z_{earth}$'s sign again.

## 5.5 Calculation of Euler Angles given an Euler Matrix

This might be an unnecessary and trivial exercise for a rotation matrix after a single rotation. However, the power of the following equations is to calculate which single transformation could do the same as a sequence of coordinate transformations.



### 5.5.1 Some Useful Trigonometry Rules

If $\sin(\alpha)$ and $\cos(\alpha)$ is known, then

$$\alpha = \begin{cases} \arctan\left(\frac{\sin(\alpha)}{\cos(\alpha)}\right) & \cos(\alpha) > 0 \\ \pi + \arctan\left(\frac{\sin(\alpha)}{\cos(\alpha)}\right) & \cos(\alpha) < 0 \\ \arcsin(\sin(\alpha)) & \text{otherwise.} \end{cases} \tag{5.4}$$

### 5.5.2 Angles for $\theta \neq 90 + 180k$

For $\theta \neq 90° + k \cdot 180°$, the entry $B_{13}$ of the Euler matrix will not be equal to zero.

Therefore, by using the Euler matrix, one can demonstrate that:

$$\begin{array}{rclrcl} \theta & = & -\arcsin(B_{13}) & & & \\ \sin(\phi) & = & \frac{B_{23}}{\cos(\theta)} & \cos(\phi) & = & \frac{B_{33}}{\cos(\theta)} \\ \sin(\psi) & = & \frac{B_{12}}{\cos(\theta)} & \cos(\psi) & = & \frac{B_{11}}{\cos(\theta)}. \end{array} \tag{5.5}$$

### 5.5.3 Angles for $\theta = 90^\circ + k \cdot 180^\circ$

If $\theta = 90^\circ + k \cdot 180^\circ$, $B_{13} = |\sin(\theta)| = 1$ and $\cos(\theta) = 0$. Then, the Euler matrix may be reduced to

$$B|_{\theta=90^\circ+k\cdot180^\circ} = \begin{pmatrix} 0 & 0 & -1 \\ \sin(\phi-\psi) & \cos(\phi-\psi) & 0 \\ \cos(\phi-\psi) & \sin(\psi-\phi) & 0 \end{pmatrix}. \tag{5.6}$$

From this matrix it is clear that, if the pitch is 90°, the yaw movement has exactly the same effect as the roll movement.

A possible solution will be $\psi = 0$, $\sin(\phi) = B_{21}$ and $\cos(\phi) = B_{31}$.

## 5.6 C++ Implementation



To implement the transformations, a C++ class `Transform.cpp` has been written. This class ensures that the mathematical detail of coordinate system transformations is separated from its implementation, as can be seen when this class is used for positioning the "Behind and Above" view.

The said class stores the position of an object on Earth as well as its orientation. The default position and rotation are both $(0, 0, 0)$. The main functions that will be used are given in Table 5.1.

## 5.7 Positioning of the "Behind and Above" View

For a realistic view from behind, the onlooker wants to be able to observe the suspension movements of the vehicle, as well as whether the vehicle is moving uphill or downhill.

Therefore, the observer should always look at the same distance from and height above a certain point of the vehicle (see Fig. 5.3 - 5.5).

Table 5.1: The main functions needed for using the Transform class.

| Function | Description |
|---|---|
| `t.setPosition(X,Y,Z)` | Set the position of the object to be at $(X, Y, Z)$. |
| `t.setEulerAnlges(psi,theta,phi)` | Set the rotation of the object at $(\psi, \theta, \phi)$. |
| `t.bodyToEarth(x_p,y_p,z_p,X_p,Y_p,Z_p)` | Determine the Earth position $(X_p, Y_p, Z_p)$ from a position $(x_p, y_p, z_p)$ relative to the object. |
| `t.earthToBody(x_p,y_p,z_p,X_p,Y_p,Z_p)` | Given the Earth position of a point $(X_p, Y_p, Z_p)$, determine the position of the point $(x_p, y_p, z_p)$ in terms of the object's coordinate system. |
| `t.addTransformation(psi_2,theta_2,phi_2)` | Add a rotation $(\psi_2, \theta_2, \phi_2)$ to the current rotation of the object. |
| `t.setToInverse()` | Replace the transformation matrix with its inverse. |
| `t.getEulerAnlges(psi,theta,phi)` | Calculate the rotation of the object $(\psi, \theta, \phi)$. |



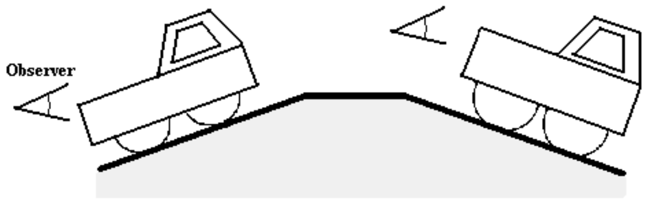


Figure 5.3: Observer position for the "Behind and Above" view.

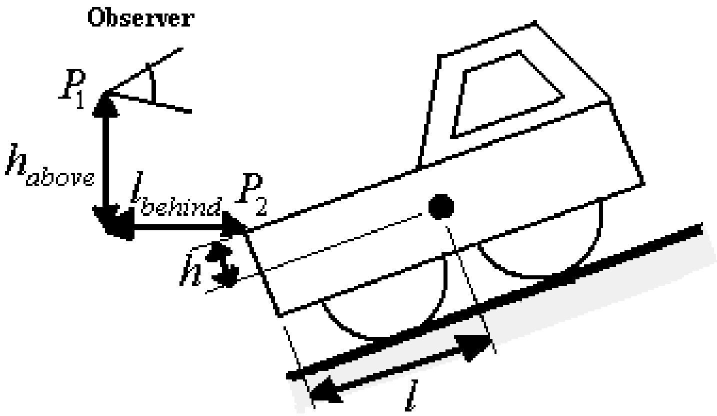


Figure 5.4: The parameters involved in positioning the "Behind and Above" view.



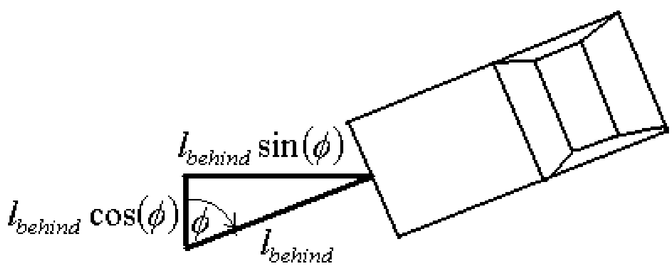


Figure 5.5: The parameters involved in positioning the "Behind and Above" view as seen from above.

### 5.7.1 Observing Roll and Pitch Movement of the Vehicle

First, set up the transformation matrix for the vehicle.

```
Transform t();
t.setPosition(x_vehicle,y_vehicle,z_vehicle);
t.setEulerAngles(psi,theta,phi);
```

The world coordinates of $P_2$ are given by

```
t.bodyToEarth(-l,0,-h,X_p2,Y_p2,Z_p2);
```

The world coordinates of $P_1$ are given by

```
t.bodyToEarth(X_p2+l_behind*cos(psi),Y_p2*sin(psi),Z_p2+h_above,
X_p1,Y_p1,Z_p1);
```

The observer position relative to the vehicle $(x_{obs}, y_{obs}, z_{obs})$ is then given by

```
t.EarthToBody(X_p1,Y_p1,Z_p1,x_obs,y_obs,z_obs)
```

The observer should have the same yaw-angle as the vehicle. The observer angles relative to the vehicle are given by

```
t.setEulerAngles(psi,theta,phi);
t.setToInverse();
t.addTransformation(psi,0,0);
t.getEulerAngles(psi_obs,theta_obs,phi_obs);
```

### 5.7.2 Observing the Yaw-movement of the Vehicle

The calculations in Section 5.7.1 give the observer the ability to view the roll and pitch movement of the vehicle. However, it will not be possible for the observer to observe that if the vehicle is turning. To achieve that effect, the observer's position and rotation should be delayed. It should be as if the vehicle is turning and thereafter the observer starts turning as well.

Denote the vehicle's current position and rotation by $(x_{now}, y_{now}, z_{now})$ and $(\psi_{now}, \theta_{now}, \phi_{now})$. Assume the vehicle's position and rotation a fraction of a second ago were $(x_{old}, y_{old}, z_{old})$ and $(\psi_{old}, \theta_{old}, \phi_{old})$.

To enable the observer to be aware of acceleration and braking, it should be positioned according to the old position of the vehicle.

First, set up the transformation matrix for the old vehicle position and determine the position of the observer in world coordinates $(x_{p1}, y_{p1}, z_{p1})$.

```
Transform t();
t.setEulerAngles(psi_old,theta_old,phi_old);
t.setPosition(x_old,y_old,z_old);
t.bodyToEarth(-l,0,-h,X_p2,Y_p2,Z_p2);
t.bodyToEarth(X_p2+l_behind*cos(psi),Y_p2 * sin(psi),Z_p2 + h_above,
X_p1,Y_p1,Z_p1);
```

The observer position relative to the vehicle should then be used using the current vehicle position:

```
Transform t();
t.setEulerAngles(psi_now,theta_now,phi_now);
t.setPosition(x_now,y_now,z_now);
t.EarthToBody(X_p1,Y_p1,Z_p1,x_obs,y_obs,z_obs);
```

To calculate the rotation of the observer, add the old yaw-movement of the observer to the inverse of the current vehicle rotation. Assume we want to let the observer look downward with an angle $\theta_{down}$ and not directly level with the horizon. The observer rotation relative to the vehicle can then be calculated as follows:

```
Transform t();
t.setEulerAngles(psi_now,theta_now,phi_now);
t.setPosition(x_now,y_now,z_now);
t.setToInverse();
t.addTransformation(psi_old,-theta_down,0);
t.getEulerAngles(psi_obs,theta_obs,phi_obs);
```



These calculations will enable the observer to observe when the vehicle is turning. However, it is still not hundred percent realistic, since the observer will not react to sudden movement. To make it more realistic, the calculated observer positions should be filtered. That could be done by a simple filtering method, such as positioning the observer using the average of the last three calculated observer positions.

## 5.8 Positioning of a Gun and Turret on a Military Vehicle

To the computational data discussed above further applications may be added. If the said vehicle is contextualized in military situations, fulfilling a combat role, for example an armed vehicle, calculations regarding the positioning of a gun and turret become necessary.

### 5.8.1 Direction Vector of the Gun

To get the direction angles of the gun relative to the ground coordinate system, the transform class could be used as follows:

```
Transform t();
t.setEulerAngles(psi_vehicle,theta_vehicle,phi_vehicle);
t.addTransformation(turretAzimuth, gunElevation, 0);
t.getEulerAngles(psi_gun,theta_gun,phi_gun);
```

The direction vector of the gun is then given by

$$\begin{aligned} \hat{\boldsymbol{r}}_{gun} &= x_{gun}\hat{\boldsymbol{x}} + y_{gun}\hat{\boldsymbol{y}} + z_{gun}\hat{\boldsymbol{z}} \\ &= -\sin(\theta_{gun})\hat{\boldsymbol{x}} + \cos(\theta_{gun})\cos(\psi_{gun})\hat{\boldsymbol{y}} + \cos(\theta_{gun})\sin(\psi_{gun})\hat{\boldsymbol{z}}. \end{aligned} \quad (5.7)$$

### 5.8.2 Position of Gun Fixed Relative to the Ground

In a military vehicle, when the gunner uses the *stab* option, the gun's orientation relative to the ground remains fixed. That is, if the gun was pointing north with a 30° angle relative to the horizon, it will stay in that position regardless of the movement of the vehicle.

However, it is still necessary to know what the gun and turret's azimuth and elevation are relative to the vehicle, to position them correctly.

#### Unit Vector Approach

Since the gun has no roll movement, it can be represented by a single unit vector. Therefore, it would be a logical reasoning to use such an approach to determine the direction vector of the gun.

The unit vectors of the vehicle's axes relative to the ground are given by

$$\begin{aligned} \hat{\boldsymbol{x}}_{vehicle} &= x_{vx}\hat{\boldsymbol{x}} + y_{vx}\hat{\boldsymbol{y}} + z_{vx}\hat{\boldsymbol{z}} \\ \hat{\boldsymbol{y}}_{vehicle} &= x_{vy}\hat{\boldsymbol{x}} + y_{vy}\hat{\boldsymbol{y}} + z_{vy}\hat{\boldsymbol{z}} \\ \hat{\boldsymbol{z}}_{vehicle} &= x_{vz}\hat{\boldsymbol{x}} + y_{vz}\hat{\boldsymbol{y}} + z_{vz}\hat{\boldsymbol{z}}. \end{aligned} \tag{5.8}$$

By using the Transform class, the direction vectors can be calculated easily:

```
Transform t();
t.setEulerAngles(psi_vehicle,theta_vehicle,phi_vehicle);
t.bodyToEarth(1,0,0,x_vx,y_vx,z_vx);
t.bodyToEarth(0,1,0,x_vy,y_vy,z_vy);
t.bodyToEarth(0,0,1,x_vz,y_vz,z_vz);
```



Therefore, in terms of the vehicle axis system, the gun position is given by

$$\begin{aligned} \hat{\boldsymbol{r}}_{gun} &= x_{gun}\hat{\boldsymbol{x}} + y_{gun}\hat{\boldsymbol{y}} + z_{gun}\hat{\boldsymbol{z}} \\ &= (\hat{\boldsymbol{r}}_{gun} \cdot \hat{\boldsymbol{x}}_{vehicle})\,\hat{\boldsymbol{x}}_{vehicle} + (\hat{\boldsymbol{r}}_{gun} \cdot \hat{\boldsymbol{y}}_{vehicle})\,\hat{\boldsymbol{y}}_{vehicle} + (\hat{\boldsymbol{r}}_{gun} \cdot \hat{\boldsymbol{z}}_{vehicle})\,\hat{\boldsymbol{z}}_{vehicle} \\ &= x_{GunVehicle}\hat{\boldsymbol{x}}_{vehicle} + y_{GunVehicle}\hat{\boldsymbol{y}}_{vehicle} + z_{GunVehicle}\hat{\boldsymbol{z}}_{vehicle}. \end{aligned} \tag{5.9}$$

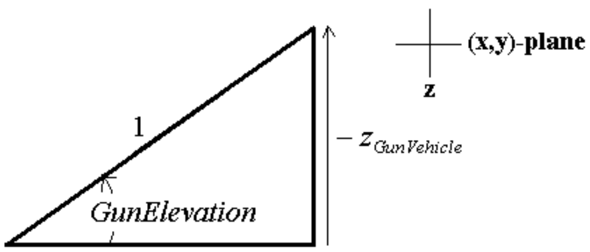


Figure 5.6: Calculation of the gun elevation angle.

The gun elevation angle (Fig. 5.6) can be expressed as

$$GunElevation = -\arcsin\left(z_{GunVehicle}\right). \tag{5.10}$$

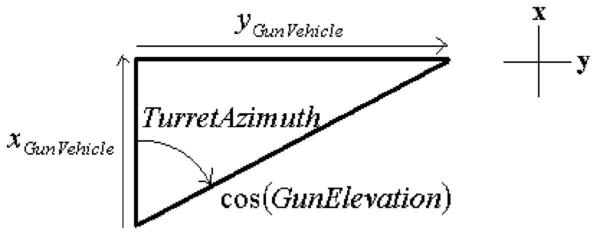


Figure 5.7: Calculation of the turret's azimuth angle.

and according to Fig. 5.7

$$\begin{aligned} \sin(TurretAzimuth) &= \frac{y_{GunVehicle}}{\cos(GunElevation)} \\ \cos(TurretAzimuth) &= \frac{x_{GunVehicle}}{\cos(GunElevation)}. \end{aligned} \tag{5.11}$$

Since its sin and cos values are now known, the $TurretAzimuth$ angle can be calculated as described in Section 5.5.1.



### Using the Transform Class only

By using the Transform class and ignoring the calculated roll angle, which will have no effect on the gun's position, the calculation of the gun's position relative to the ground can be greatly simplified. Let $\psi_{gun}$ and $\theta_{gun}$ be the turret's azimuth and the gun's elevation relative to the ground. The following C++ code will calculate the gun's parameters relative to the vehicle.

```
Transform t();
t.setEulerAngles(psi_vehicle,theta_vehicle,phi_vehicle);
t.setToInverse();
t.addTransformation(psi_gun,theta_gun,0);
t.getEulerAngles(turretAzimuth,gunElevation,n);
```

## 5.9 Conclusion

In this chapter the mathematical framework for implementing tree-dimensional coordinate transformations was presented. This framework is currently used for positioning of an observer for a driving simulator. In presenting this framework, special attention was given to achieve clarity for the purpose of implementation.

# Chapter 6

# Phase Vocoder Technology for the Simulation of Engine Sound

## 6.1 Introduction



Although the simulation of the sound of a vehicle is not a general research area, many people spend their time on the creation, control and damping of engine sounds.

In 2003, the vehicle manufacturer, Audi, had 45 engineers who worked on the design of appropriate engine sounds. A sound that is too loud will be irritating, but if it is too soft, one may wonder if the car is working properly [72]. To evaluate a sound, first it must be modelled.

Ammon and Das (2001) extracted each deterministic component of an engine sound, and proposed a simple method for modelling the remaining stochastic component of the engine sound. In this way, one of the sound components could be changed and evaluated before the physical implementation thereof [22].

The development of traffic noise prediction models is another research domain regarding engine sounds. The models are used by several groups of people such as roadway engineers to determine the spacing needed between a road and adjacent buildings and acoustic specialists for environmental impact studies. In a study done by Steele (2001) several noise prediction models were evaluated. He found that all the selected models tested proved to satisfy government regulations and could be used by roadside engineers, but would not meet the requirements of other users of traffic models. There does not yet exist a model suitable for all requirements, and he proposed the requirements for an ideal model to overcome the identified deficiencies [164].

Stankovic and Bohme (1999) did research about the possibility to use the multiple resonance in combustion engine signals as an input for engine control, rather than pressure. For effective engine control, a sensor is needed inside the cylinder to measure the pressure at a suitable point to determine the combustions. The pressure sensors are, however, difficult to mount, expensive and not robust enough. The sound analysis proved to be a much cheaper and faster tool for engine control [162].

The sound of an emergency engine generator is one indication if it is in a full working condition. Sumita *et al.* (1998) used sound analysis to automate the process of keeping an ear on the engine generator's sound. They found that the calculated frequency intensity of a malfunctioning engine generator was lower than that of a proper working generator [166].

Fukuhar *et al.* (2002) used a driving simulator to evaluate the engine acceleration sound. The effect of vehicle performance and the controllability of the engine sound by means of the accelerator pedal were measured quantitatively. It was found that the evaluation of engine sound does not depend on the sound only, but also on the action performed with that sound, such as acceleration [57].

Perception of sound and associations that go along with it, is a human activity and prone to subjectivity. Gonzalez *et al.* (2003) assessed the ability of active noise control systems to achieve a more pleasant sound. The sound quality study focused on estimating changes in the noise quality by evaluating the sense of comfort of the hearer. The conclusion was that the active noise control positively affects acoustic comfort, but that it is unable to reduce the loudness of the sounds [68].

Vastifall *et al.* (2002) did research on the affective evaluations of and reactions to exterior and interior vehicle quality. In three experiments, participants rated their affective reactions ("how pleasant I feel") and preferences for these affective reactions ("how much I like the way I feel") as well as affective evaluations ("how pleasant the sound is") to interior binaurally recorded vehicle sounds varying in physical properties. The deduction can thus be made that affect is an important component in product auditory quality optimization [173].

In addition to be pleasing, sound can also irritate. Versfeld and Vos (2002) studied the relationship between noise annoyance and the proportion of heavy vehicles in a mixture of trucks and passenger cars. Twenty normal-hearing people were asked to judge the annoyance caused by the sounds of a continuous stream of vehicles, assuming they were exposed to it at home on a regular basis. The number of vehicles driving past was kept constant. Results showed that in such conditions, the annoyance is virtually independent of the proportion of heavy vehicles [174].



Martin (1999) looked into the active noise control of a moving car. This cannot be achieved directly by using active control of an immobile source. In their study, a method is described for installing a secondary source screen in the vicinity of the controlled domain, and has been proved to be successful according to the numerical modelling done in the frequency and time domains [117].

To the author's present knowledge, no active research has yet been published for the modelling of engine sound for driving simulation and computer driving games. Most driving games use only three engine sounds and choose from them according to the engine speed. This approach is not sufficient for giving the driver enough cues for a realistic driving exercise. Mourant and Refsland (2003) described the modelling and rendering of sounds in a 3D virtual environment driving simulator. The sound of a particular engine speed is determined through linear interpolation. A set of engine speeds and their corresponding sound intensity levels are created. The intensity level of a particular engine speed is calculated by linearly interpolating between the sound levels of the key engine speeds it falls between. Wind noise is added depending on the vehicle's velocity [128].

This chapter proposes the modelling of engine sound by using vocoding. For a driving simulator where a person is learning to drive, an accurate sound model is necessary. Certain actions, such as gear changing, relies primarily on the current engine sound. Section 6.2 gives an overview of the phase vocoder, and section 6.3 explains its implementation detail. Some experimental results are given in section 6.4 and concluding remarks follow in section 6.5.

## 6.2 The Phase Vocoder

The phase vocoder is a tool for independent time scaling and pitch shifting of speech and audio signals via modification of their short-time Fourier transforms [98]. The phase vocoder was described as early as 1966 in an article by Flanagan and Golden. They gave much detail on the implementation of the phase vocoder on an IBM 7094 computer [53]. The vocoder technology was one of the first steps towards digital sound. Using vocoder technology, much less disk space is needed for storing the necessary information than it would be to store all the possible words and word combinations [158]. The vocoder also reduces the bandwidth necessary for transmitting audio. If a telephone cable has a bandwidth of 3kHz, it can only carry one speech signal. If a vocoder reduces the necessary bandwidth to 600Hz, five simultaneous conversations on one telephone cable will be possible [66].

Although the phase vocoder is a successful instrument for time-scale and pitch modifications of speech, it has its limitations, such as the general problem of the vocoder called the phasiness. The phasiness of vocoders relates to the fact that the modified signal often sounds as if it had been recorded in a small room. In particular, time-expanded speech sounds produced by a speaker sounds much further from the microphone than it was in the original sound. Laroche and Dolson (1999) studied the reasons for this phasiness, and two phase-locking techniques were proposed which dramatically reduce the the phasiness in the modified signal [97].

The quality of a vocoder's sound is not always easy to evaluate. Several factors will also influence the way a person listens to a vocoder's output, such as the specific voice and sentence used, the loudspeaker, the size of the room, knowing the sentence beforehand, and which sample was first [66].

The phase vocoder technology is not only a benefit to the signal processing of the human voice. It has been used successfully for several applications within music. Pielemeier *et al.* (1996) highlighted the applications of phase vocoders and general sound syntheses within music. Vocoder technology has been utilized for the analysis and re-synthesis of specific instruments' sounds, for transcription of music into written form and the mapping of an acoustic signal into visual form in order to improve highlighting the desired features of the signal over others [139]. In order to design a proper tuner device for a wind instrument, it is necessary to estimate the frequency of a note to analyse if it is on the correct pitch. Several frequency estimation techniques exist that make use of the phase vocoder [15]. Puckette and Brown did a study to compare the frequency estimation of the phase vocoder with that of the maximum likelihood (ML) frequency estimator. The phase vocoder was evidently more successful for any type of noise, as which may appear in wind instruments. The ML technique assumes that the disturbance is Gaussian white noise, and has proved to have limited functionality [143]. Moorer used vocoder techniques to identify the differences between a cello, clarinet and trumpet sounds. Every note has an "attack" phase, a "steady state" position and a "decay position", which differs for each instrument. This information can then be used to "generate" new sounds for modern or contemporary music [125].

The next section describes the implementation of a phase vocoder. Up to now, several algorithms have been proposed in literature to optimize the speed of the algorithm or the quality of its output. Laroche and Dolson (1999) proposed, for instance, a method for doing the time-scale and sample rate conversion for pitch scale modification within one step, directly in the frequency domain [99]. For voice applications, the phase vocoder is applied to a speech production model [118, 142, 144, 145]. The vocoder principles, however, do not change within any application.

## 6.3 Implementation of the Phase Vocoder

The modification of audio happens in four phases. The *analysis* phase represents the signal using the *short time Fourier transform* (STFT). The *modification* phase modifies the STFT to change the speed of the signal. The *synthesis* stage estimates the representation of the modified signal in time. The *resampling* phase changes the sampling rate of the signal.

For a time-scale modification, the resampling phase is not needed. For a pitch scale modification, the modification phase will need to slow down the signal by a certain amount $x$, and the signal must then be resampled $x$ times faster for the desired effect.

The resampling phase might happen before the analysis stage, or after the synthesis stage. If the pitch of an audio signal must be scaled down, the audio must be resampled before the analysis stage to prevent the loss of too much audio information.

By using the phase vocoder to change the pitch of the signal, the length and the rate at which the sound sample must be played will always remain the same. That property makes it attractive for a driving simulator. Typically, everything happens at fixed time instances, and a variable-length audio signal does not conform with that. The four phases of the phase vocoder are described below.

### 6.3.1 Analysis

For the *analysis* stage, the idea is to perform a Fourier transform on a limited portion of the signal, then shifting to another portion of the signal and repeating the operation. The signal is then described by the values of the Fourier transforms obtained at the different window locations [126]. A digital filter must be implemented to divide the signal in such portions.

The Short Time Fourier Transform (STFT) represents the signal as the sum of sine waves by applying the Fourier Transform to a small part of the signal. It is defined by [141]

$$X_k(t_{ai}) = \sum_{r=-\infty}^{\infty} x(r)h_a(t_{ai} - r)e^{-j\left(\frac{2\pi}{N}\right)rk}, \; i = 1, 2, \ldots, m_a, \; k = 0, 1, \ldots, N-1. \tag{6.1}$$

where $h_a(n)$ is the chosen analysis window function, $t_{ai}$ is the centre of the $i^{th}$ window, and $N$ is the size of the chosen Fourier transform.

The short time Fourier transform is used for a non-periodic signal. On the other hand, the *Discrete Fourier Transform* (DFT), which assumes a periodic signal, is given by [115]

$$X(k) = \sum_{n=0}^{N-1} x(n)e^{-j\left(\frac{2\pi}{N}\right)kn}, \; k = 0, 1, \ldots, N-1. \tag{6.2}$$

One can see the similarities between Eq. (6.1) and (6.2). A mathematical formulation of the relation between these two equations was done by Portnoff [141]. For a practical implication, if the window is of width $N$, $r$ does not need to be within the range $r \in (-\infty, \infty)$, because all values of $r$ will only consist of zero's for all $r < 0$ or $r \geq N$. Then, the signal within each frequency window $X_k$ in Eq. (6.1) can be written as the DFT of $[x(r)h(n-r)]$. The signal can then be represented in the frequency domain by

$$\begin{aligned} \boldsymbol{X} &= [\boldsymbol{X}(t_{a1})\boldsymbol{X}(t_{a2})..\boldsymbol{X}(t_{am_a})] \\ &= \begin{bmatrix} X_0\left(t_{a1}\right) & X_0\left(t_{a2}\right) & \cdots & X_0\left(t_{am_a}\right) \\ X_1\left(t_{a1}\right) & X_1\left(t_{a2}\right) & \cdots & X_1\left(t_{am_a}\right) \\ \vdots & & & \vdots \\ X_{N-1}\left(t_{a1}\right) & X_{N-1}\left(t_{a2}\right) & \cdots & X_{N-1}\left(t_{am_a}\right) \end{bmatrix}. \end{aligned} \tag{6.3}$$

If $N$ is a power of 2, computational power can be diminished by applying the Fast Fourier Transform of $[x(r)h(n-r)]$. If $N$ is not a power of 2, the window can be enlarged by adding zero's on both sides of the window until the window length will be a multiple of two [131].

Mostly a window function such as the Hamming or Hanning window is used. A proper choice of the analysis window, $h_a\left(n\right)$, will ensure that the original signal is exactly recoverable from the model. To have this property, a window should be as close as possible to the ideal window, represented by [141]

$$h_{ideal}(n) = \frac{\sin\left(\frac{n\pi}{N}\right)}{\frac{n\pi}{N}}. \tag{6.4}$$

The length of the window is a separate consideration. According to the Nyquist criterion, a signal can be reconstructed from its sampling rate $R$ if $R$ is greater than twice the highest frequency present in the signal [115]. For a proper reconstruction of the signal, each window should not contain more than one harmonic of the fundamental frequency within the range 0 Hertz to $\frac{R}{2}$ Hertz [46].

For the proper reconstruction of the signal after modifications, an overlap is needed between consecutive windows. For rapidly varying sounds, more overlapping is necessary than for slow-varying sounds [46]. The more overlap between filters, the more filters are needed and that causes an increase in the computational intensity. However, it is suggested that for Hanning and Hamming windows, there must be an overlap of at least 75% [98].



### 6.3.2 Modification

The modification stage results in a change in the speed of the signal, without altering the pitch. The role of the phase vocoder is to preserve the amplitude and phase of the signal.

To slow down a signal to $v_s$ times its original speed, $\frac{1}{v_s}$ times as many columns will be needed in the modified short time Fourier representation of the signal. Let the number of columns of the modified STFT be $m_s$, where $m_s = \left\lceil \frac{m_a}{v_s} \right\rceil$. If the windows of the STFT is equally spaced the centre of each synthesis window $t_{si}$ will be at

$$t_{si} = \frac{t_{sa}}{m_s} i, \ i = 1, 2, \ldots, m_s. \tag{6.5}$$

The modified STFT will then be of the form

$$\boldsymbol{Y} \;=\; [\boldsymbol{Y}(t_{s1})\boldsymbol{Y}(t_{s2})..\boldsymbol{Y}(t_{sm_s})]$$

$$= \begin{bmatrix} Y_0(t_{s1}) & Y_0(t_{s2}) & \cdots & Y_0(t_{sm_s}) \\ Y_1(t_{s1}) & Y_1(t_{s2}) & \cdots & Y_1(t_{sm_s}) \\ \vdots & & & \vdots \\ Y_{N-1}(t_{s1}) & Y_{N-1}(t_{s2}) & \cdots & Y_{N-1}(t_{sm_s}) \end{bmatrix}. \tag{6.6}$$

Each of these columns must be estimated using the original STFT-signal $\boldsymbol{X}$. Each column $\boldsymbol{Y}(t_{si})$ will be estimated using the two columns of $\boldsymbol{X}$ closest to that signal. Assume

$$t_{a(i-1)} \leq t_{sp_i} \leq t_{ai}. \tag{6.7}$$

The amplitude of $Y_k(t_{sp_i})$ can be estimated using linear interpolation. That is

$$|Y_k(t_{sp_i})| = \left(\frac{t_{ai} - t_{sp_i}}{t_{ai} - t_{a(i-1)}}\right)\left|X_k\left(t_{a(i-1)}\right)\right| + \left(\frac{t_{sp_i} - t_{a(i-1)}}{t_{ai} - t_{a(i-1)}}\right)\left|X_k\left(t_{ai)}\right)\right|. \tag{6.8}$$

The preservation of the phase needs a little bit more effort. The initial phase of the STFT-signal must remain constant. That is

$$\angle Y_k(t_{s1}) = \angle X_k(t_{a1}). \tag{6.9}$$

To estimate the rest of the phases of $\boldsymbol{Y}$, phase wrapping must be used. That is, the phase increment between two consecutive frames is used to estimate the instantaneous frequency of a nearby sinusoid for each $k \in \{0, 1, \ldots, N-1\}$ [98].

The equations for the phase wrapping process is described by Laroche and Dolson [98]. The idea is to determine the instantaneous frequency $\hat{\omega}_{ki}$ of the sinusoid closest to $X_k(t_{ai})$. This value must be close to $\frac{2\pi k}{N}$. To achieve that, first the heterodyned phase increment $\Delta\Phi_{ki}$ must be calculated. That will be the phase difference minus the expected phase difference $\left[t_{ai} - t_{a(i-1)}\right]\frac{2\pi k}{N}$. The heterodyned phase increment is given by

$$\Delta\Phi_{ki} = \angle X_k(t_{ai}) - \angle X_k\left(t_{a(i-1)}\right) - \left[t_{ai} - t_{a(i-1)}\right]\frac{2\pi k}{N}. \tag{6.10}$$

This value must then be modified so that $\Delta\Phi_{ki} \in [-\pi, \pi]$. Once that is done, the instantaneous frequency of the closest sinusoid can then be calculated by

$$\hat{\omega}_{ki} = \frac{2\pi k}{N} + \frac{1}{t_{ai} - t_{a(i-1)}}\Delta\Phi_{ki} \tag{6.11}$$

and the phase propagation formula will then be

$$\angle Y_k\left(t_{sp_i}\right) = \angle Y_k\left(t_{sp(i-1)}\right) + \left[t_{sp_i} - t_{sp(i-1)}\right]\hat{\omega}_{ki}. \tag{6.12}$$

### 6.3.3 Synthesis

The synthesis stage is to represent the model in the time domain. First, the inverse short time Fourier transform must be calculated for each window, defined by [98, 141]

$$y^u\left(n\right) = \sum_{k=0}^{N-1} X_k\left(t_{su}\right) e^{j\left(\frac{2\pi}{N}\right)kn}, \; u = 1, 2, \ldots, m_s \tag{6.13}$$

where the output of the $u^{th}$ filter is given by $y^u$. The output signal $y\left(n\right)$ is then given by [98]

$$y\left(n\right) = \sum_{u=1}^{m_s} y^u(n) h_s(t_{si} - n) \tag{6.14}$$

where $h_s$ is the synthesis window. The synthesis window need not be the same as the analysis window, and is optional. Several considerations exist for choosing the synthesis window. Practically, it must be of finite duration, and to avoid time-aliasing, its duration must be smaller as N, the number of FFT coefficients [126].

### 6.3.4 Resampling at a Different Speed

As discussed previously, for a pitch scale modification, the modification phase will need to slow down the signal by a certain amount $x$, and the signal must then be played $x$ times faster for the desired effect. However, computer hardware do not always allow a continuous change in sampling speed, and most of the sound cards stall after a few alterations in sampling rate. For that reason, it might be a better option to resample the sound signal to the required speed. Several resampling algorithms exists, and a `resample` function exist in most audio software such as MATLAB.

## 6.4 Experimental Results

The vocoder technique was subsequently applied to the sound modelling of a commercial truck simulator. This was done to evaluate the efficiency of this technique and the level of realism for such applications.

Only one clear sound sample could be obtained for this truck, and this sample was at an engine speed of $1300rpm$. A few other sound samples at other engine speeds were also available, but they contained background noise which could not be filtered out completely. For the imitation of vehicle sound, a continuous sound is needed, and this can be obtained more successfully by using one sound sample only.

In order to simulate the engine sound at different pitches, it first had to be determined how much the pitch of the sound sample should be altered for the desired effect. This was done by determining the dominating frequency of each of the other sound samples and comparing them to the sound sample at $1300rpm$.

Let $f(n_e)$ be the frequency of the engine at an engine speed $n_e$. A linear estimation of $f(n_e)$ is given by

$$f(n_e) = (0.00019n_e + 0.70758)\, f(1300)\,. \tag{6.15}$$

The average human ear cannot distinguish between small variations in engine pitch. For that reason, it was not necessary to change the sound of the engine constantly. For this simulator, sound samples were generated for each engine speed between $1800rpm$ and $2800rpm$, which is a multiple of 100.

The program written for generating the sound samples is based on the vocoder MATLAB program written by Dan Ellis [49].

Fig.6.1 shows the engine sound at different engine speeds. One can observe the effect of the vocoder: Although the frequency of the sound is different at each engine speed, the shape or envelope of the audio signal remains the same.

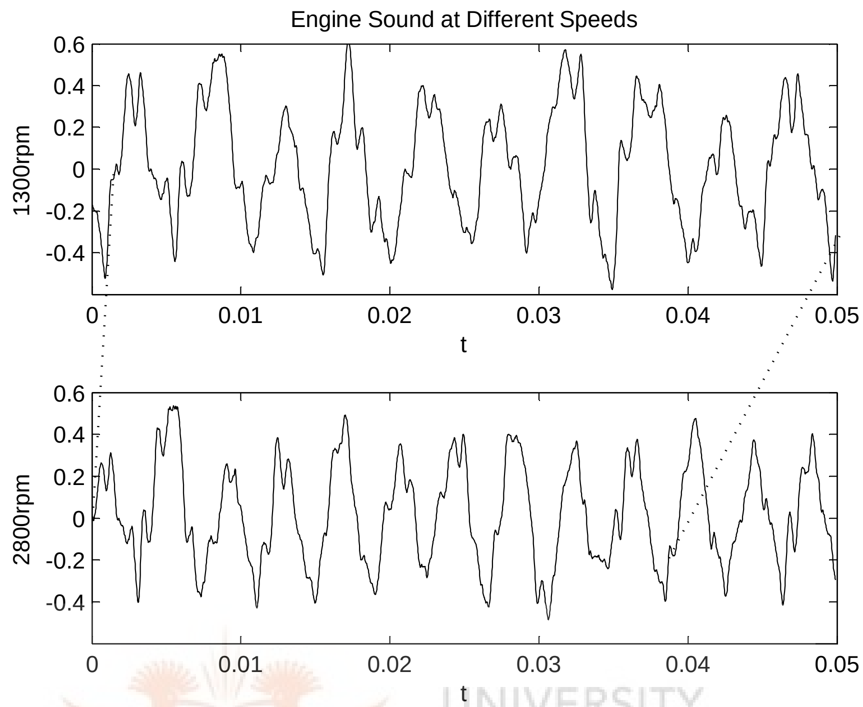


Figure 6.1: Engine sound at different speeds.

Within the driving simulator, the vehicle dynamics model updates the engine speed, vehicle speed, vehicle position and type of terrain every $30ms$. The sound model then decides which sound sample is required for the next $30ms$, and that is added to the sound of wheels on the specific terrain for the desired effect.

During the experiments it was found that special care should be taken in concatenating the sound samples, since a discontinuity results in a "click" sound every time the sample starts again. The end of the sample should be chosen in such a way as to form a continuous wave with the beginning of next sample. If this cannot be achieved manually, the solution is to use a low pass filter with a high cut-off frequency in order to filter out the discontinuity between the sound samples.

To test the realism of the sound model, a few driving instructors of the specific truck were invited to a demonstration. The truck was accelerated in first gear at full throttle. The instructors became stressed, and some even aggressive, when no attempt was made to change gears at the desired moment. More than one left hand was also noticed trying to grip an invisible gear lever from where he stood.

## 6.5 Conclusion

This chapter presented the use of vocoder technology for the modelling of vehicle sound for a driving simulator. An overview was given of the existing research of vehicle sound applications within the literature, as well as background information on the phase vocoder. The vocoder modifies the audio sample in four stages, namely analysis, modification, synthesis and resampling, and the mathematics of each of these stages was presented. The sound model was implemented in a commercial driving simulator with exceptionally good results. The vocoder proved to be a successful method for the realistic alteration of the pitch of the engine sound to imitate a vehicle sound at different speeds.

# Chapter 7

# Conclusion and Recommendations



## 7.1 Conclusion

In conclusion the key features of the thesis are briefly highlighted.

Essentially the study focuses on particular aspects of simulation applied within a particular field, the driving simulator.

A driving simulator provides a safe and less expensive way of training people how to drive. It furnishes a method for getting a person used to a specific vehicle in a specific geographic area which he or she possibly never seen before. For a driver the only noticeable difference should be computer screens instead of windows and mirrors.

Driving simulators have many fields of scientific applications, such as automated highway systems and the modelling and control of unmanned vehicles. It can be used for the analysis and prevention of road accident and to analyse the effect of cellphones on driving performance. Simulators make it easier to test new technology, to do research on transportation and to improve the efficiency of vehicle equipment. Within the domain of humanities, it is used to analyse driving behaviour and to study the effect of fatigue on driving performance. With regard to the the field of medicine, driving simulators have proved to be an effective method for analysing the effect of a certain medicine on driving. All these applications contextualize the present study within the greater simulation environment and indicate research opportunities with regard to driving simulators.

For reliable driving simulator results, however, close attention has to be paid to the ongoing development of the technical aspects of dynamical modelling. It is in this area that the thesis endeavoured to make its main contributions.

Broadly seen, a driving simulator consists of a vehicle dynamics model, terrain model, scenario generator, visual display, sound and a driver. The *vehicle dynamics model* includes models of several subsystems of the vehicle, such as for the engine, drive train, aerodynamics, vehicle-road interaction, suspension and handling. The *terrain model* contains a database of all the terrain information. This information is then used to visualize the terrain by means of a graphic display. The *visual model* generates a picture of all the information given by the terrain model, the vehicle model and the scenario generator. To simulate the "look and feel" of a vehicle, the more sophisticated simulators have a *motion system* which might provide an exact replica of the interior of the vehicle. The *sound model* generates a sound according to the engine and vehicle speed and the noise caused by the wind and type of terrain. The *driver* is the user of the simulator. He uses his senses to combine the visual information, motion and sound feedback in order to make decisions about how to drive.

With regard to vehicle dynamics modelling, in available research the focus is primarily on the vehicle dynamics modelling of commercial four wheel vehicles. However, many of the military armoured vehicles have six or eight wheels. Their capabilities completely differ from that of the aforementioned vehicles. These multi-wheeled vehicles are, for example, able to cross trenches of approximately two meters, and can climb steps of as high as one meter. In this thesis, attention is therefore predominantly given to an eight wheel vehicle dynamics model for use in an off road driving simulator [88]. An overview is given of the coordinate transformations and transformation of speed, linear and angular velocity and acceleration between two coordinate systems in three dimensions. The basic vehicle dynamics modelling components such as acceleration, braking and turning properties of the vehicle are explained. A suspension model for eight wheel vehicles is suggested together with a terrain model for addressing extreme terrain conditions such as trenches and steps. A control sequence is given to show how all the models could be integrated for a real-time simulation, where all parameters change after each time interval. The experimental results are provided to illustrate the model's ability to realistically simulate the climbing of a 0.5m step.

To prove the validity of a vehicle model, it is necessary to provide a method of testing the model. Proper testing of a driving simulator is not only the verification of standard vehicle dynamics equations. Integration methods and other numerical methods used may also influence the final result. Detail about the vehicle dynamics model used is not always available when developed by a third party. This testing scenario has not yet been discussed within the literature. In this thesis, the simulation of a "black box" testing environment for a vehicle dynamics model is elucidated [89]. Such a simulation is necessary for the validation of a commercial off-the-shelf vehicle model where the implementation detail is unknown. The subsystems of a standard driving simulator, that is the vehicle dynamics model, terrain model, scenario generator, visual display, sound, motion base and driver are discussed. It is shown how these interfaces can be adjusted to use a main test program, terrain model and automatic driver to simulate various test scenarios and log the vehicle dynamics output. In the discussion of experimental results on an off-road truck, the value of a proper test simulator has been shown.

Normally, the focus on driving simulators is on the modelling of realistic vehicle dynamics models. However, the design of a realistic simulation environment is of equal importance. A human driver usually steers one vehicle, but the rest of the vehicles used in the simulation should be managed by a computer program. In this thesis, an automatic driver model is described which can be used within the simulation environment [86]. By using the vehicle output and with the way points defined, the automatic driver determines the inputs to the vehicle dynamics model. It uses the vehicle specifications to achieve the optimal performance of the vehicle. By using this automatic driver model, it is possible to simulate the movement of vehicles controlled by the computer more realistically.

An understanding of three-dimensional coordinate system transformations is one of the most important parts of a flight or driving simulator. Although the procedure of using Euler angles for coordinate system transformations is nothing new, almost no literature is available on how it can be applied for more complex situations. In this thesis, the mathematical framework for implementing tree-dimensional coordinate transformations has been presented. [87] This includes the positioning of an observer relative to a vehicle, and controlling the position of a gun and turret on a military vehicle. More information is also given on how to use a program language such as C++ for more complex coordinate transformations in real-life situations. This framework is currently used for the positioning of an observer for a commercial driving simulator.



For a driving simulator which should be an exact replica of a certain vehicle, an accurate sound model is of extreme importance. The most computer games select from three or more pre-recorded engine sounds, depending on the engine speed. Other methods use linear interpolation between engine sounds for a more accurate model, but this modus operandi is still not ideal. This thesis proposes the use of vocoders for the modelling of engine sound [85]. By using vocoders, a technique used for the manipulation of voice, a much higher level of accuracy and realism was obtained. An overview is given of the existing research of vehicle sound applications within the literature, as well as background information regarding the phase vocoder. The vocoder modifies the audio sample in four stages, namely analysis, modification, synthesis and resampling, and the mathematics of each of these stages is presented. The sound model was implemented in a commercial driving simulator with exceptionally good results. The vocoder has proved to be a successful method for the realistic alteration of the pitch of the engine sound to imitate the noise made by a vehicle at different speeds.

## 7.2 Recommendations and Future Work

This thesis presented new models for aspects of driving simulation which have not been covered sufficiently within the literature before. However, several techniques could still be applied to achieve even more accurate results.

For the modelling of eight wheel vehicle dynamics, further research needs to focus on the incorporation of proper numerical analysis techniques and the use of quaternions for ensuring stability and a higher level of accuracy within the model.

The applications of the vehicle dynamics testing simulator could be extended to include the typical tests needed for the simulation of automated highway systems. This includes the exact modelling of slowly increasing steer, step steer and lane changing manoeuvres.

The autodriver model could be refined by taking into account many more vehicle subsystems such as the suspension, aerodynamics and vehicle-road interaction. A study can also be made to determine the optimal placement of way points.

For the three dimensional geometry used within driving simulators, the use of quaternions could still be investigated.

The vehicle sound modelling could still be refined by applying the voice modelling techniques for improving the sound quality of the output of the vocoder. More research can also be done for the optimised concatenation of the sound samples at different engine speeds to ensure a continuous engine sound.

# Bibliography


[1] ABS may increase your chances of crashing. Available from:
http://www.ambulancedriving.com/research/r-u1-e4-pce-09-01.html
(Accessed 15 February 2005).

[2] ADS information brochure. Available from:
http://www.ads.co.za
(Accessed 10 February 2005).

[3] A brief history of aircraft flight simulation. Available from:
http://homepage.ntlworld.com/bleep/SimHist1.html
(Accessed 10 February 2005).

[4] Demeter terrain engine home page. Available from:
http://www.terrainengine.com
(Accessed 1 August 2005).

[5] DFAD summary. Available from:
http://www.meteostar.com/esms/sme_spre/dfad.html
(Accessed 1 August 2005).

[6] DTED summary. Available from:
http://www.vterrain.org/Elevation/dted.html
(Accessed 1 August 2005).

[7] Honda: The 33rd Tokyo motor show. Available from:
http://www.firstmoto.ch/gallery/Tokyo/safety.html
(Accessed 10 February 2005).

[8] ICE Fahrsimulator. Available from:
`http://www.bahn.de/konzern/holding/angebote/die_bahn_ice_simulator.shtml`
(Accessed 10 February 2005).

[9] Jacobs vehicle systems - FAQ's. Available from:
`http://www.jakebrake.com/content.php4?doc_vid=17`
(Accessed 10 February 2005).

[10] Motorradfahrsimulator SAFE II. Available from:
`http://wsvst25.site.uni-wuppertal.de/dirk/motsim1.html`
(Accessed 10 February 2005).

[11] Port crane. Available from:
`http://glup.irobot.uv.es/grupos/artec/English/gruas.html`
(Accessed 10 February 2005).

[12] Thoroughtec Technologies. Available from:
`www.thoroughtec.com`
(Accessed 10 February 2005).

[13] The website for the defence industries - Army. Available from:
`http://www.army-technology.com`.
(Accessed 10 February 2005).

[14] G. Abe and J. Richardson. The effect of alarm timing on driver behaviour: An investigation of differences in driver trust and response to alarms according to alarm timing. *Transportation Research Part F*, 7:307–322, 2004.

[15] S.S. Abeysekera, K.P. Padhi, J. Absar, and S. George. Investigation of different frequency estimation techniques using the phase vocoder. *Circuits and Systems*, 2:265–268, 2001.

[16] E. Ahlgren, A. Lundqvist, A. Nordlund, C. Aren, and H. Rutberg. Nerocognitive impairment and driving performance after coronary artery bypass surgery. *European Journal of Cardio-thoacic Surgery*, 23:334–340, 2003.

[17] H.B. Ahn, J.H. Ku, B.H. Cho, H. Kim, H.J. Jo, J.M. Lee, I.Y. Kim, and S.I. Kim. The development of virtual reality driving simulator for rehabilitation. *Proceedings of the 23rd Annual EMBS International IEEE Conference*, 4:3780 – 3783, 2001.

[18] T. Alderete. Simulator aero model implementation. NASA Ames Research Center, Moffet Field, California, 1993.

[19] J. Alexander, P. Barham, and I. Black. Factors influencing the probability of an incident at a junction: results from an interactive driving simulator. *Accident Analysis and Prevention*, 34(6):779–792, 2002.

[20] R.W. Allen, T.J. Rosenthal, B.L. Aponso, D.H. Klyde, F.G. Hogue, and J.P. Christos. A low cost PC based driving simulator for prototyping and hardware-in-the-loop applications. *Society of Automotive Engineers*, SAE Paper 980222, 1998.

[21] H. Alm and L. Nilsson. The effects of a mobile telephone task on driver behaviour in a car following situation. *Accident Analysis and Prevention*, 27(5):707–715, 1995.

[22] S.A. Amman and M.D. Das. An efficient technique for modeling and synthesis of automotive engine sounds. *IEEE Transactions on Industrial Electronics*, 48(1):225–234, 2001.

[23] H. Anton and C. Rorres. *Elementary Linear Algebra: Applications Version*. John Wiley and Sons, New York, $7^{th}$ edition, 1994.

[24] B. Artmann. *The Concept of Number: from quaternions to monads and topological fields*. John Wiley and Sons, New York, 1988.

[25] D. Bastow. *Car Suspension and Handling*. Pentech, London, $2^{nd}$ edition, 1988.

[26] J Bernard, J. Gruening, and K. Hoffmeister. Evaluation of vehicle/driver performance using genetic algorithms. *Society of Automotive Engineers*, SAE Paper 980227, 1998.

[27] J.P. Bliss and S.A. Acton. Alarm mistrust in automobiles: how collision alarm reliability affects driving. *Applied Ergonomics*, 34:499–509, 2003.

[28] R. Bosch. *Automotive Handbook*. Society of Automotive Engineers, Warrendale, $5^{th}$ edition, 2000.

[29] L.N. Boyle and F. Mannering. Impact of traveler advisory systems on driving speed: some new evidence. *Transportation Research Part C*, 12:57–72, 2004.

[30] A. Campagne, T. Pebayle, and A. Muzet. Correlation between driving errors and vigilance level: influence of the driver's age. *Physiology Behavior*, 80:515–524, 2004.

[31] D. Cebon. *Handbook of Vehicle-Road Interaction*. Swets and Zeitlinger, Netherlands, 2000.

[32] S.G. Charlton. Perceptual and attentional effects on drivers' speed selection at curves. *Accident Analysis and Prevention*, 36:877–884, 2004.

[33] B. Cheng, M. Hashimoto, and T. Suetomi. Analysis of driver response to collision warning during car following. *JSAE Review*, 23:231–237, 2002.

[34] J.C.K. Chou. Quaternion kinematic and dynamic differential equations. *IEEE Transactions on Robotics and Automation*, 8(2):53–64, 1992.

[35] J.P. Chrstos and P.A. Grygier. Experimental testing of a 1994 Ford Taurus for NADSdyna validation. *Society of Automotive Engineers*, SAE Paper 970563, 2000.

[36] T. Chung, J. Kim, and K. Yi. Human-in-the-loop evaluation of a vehicle stability controller using a vehicle simulator. *International Journal of Automotive Technology*, 5(2):109–114, 2004.

[37] S.L. Comte and A.H. Jamson. Traditional and innovative speed-reducing measures for curves: an investigation of driver behaviour using a driving simulator. *Safety Science*, 36(3):137–150, 2000.

[38] S. Contardi, F. Pizza, E. Sancisi, S. Mondini, and F. Cirignotta. Reliability of a driving simulation task for evaluation of sleepiness. *Brain Research Bulletin*, 63:427–431, 2004.

[39] J.M. Cooke, M.J. Zyda, D.R. Pratt, and R.B. KcGhee. NPSNET: Flight simulation dynamic modeling using quaternions. *Presence*, 1(4):404–420, 1994.

[40] T. Daimon and H. Kawashima. Study of aged drivers' behaviors when using the advanced cruise-assist highway systems at an intersection. *JSAE Review*, 24:393–402, 2003.

[41] A.P. de Vos, J. Theeuwes, W. Hoekstra, and M.J. Coemet. Behavioural aspects of automatic vehicle guidance: relationships between headway and driver comfort. *Transportation Research Record*, (1573):17–22, 1997.

[42] D. de Waard, F.J.J.M. Steyvers, and K. Brookhuis. How much visual road information is needed to drive safely and comfortably. *Safety Science*, 42:639–655, 2004.

[43] D. de Waard, M. van der Hulst, and K.A. Brookhuis. Elderly and young driver's reaction to an in-car enforcement and tutoring system. *Applied Ergonomics*, 30:147–157, 1999.

[44] P.A. Desmond and G. Matthews. Implications of task-induced fatigue effects for in-vehicle countermeasures to driver fatigue. *Accident Analysis and Prevention*, 29(4):515–523, 1997.

[45] J.C. Dixon. *Tires, Suspension and Handling.* Society of Automotive Engineers, Warrendale, $2^{nd}$ edition, 1996.

[46] M. Dolson. The phase vocoder: A tutorial. *Computer Music Journal*, 10(4):14–27, 1986.

[47] L. Dorn and D. Barker. The effects of driver training on simulated driving performance. *Accident Analysis and Prevention*, 37(1):63–69, 2005.

[48] A. Dutta, D.L. Fisher, and D.A. Noyce. Use of a driving simulator to evaluate and optimize factors affecting understandability of variable message signs. *Transportation Research Part F*, 7:209–227, 2004.

[49] D. Ellis. A phase vocoder in Matlab. Vocoder notes and MATLAB code, Available from:
`http://www.ee.columbia.edu/~dpwe/resources/matlab/pvoc/`
(Accessed 2 November 2005).

[50] K.A. Featherstone, J.R. Bloomfield, A.J. Lang, M.J. Miller-Meeks, G. Woodworth, and R.F. Steinert. Driving simulation study: Bilateral array multifocal versus bilateral AMO monofocal intraocular lenses. *Journal of Cataract Refract Surgery*, 25:1254–1262, 1999.

[51] D.A. Fishbain, R.B. Cutler, H.L. Rosmoff, and R.S. Rosomoff. Are opioid-dependent/tolerant patients impaired in driving-related skills? A structured evidence-based review. *Journal of Pain and Symptom Management*, 25(6):559–577, 2003.

[52] J.W. Fitch. *Motor Truck Engineering Handbook*. James W. Fitch Publisher, San Francisco, $2^{nd}$ edition, 1972.

[53] J.L. Flanagan and R.M. Golden. Phase vocoder. *Bell Systems Technical Journal*, 45:1493–1500, 1966.

[54] G.R. Fowles and G.L. Cassiday. *Analytical Mechanics*. Saunders College Publishing, London, $6^{th}$ edition, 1990.

[55] J.S. Freeman, G. Watson, Y.E. Papelis, T.C. Lin, A. Tayyab, R.A. Romano, and J.G. Kuhl. The Iowa driving simulator: An implementation and application overview. *Society of Automotive Engineers*, SAE Paper 950174, 1995.

[56] C.-E. Fröberg. *Numerical Mathematics, Theory and Computer Applications*. The Benjamin/Cummings Publishing Company, Amsterdam, 1985.

[57] C. Fukuhara, T. Kamura, and T. Suetomi. Subjective evaluation of engine accelerator sound with driving simulator. *JSAE Review*, 23:435–441, 2002.

[58] J. Funda, R.H. Taylor, and R.P. Paul. On homogeneous transforms, quaternions, and computational efficiency. *IEEE Transactions on Robotics and Automation*, 6(3):382–388, 1990.

[59] T.K. Garret. *The Motor Vehicle*. Society of Automotive Engineers, Warrendale, $13^{th}$ edition, 2001.

[60] G. Genta. *Motor Vehicle Dynamics, Modeling and Simulation*, volume 43 of *Series on Advances in Mathematics for Applied Sciences*. World Scientific, London, 1997.

[61] C.F.P. George. Driving simulators in clinical practice. *Sleep Medicine Review*, 7(4):311–320, 2003.

[62] R. Gianutsos and A. Beattie. Elemental driving simulator. *Proceedings of the IEEE Johns Hopkins National Search for Computing Applications to Assist Persons with Disabilities*, pages 117 – 120, 1992.

[63] T. Gillespie. *Fundamentals of Vehicle Dynamics*. Society of Automotive Engineers, Warrendale, 1992.

[64] A.I. Glendon, T.W. Hoyes, D.E. Haigney, and R.G. Taylor. A review of risk homoeostasis theory in simulated environments. *Safety Science*, 22(1-3):15–25, 1996.

[65] S.T. Godley, T.J. Triggs, and B.N. Fildes. Driving simulator validation for speed research. *Accident Analysis and Prevention*, 34:589–600, 2002.

[66] B. Gold and C. Rader. The channel vocoder. *IEEE Transactions on Audio and Electroacoustics*, 15(4):148–161, 1967.

[67] H. Goldstein, C. Poole, and J. Safko. *Classical Mechanics*. Addison Wesley, London, 2002.

[68] A. Gonzalez, M. Ferrer, M. de Diego, G. Pinero, and J. J. Garcia-Bonito. Sound quality of low-frequency and car engine noises after active noise control. *Journal of Sound and Vibration*, 265:663–679, 2003.

[69] P.G. Griffiths and R.B. Gillespie. A driving simulator for teaching embedded automotive control applications. *Proceedings of the 2005 American Control Conference*, pages 722–726, 2005.

[70] J. Gruening, J. Bernard, C. Clover, and K. Hoffmeister. Driving simulation. *Society of Automotive Engineers*, SAE Paper 980223, 1998.

[71] K. Guo, H. Guan, and C. Zong. Development and applications of JUT-ADSL driving simulator. *Proceedings of the IEEE Vehicle Electronics Conference*, 1:1–5, 1999.

[72] M. Hattingh. Die simfonie van motorenjins wat ontwerpersdeuntjies sing. *Naweek-Beeld*, page 9, 20 December 2003.

[73] E.J. Haug, D. Negrut, R. Serban, and D. Solis. Numerical methods for high speed vehicle dynamic simulation. *Mechanics of Structures and Machines*, 27(4), 1999.

[74] M. Hoedemaeker and K.A. Brookhuis. Behavioural adaption to driving with an adaptive cruise control. *Transportation Research Part F*, 1:95–106, 1998.

[75] A. Horiguchi and T. Suetomi. A Kansei engineering approach to a driver/vehicle system. *International Journal of Industrial Ergonomics*, 15:25–37, 1995.

[76] R. Horowitz and P. Varaiya. Control design of an automated highway system. *IEEE Proceedings of the IEEE*, 88(7):913–925, 2000.

[77] T.W. Hoyes, L. Dorn, P.A. Desmond, and R. Taylor. Risk homeostasis theory, utility and accident loss in a simulated driving task. *Safety Science*, 22(1-3):49–62, 1996.

[78] A.R.W. Huang and C. Chen. A low-cost driving simulator for full vehicle dynamics simulation. *IEEE Transactions on Vehicular Technology*, 52(1):162–172, 2003.

[79] W.-H. Hucho. *Aerodynamics of Road Vehicles*. Butterworths, London, 1987.

[80] A. Ikeda, T. Katou, M. Kinoshita, and M. Aihara. Study of driver characteristics using driving simulator considerations on difference in accident avoidance performance due to age. *JSAE Review*, 23(2):219–222, 2002.

[81] M. Iwao, A. Horiguchi, and M. Kobayashi. Study on behavior of cab-over truck driver looking at a display while driving. *JSAE Review*, 23:489–494, 2002.

[82] T. Janse van Rensburg. *A Generic vehicle model for real-time simulation applications*. B. Ing mini-dissertation, Department of Electrical and Electronic Engineering, Rand Afrikaans University, 2002.

[83] T. Janse van Rensburg. *Implicit Runge-Kutta Methods*. BSc Hons mini-dissertation, Department of Applied Mathematics, Rand Afrikaans University, 2003.

[84] T. Janse van Rensburg and M.A. van Wyk. Camera positioning within a driving simulator. *WSEAS Transactions on Circuits and Systems*, 2(4):814–819, October 2003.

[85] T. Janse van Rensburg, M.A. van Wyk, A.T. Potgieter, and W.-H. Steeb. Phase vocoder technology for the simulation of engine sound. 2006. Submitted to the *International Journal of Modern Physics C*.

[86] T. Janse van Rensburg, M.A. van Wyk, and W.-H. Steeb. Mathematical modeling of an automatic driver. *International Journal of Modern Physics C*, 16(6):895–908, 2005.

[87] T. Janse van Rensburg, M.A. van Wyk, and W.-H. Steeb. Three dimensional geometry within a driving simulator. *International Journal of Modern Physics C*, 16(6):909–920, 2005.

[88] T. Janse van Rensburg, M.A. van Wyk, and W.-H. Steeb. Modeling and simulation of eight wheel vehicle dynamics. 2006. Submitted to the *International Journal of Modern Physics C*.

[89] T. Janse van Rensburg, M.A. van Wyk, and W.-H. Steeb. Simulating a test environment for vehicle dynamics models. 2006. Submitted to the *International Journal of Modern Physics C*.

[90] A. Kemeny and F. Panerai. Evaluating perception in driving simulation experiments. *Trends in Cognitive Science*, 7(1):31–37, 2003.

[91] U. Kiencke and L. Nielsen. *Automotive Control Systems*. Society of Automotive Engineers, Warrendale, 2000.

[92] S.G. Kim and J.H. Kim. Unmanned vehicle control and modeling for obstacle avoidance. *International Journal of Automotive Technology*, 4(4):173–180, 2003.

[93] S. Kotterba, N. Mueller, M. Leidag, W. Widdig, K. Rasche, J.-P. Malin, G. Schultze-Werninghaus, and M. Orth. Comparison of driving simulator performance and neuropsychological testing in narcolepsy. *Clinical Neurology and Neurosurgery*, 106:275–279, 2004.

[94] H. Koutspouluos, A. Plydorpoulou, and M. Ben-Akiva. Travel simulators for data collection on driver behavior in the presence of information. *Journal of Transportation Research C*, 3(2):143–159, 1995.

[95] B.C. Kuo and F. Golnaraghi. *Automatic Control Systems*. John Wiley and Sons, New York, $8^{th}$ edition, 2003.

[96] S.J. Kwon, M. Omae, K.Y. Cho, and M.W. Suh. A study on the model-matching control in the longitudinal autonomous driving system. *International Journal of Automotive Technology*, 5(2):135–144, 2004.

[97] J. Laroche and M. Dolson. Phase-vocoder: About this phasiness business. *Proceedings IEEE ASSP workshop on Applications of Signal Processing to Audio and Acoustics*, 1997.

[98] J. Laroche and M. Dolson. Improved phase vocoder time-scale modification of audio. *IEEE Transactions on Speech and Audio Processing*, 7(3):323–332, 1999.

[99] J. Laroche and M. Dolson. New phase-vocoder techniques for pitch-shifting, harmonizing and other exotic effects. *Proceedings IEEE Workshop on Applications of Signal Processing to Audio and Acoustics*, pages 91–94, 1999.

[100] N.E. Laurie, R.O. Andres, and D. Fisher. Case study: Increasing usability of voice activated dialing systems. *International Journal of Industrial Ergonomics*, 23:621–627, 1999.

[101] N.E. Laurie, R.O. Andres, and D.L Fisher. The role of instruction sets in operator satisfaction while using a voice activated dialing system. *International Journal of Industrial Ergonomics*, 22:307–312, 1998.

[102] N.E. Laurie, S. Zhang, R. Mundoli, S.A. Duffy, J. Collura, and D. Fisher. An evaluation of alternative do not enter signs: failures of attention. *Transportation Research Part F*, 7:151–166, 2004.

[103] G.C.H. Lee, Y. Yoo, and S. Jones. Investigation of driving performance, vection, postural sway and simulator sickness in a fixed-based driving simulator. *Computers and Industrial Engineering*, 33(3-4):533–536, 1997.

[104] H.C. Lee, D. Cameron, and A.H. Lee. Assessing the driving performance of older adult drivers: on-road versus simulated driving. *Accident Analysis and Prevention*, 35:797–803, 2003.

[105] H.C. Lee, A.H. Lee, D. Cameron, and C. Li-Tsang. Using a driving simulator to identify older drivers at inflated risk of motor vehicle crashes. *Journal of Safety Research*, 34:453–459, 2003.

[106] W.S. Lee, J.H. Kim, and J.H. Cho. A driving simulator as a virtual reality tool. *IEEE International Conference on Robotics and Automation*, 1:71–76, 1998.

[107] M.R. Lehto, J.D. Papastavrou, T.A. Ranney, and L.A. Simmons. An experimental comparison of conservative versus optimal collision avoidance warning system thresholds. *Safety Science*, 36:185–209, 2000.

[108] M.G. Lenne, P. Dietze, G.R. Rumbold, J.R. Redman, and T.J. Triggs. The effects of the opoid pharmacotherapies methadone, laam and buprenorphine, alone and in combination with alcohol on simulated driving. *Drug and Alcohol Dependence*, 72:271–278, 2003.

[109] M.G. Lenne, T.J. Triggs, and J.R. Redman. Time of day variations in driving performance. *Accident Analysis and Prevention*, 29(4):431–437, 1997.

[110] M.D. Letherwood and D.D. Gunter. Virtual modeling and simulation of military ground vehicles. *Society of Automotive Engineers*, SAE Paper 2000-01-1580, 2000.

[111] M.D. Letherwood and D.D. Gunter. Ground vehicle modeling and simulation of military vehicles using high performance computing. *Parallel Computing*, 27(1-2):109–140, 2001.

[112] Y.-C. Liu. Effects of Taiwan in-vehicle cellular audio phone system on driving performance. *Safety Science*, 41:531–542, 2003.

[113] Y.-C. Liu. Effects of using head-up display in automobile context on attention demand and driving performance. *Displays*, 24:157–165, 2003.

[114] R.E. Llaneras, R.W. Swezey, J.F. Brock, W.C. Rogers, and H.P. van Cott. Enhancing the safe driving performance of older commercial vehicle drivers. *International Journal of Industrial Ergonomics*, 22:217–245, 1998.

[115] L.C. Ludeman. *Fundamentals of Digital Signal Processing*. John Wiley and Sons, Inc., New York, 1986.

[116] M.M. Macchi, Z. Boulos, T. Ranney, L. Simmons, and S.S. Campbell. Effects of an afternoon nap on nighttime alertness and performance in long-haul drivers. *Accident Analysis and Prevention*, 34:825–834, 2002.

[117] V. Martin. Active control of moving sound source radiation - Numerical modeling in the space-frequency and space-time domains. *Journal of Sound and Vibration*, 228(3):477–509, 1999.

[118] R.J. McAuly and T.F. Quatieri. Speech analysis/synthesis based on a sinusoidal representation. *IEEE Transactions on Acoustics, Speech and Signal Processing*, ASSP-34(4):744–754, 1986.

[119] D.V. McGehee, J.D. Lee, M. Rizzo, J. Dawson, and K. Bateman. Quantitative analysis of steering adaptation on a high-performance fixed-base driving simulator. *Transportation Research Part F*, 7:181–196, 2004.

[120] D.J. McGill and W.W. King. *Engineering Mechanics: Statics and an Introduction to Dynamics.* PWS Publishing Company, Boston, $3^{rd}$ edition, 1995.

[121] R.C. McLane and W.W. Wierwille. The influence of motion and audio cues on driver performance in an automobile simulator. *Human Factors*, 17:488–501, 1975.

[122] D. McRuer, I. Ashkenas, and D. Graham. *Aircraft Dynamics and Automatic Control.* Princeton University Press, New Yersey, 1973.

[123] W.F. Milliken and D.L. Miliken. *Race Car Vehicle Dynamics.* Society of Automotive Engineers, Warrendale, 1995.

[124] J. Miura, M. Ito, and Y. Shirai. A three-level control architecture for autonomous vehicle driving in a dynamic and uncertain traffic environment. *Proceedings IEEE Conference on Intelligent Transportation Systems*, pages 706–711, 1997.

[125] J.A. Moorer. Signal processing aspects of computer music: A survey. *Proceedings of the IEEE*, 65(8):1108–1137, 1977.

[126] E. Moulines and J. Laroche. Non-parametric techniques for pitch-scale and time-scale modifications of speech. *Speech Communication*, 16:175–205, 1995.

[127] R.R. Mourant, N. Qiu, and S.A. Chiu. A distributed virtual driving simulator. *IEEE Virtual Reality Annual International Symposium*, page 208, 1997.

[128] R.R. Mourant and D. Refsland. Developing a 3D sound environment for a driving simulator. *Proceedings of the Ninth International Conference on Virtual Systems and Multimedia*, pages 711–719, 2003.

[129] S. Namba, S. Kuwano, A. Kinoshita, and Y. Hayakawa. Psychological evaluation of noise in passenger cars - the effect of visual monitoring and the measurement of habituation. *Journal of Sound and Vibration*, 205(4):427–433, 1997.

[130] C. Newton, R.N. Mussa, E.K. Sadalla, E.K. Burns, and J. Matthias. Evaluation of an alternative traffic light change anticipation system. *Accident Analysis and Prevention*, 29(2):201–209, 1997.

[131] P.M. Nielsen and S. Brandorff. Sound manipulation in the frequency domain. Available from:
`http://www.daim.au.dk/~pmn/sound/soundman/soundman_041202.doc`
(Accessed 1 November 2005).

[132] H. Ohno. Analysis and modeling of human driving behaviors using adaptive cruise control. *Applied Soft Computing*, 1:237–243, 2001.

[133] H.B. Pacejka. *Tire and Vehicle Dynamics*. Society of Automotive Engineers, Warrendale, 2002.

[134] E.H. Page and R. Smith. Introduction to military training simulation: A guide for discrete event simulationists. In D. J. Medeiros, E. F. Watson, J. S. Carson, and M. S. Manivannan, editors, *Proceedings of the 1998 Winter Simulation Conference*, 1998.

[135] M.K. Park, M.C. Lee, K.S. Yoo, K. Son, W.S. Yoo, and M.C. Han. Development of the PNU vehicle driving simulator and its performance evaluation. *Proceedings of the IEEE International Conference on robotics and Automation*, 3:2325 – 2330, 2001.

[136] M. Partinen, K. Hirvonen, C. Hublin, M. Halavaara, and H. Hiltunen. Effects of after-midnight intake of zolpidem and temazepam on driving ability in woman with non-organic insomnia. *Sleep Medicine*, 4(4):553–561, 2003.

[137] M. Pasquier, C. Quck, and M. Toh. Fuzzylot: a novel self-organizing fuzzy-neural rule-based pilot system for automated vehicles. *Neural Networks*, 14:1099–1112, 2001.

[138] P. Philip, J. Taillard, E. Klein, P. Sagaspe, A. Charles, W.L. Davies, C. Guilleminault, and B. Bioulac. Effect of fatigue on performance measured by a driving simulator in automobile drivers. *Journal of Psychosomatic Research*, 55:197–200, 2003.

[139] W.J. Pielemeier, G.H. Wakefield, and M.H Simone. Time-frequency analysis of music signals. *Proceedings of the IEEE*, 84(9):1216–1230, 1996.

[140] F. Pizza, S. Contardi, B. Mostacci, S. Mondini, and F. Cirignotta. A driving simulation task: correlations with multiple sleep latency test. *Brain Research Bulletin*, 63:423–426, 2004.

[141] M.R. Portnoff. Implementation of the digital phase vocoder using the Fast Fourier Transform. *IEEE Transactions on Acoustics, Speech and Signal Processing*, ASSP-24(3):243–248, 1976.

[142] M.R. Portnoff. Time-scale modification of speech based on short-time Fourier analysis. *IEEE Transactions on Acoustics, Speech and Signal Processing*, ASSP-29(3):374–390, 1981.

[143] M.S. Puckette and J.C. Brown. Accuracy of frequency estimates using the phase vocoder. *IEEE Transactions on Speech and Audio Processing*, 6(2):166–176, 1998.

[144] T.F. Quatieri and R.J. McAuly. Speech transformations based on a sinusoidal representation. *IEEE Transactions on Acoustics, Speech and Signal Processing*, ASSP-34(6):1449–1464, 1986.

[145] T.F. Quatieri and R.J. McAuly. Shape invariant time-scale and pitch modification of speech. *IEEE Transactions on Signal Processing*, 40(3):497–510, 1992.

[146] M.E. Rakauskas, L.J. Gugerty, and N.J. Ward. Effects of naturalistic cell phone conversations on driving performance. *Journal of Safety Research*, 35:453–464, 2004.

[147] F.M. Ravin. *Automatic Control Engineering.* McGraw-Hill, New York, $5^{th}$ edition, 1995.

[148] J. Reimpell and H. Stoll. *The Automotive Chassis: Engineering Principles.* Arnold, London, 1996.

[149] J. Roge, T. Pebayle, and A. Muzet. Variations on the level of vigilance and of behavioural activities during simulated automobile driving. *Accident Analysis and Prevention*, 33:181–186, 2001.

[150] R. Romano. Real-time multi-body vehicle dynamics using a modular modeling methodology. *Society of Automotive Engineers*, SAE Paper 2003-01-1286, 2003.

[151] M.K. Salani and G.J. Heydinger. Model validation of the 1997 Jeep Cherokee for the national advanced driving simulator. *Society of Automotive Engineers*, SAE Paper 01-0700, 2000.

[152] G. Salgian. *Tactical Driving using Visual Routines.* Ph.D. thesis, Department of Computer Science, University of Rochester, 1998.

[153] G. Salgian and D. Ballard. Developing autonomous navigation algorithms using photorealistic simulation. *IEEE Conference on Intelligent Transportation Systems*, pages 882–887, 1997.

[154] D. Salvucci and A. Liu. The time course of a lane change: driver control and eye-movement behavior. *Transportation Research Part F*, 5:123–132, 2002.

[155] D.D. Salvucci. Predicting the effects of in-car interface use on driver performance: an integrated model approach. *Transportation Research Part F*, 55:85–107, 2001.

[156] D.D. Salvucci and K.L. Macuga. Predicting the effects of cellular-phone dialing on driver performance. *Cognitive System Research*, 3:95–102, 2002.

[157] N. Samyn, G. de Boeck, M. Wood, C.T.J. Lamers, D. de Waard, K.A. Brookhuis, A.G. Verstraete, and W.J. Riedel. Plasma, oral fluid and sweat wipe ecstasy concentrations in controlled and real life conditions. *Forensic Science International*, 128:90–97, 2002.

[158] L. Schweizer. Problems in realizing a digital vocoder and novel solutions. *IEEE Transactions on Audio and Electroacoustics*, AU-19(1):94–96, 1971.

[159] E. Seckel. *Stability and Control of Airplanes and Helicopters*. Academic Press, New York, 1964.

[160] M. Segwa, S. Nakan, O. Nishihara, and H. Kumamoto. Vehicle stability control strategy for steer by wire system. *JSAE Review*, 22:383–388, 2001.

[161] T. Shiiba and Y. Suda. Development of driving simulator with full vehicle model of multibody dynamics. *JSAE Review*, 23:223–230, 2002.

[162] L. Stankovic and J. Bohme. Time-frequency analysis of multiple resonances in combustion engine signals. *Signal Processing*, 79:15–28, 1999.

[163] R.L. Stapleford, D.H. Weir, N.L. Broen, D.P. Chiang, and R. Igarashi. The DRI driving simulator 1997, description and applications to the study of intelligent transportation systems. *IEEE Conference on Intelligent Transportation System*, pages 478–483, 1997.

[164] C. Steele. A critical review of some traffic noise prediction models. *Applied Acoustics*, 62:271–287, 2001.

[165] B.L. Stevens and F.L. Lewis. *Aircraft Control and Simulation*. John Wiley & Sons, New York, 1992.

[166] J. Sumita, H. Takada, Y. Konya, and S. Muroyama. A new visual and sound monitoring system for emergency engine generators. *IEEE Telecommunications Energy Conference*, pages 732–737, 1981.

[167] J. Tornros. Driving behaviour in a real and a simulated road tunnel: a validation study. *Accident Analysis and Prevention*, 30(4):497–503, 1998.

[168] M. van der Hulst, T. Meijman, and T. Rothengatter. Maintaining task set under fatigue: a study of time-on-task effects in simulated driving. *Transportation Research Part F*, 4:103–118, 2001.

[169] M. van der Hulst, T. Rothengatter, and T. Meijman. Strategic adaptions to lack of preview in driving. *Transportation Research Part F*, 1:59–75, 1998.

[170] M. van der Voort, M.S. Dougherty, and M. van Maarseveen. A prototype fuel-efficiency support tool. *Transportation Research Part C*, 9:279–296, 2001.

[171] M.B.F. van Erp and H.A.H.C. van Veen. Vibrotactile in-vehicle navigation system. *Transportation Research Part F*, 7:247–256, 2004.

[172] W. van Winsum, D. de Waard, and K. A. Grookhuis. Lane change manoeuvres and safety margins. *Transportation Research Part F*, 2:139–149, 1999.

[173] D. Vastifall, M.A. Gulbol, and M. Kleiner. Affective evaluations and reactions to exterior and interior vehicle auditory quality. *Journal of Sound and Vibration*, 253(3):501–518, 2002.

[174] N.J. Versfeld and J. Vos. A weighted equivalent sound level as a predictor of the annoyance caused by road traffic consisting of various proportions of light and heavy vehicles. *Journal of Sound and Vibration*, 253(2):389–399, 2000.

[175] J.C. Verster, D.S. Veldhuijzen, and E.R. Volkerts. Residual effects of sleep medication on driving ability. *Sleep Medicine Reviews*, 8:309–325, 2004.

[176] W.B. Verwey and D.M. Zaidel. Preventing drowsiness accidents by an alertness maintenance device. *Accident Analysis and Prevention*, 31:199–211, 1999.

[177] G.R. Watts. A comparison of noise measures for assessing vehicle noisiness. *Journal of Sound and Vibration*, 180(3):493–512, 1995.

[178] J.Y. Wong. *Terramechanics and Off-Road Vehicles.* Elsevier, New York, 1973.

[179] J.Y. Wong. *Theory of Ground Vehicles.* John Wiley and Sons, New York, $3^{rd}$ edition, 2001.

[180] Y. Xu, J. Song, M.C. Nechyba, and Y. Yam. Performance evaluation and optimization of human control strategy. *Robotics and Autonomous Systems*, 39:19–36, 2002.